

**Monomeric Organo–Aluminum and Gallium Monohydroxides as
Precursor for Homo– and Hetero–Bimetallic Oxides:
Synthetic, Reactivity and Structural Investigations
Including Gold(I) *N*-heterocyclic Carbene Complexes**

Dissertation
zur Erlangung des Doktorgrades
der Mathematisch–Naturwissenschaftlichen Fakultäten
der Georg–August–Universität zu Göttingen

Vorgelegt von

Sanjay Singh
Aus Varanasi
(Indien)

Göttingen 2005

D 7

Referent: Prof. Dr. Dr. h. c. mult. H. W. Roesky

Korreferent: Prof. Dr. Dietmar Stalke

Tag der mündlichen Prüfung: 12.01. 2006

*Dedicated to my parents
for their love and affection*

Acknowledgement

The work described in this doctoral thesis has been carried out under the guidance and supervision of Prof. Dr. Dr. h. c. mult. H. W. Roesky at the Institut für Anorganische Chemie der Georg-August-Universität in Göttingen between January 2003 and October 2005.

My grateful thanks to

Prof. Dr. Dr. h. c. mult. H. W. Roesky

for his constant advice, guidance, motivation, suggestions, and discussions throughout this work. I would like to thank him for his personal attention and the freedom I enjoyed during my stay in Göttingen.

I profoundly take this opportunity in expressing my sincere thanks to Dr. Ganapathi Anantharaman for teaching me the experimental skills at the initial phase of my work and for being supportive throughout my work. I would like to thank Prof. G. M. Sheldrick, Dr. Vojtech Jancik, Mr. Aritra Pal, Dr. M. Noltemeyer, and Mr. H.-G. Schmidt for their kind help in X-ray crystallographic studies. I express my sincere thanks to Prof. Dr. V. Chandrasekhar, IIT Kanpur and Prof. Dr. Narayan S. Hosmane, Northern Illinois University, Dekalb USA for sharing their ideas with me during their stay in Göttingen. I thank Mr. W. Zolke, Mr. J. Schöne, Dr. G. Elter (NMR studies), Dr. D. Böhler, Mr. T. Schuchhardt (mass spectral measurements), Mr. Mathias Hesse, Mr. H.-J. Feine (IR spectral measurements), Mr. J. Schimkowiak, Mr. M. Schlote, Frau H. Tappe and the staff of analytical division for their timely help.

I thank all my colleagues for creating a lively work atmosphere and for having good rapport with me. I am grateful to Dr. Shravan Kumar, Dr. D. Neculai, Dr. A. M. Neculai, Dr. M. Schiefer, Dr. A. Stasch, Dr. M. Gorol, Dr. S. Nagendran, Dr. G. Bai, Dr. P. Lobinger, Dr. Jansen, Dr. Y. Peng, Dr. J. Chai, Dr. Ahn, Mr. T. Blunck, Mr. L. Pineda, Mr. U. Nehete, Mr. Guru Basvaraja, Miss. Kerstin, Mr. N. Sharanappa, Dr. He, Dr. So, Mr. Christian Ene and Dr. Zhu for providing friendly

work atmosphere. I thank Dr. Ostwald for his timely assistance in computer related work. I thank my sisters Bindu, and Nisha, my brother Anil, my nephew Yash and my friends Ravi Chandra Diwedi, Ganna Lyashenko, Sunil Jagtap and Dheeraj Jain for their motivation and support in accomplishing this work.

The financial support from the Göttinger Akademie der Wissenschaften and the Deutsche Forschungsgemeinschaft is gratefully acknowledged. My special thanks to the Graduiertenkolleg (GRK782) Spektroskopie und Dynamik molekularer Aggregate, Ketten und Knäuel and to Prof. Martin Suhm for a graduate student fellowship.

1. Introduction	1
1.1. β-Diketiminato ligands	1
1.2. Group 13 chlorides	3
1.3. Group 13 fluorides and hydrides	4
1.4. Organoaluminum hydroxides	7
1.5. Organogallium hydroxides	11
1.6. Homo- and heterometallic oxides containing aluminum	12
1.7. Heterometallic oxides containing gallium	15
1.8. N-Heterocyclic carbene complexes of gold(I)	17
1.9. Aim and scope of the present work.....	19
 2. Results and Discussion	 20
2.1. Compounds containing Group 13 element-halogen bonds	20
2.1.1. Reaction of $LLi \cdot OEt_2$ with $MeMCl_2$ ($M = Al$ (1), Ga (2), In (3)).....	20
2.1.2. Molecular crystal structures of $LM(Me)Cl$ ($M = Al$ (1), Ga (2), In (3)).....	21
2.1.3. Reaction of $LAl(Me)Cl$ (1) with Me_3SnF and X-ray crystal structural characterization of $LAl(Me)F$ (4).....	25
2.1.4. Reaction of $LAlH_2$ with $BF_3 \cdot OEt_2$ and X-ray crystal structure of $LAlF_2$ (5).....	27
2.1.5. Reduction of $LGa(Me)Cl$ (2) with $LiBEt_3H$ and X-ray crystal structure of $LGa(Me)H$ (6)	28
 2.2. Hydrolysis of $LAl(Me)Cl$ (1), $LGa(Me)Cl$ (2) in the presence of N-heterocyclic carbene as HCl scavenger	 31
2.2.1. Hydrolysis of $LAl(Me)Cl$ (1) and molecular crystal structure of $LAl(Me)OH$ (7)	31
2.2.2. Hydrolysis of $LGa(Me)Cl$ (2) and molecular crystal structure of $LGa(Me)OH$ (8)	34
2.2.3. The OH functional group of $LAl(Me)OH$ (7) and $LGa(Me)OH$ (8)	37

2.3. Reactions of LAl(Me)OH; syntheses of homo- and heterobimetallic oxides	38
2.3.1. Reaction of LAl(Me)OH (7) with AlH ₃ ·NMe ₃ and GaH ₃ ·NMe ₃	38
2.3.2. Reaction of LAl(Me)OH (7) with Sb(NMe ₂) ₃	43
2.3.3. Reaction of LAl(Me)OH (7) with Sn[N(SiMe ₃) ₂] ₂	45
2.3.4. Lithiation of LAl(Me)OH (7) and X-ray crystal structure of [LAl(Me)OLi] ₃ (14).....	46
2.4. Reaction of LGa(Me)OH; syntheses of heterobimetallic derivatives	50
2.4.1. Lithiation of LGa(Me)OH (8) and X-ray crystal structure of [LGa(Me)OLi] ₃ (15)	50
2.4.2. Reaction of LGa(Me)OH (8) with Cp ₂ ZrMe ₂	52
2.4.3. Reaction of LGa(Me)OH (8) with Cp ₃ Ln (Ln = Sm (17), Nd (18), Yb (19)).....	54
2.4.4. Molecular crystal structure of LGa(Me)(μ-OH)Ln Cp ₃ (Ln = Sm (17), Nd (18))...	55
2.5. N-Heterocyclic carbene complexes of gold(I).....	58
2.5.1. Synthesis and X-ray crystal structure of C _{tBu} AuCl (20) and C _{MeS} AuCl (21).....	58
2.5.2. Preparation of C _{tBu} AuC≡CH (22) and C _{MeS} AuC≡CH (23) and molecular crystal structure of C _{tBu} AuC≡CH (22)	64
3. Summary And Future Directions	68
3.1. Summary	68
3.2. Future directions	74
4. Experimental Section	75
4.1. General procedure.....	75
4.2. Physical measurements	75
4.3. Starting materials	76
4.4. Synthesis of compounds 1–23	77
4.4.1. Synthesis of LAl(Me)Cl (1).....	77

4.4.2.	Synthesis of $LGa(Me)Cl$ (2).....	78
4.4.3.	Synthesis of $LIn(Me)Cl$ (3)	78
4.4.4.	Synthesis of $LAl(Me)F$ (4)	79
4.4.5.	Synthesis of $LAlF_2$ (5).....	80
4.4.6.	Synthesis of $LGa(Me)H$ (6)	80
4.4.7.	Synthesis of $LAl(Me)OH$ (7).....	81
4.4.8.	Synthesis of $LGa(Me)OH$ (8).....	82
4.4.9.	Synthesis of $[LAl(Me)(\mu-O)AlH_2]_2$ (9)	82
4.4.10.	Synthesis of $[LAl(Me)(\mu-O)GaH_2]_2$ (10).....	83
4.4.11.	Synthesis of $[LAl(Me)(\mu-O)]_2SbNMe_2$ (11)	84
4.4.12.	Synthesis of $[LAl(Me)(\mu-O)]Sn\{N(SiMe_3)_2\}$ (12)	85
4.4.13.	Synthesis of $[LAl(Me)(\mu-O)]_2Sn$ (13)	85
4.4.14.	Synthesis of $[LAl(Me)OLi]_3$ (14)	86
4.4.15.	Synthesis of $[LGa(Me)OLi]_3$ (15).....	86
4.4.16.	Synthesis of $LGa(Me)(\mu-O)Zr(Me)Cp_2$ (16)	87
4.4.17.	Synthesis of $LGa(Me)(\mu-OH)SmCp_3$ (17)	88
4.4.18.	Synthesis of $LGa(Me)(\mu-OH)NdCp_3$ (18).....	88
4.4.19.	Synthesis of $LGa(Me)(\mu-OH)YbCp_3$ (19)	89
4.4.20.	Synthesis of $C_{tBu}AuCl$ (20).....	89
4.4.21.	Synthesis of $C_{Mes}AuCl$ (21).....	90
4.4.22.	Synthesis of $C_{tBu}AuC\equiv CH$ (22).....	91
4.4.23.	Synthesis of $C_{Mes}AuC\equiv CH$ (23).....	91
5.	Handling and Disposal of Solvents and Residual Waste	93
6.	Crystal Data and Refinement Details	94
7.	References	113

List of Publications

Lebenslauf

Abbreviations

δ	chemical shift
λ	wavelength
μ	bridging
$\tilde{\nu}$	wave number
Ar	aryl
av	average
b	broad
<i>t</i> Bu	<i>tert</i> -butyl
C	Celsius
calcd.	calculated
C _{Mes}	1,3-di-mesitylimidazolyl carbene
Cp	cyclopentadienyl
Cp*	pentamethylcyclopentadienyl
C _{<i>t</i>Bu}	1,3-di- <i>tert</i> -butylimidazolyl carbene
d	doublet
decomp.	decomposition
EI	electron impact ionization
Et	ethyl
eqv.	equivalents
eV	electron volt
g	grams, gaseous
h	hours
Hz	Hertz
<i>i</i> Pr	<i>iso</i> -propyl
IR	infrared
<i>J</i>	coupling constant
K	Kelvin
L	ligand
M	metal
m	multiplet
<i>m/z</i>	mass/charge

Mp	melting point
M^+	molecular ion
Me	methyl
Mes	mesityl
min.	minutes
MS	mass spectrometry, mass spectra
NMR	nuclear magnetic resonance
ppm	parts per million
q	quartet
R, R', R''	organic substituents
s	singlet
sept	septet
st	strong
t	triplet
THF	tetrahydrofuran
TMS	tetramethylsilane
V	volume
w	weak
Z	number of molecules in the unit cell

1. Introduction

This section of the thesis gives the background and an overview of the area in several sections before the present work is presented.

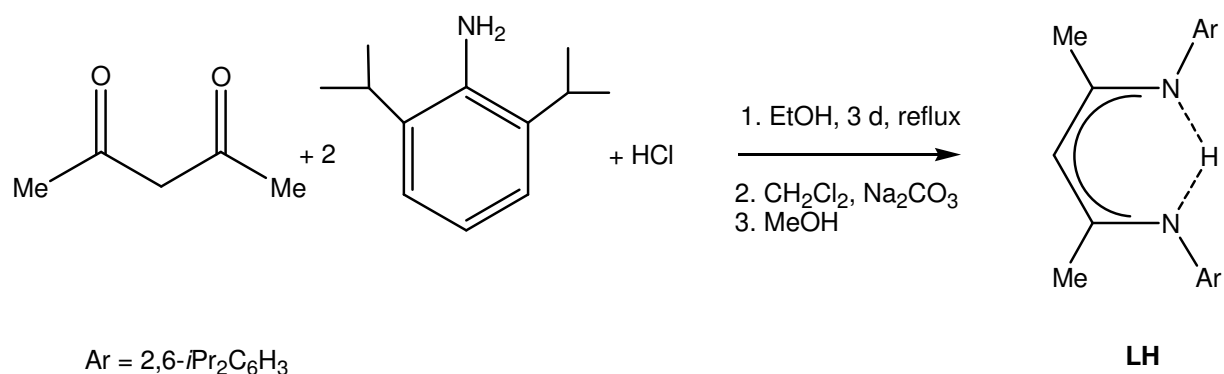
1.1. β -Diketiminato ligands

The first complexes of β -diketiminato ligands were prepared in the mid to late 1960's as homoleptic complexes of Co, Ni, Cu, and Zn.^[1-14] They contain two different bonding modes of the ligands, one with $RN-C(R')-C(R'')-C(R')-NR$ acyclic arrangement ($R = H$, alkyl, aryl, $R' = H$, alkyl and $R'' = H$ or Me)^[2,3,5,7-9,12-14] and the other is comprised of two pyrrol rings bridged in position 2 by a CH moiety.^[8,10,11] The major breakthrough in this area was achieved in the mid 1990's, when β -diketiminato ligands were used as *spectator* ligands, thus offering strong metal–ligand bonds like cyclopentadienyls. In contrast to the latter, β -diketiminato ligands offer a possibility of subtle tuning of their electronic and steric properties by simple variation of the substituents on nitrogen and adjacent carbon atoms. When R is small moiety such as H , Me or the $SiMe_3$, the substance easily forms dimer and allows higher coordination to the metal center, whereas bulky aryl groups on nitrogen usually leads to the isolation of monomeric species with low coordination numbers at the metal. To date, there are numerous reports on a wide variety of these ligands and their complexes with almost all elements across the periodic table, that have found application in catalysis (e.g. Cr ,^[15-18] Mg ,^[19] Ni ,^[20] Pd ,^[20] Ti ,^[21] V ,^[22] Zn ,^[19] and Zr ^[23]) and as models in bioinorganic chemistry (Cu),^[24,25] or are interesting compounds in terms of reaction chemistry (e.g. Al ,^[26,27] Fe ,^[28,29] Ga ,^[30] Ge ,^[31,32] and Zn ^[33]).

The N -aryl substituted ligands $[HN(Ar)C(Me)CHC(Me)N(Ar)]$ ^[34,35] (L) and $[HN(Ar)C(*i*Bu)CHC(*i*Bu)N(Ar)]$ (L') ($Ar = 2,6\text{-}iPr_2C_6H_3$) when coordinate with the appropriate metal fragments the newly formed ring would be delocalized in two different ways, $(Ar)N=C(Me)-CH=C(Me)-N(Ar)^- \leftrightarrow (Ar)N=C(Me)-CH^--C(Me)=N(Ar)$. Additionally, the

ligands L and L' are also useful in stabilization of low coordination numbers of electropositive elements such as Mg^{2+} in $\text{L}'\text{MgMe}$ ^[36] and Fe^{2+} in $\text{L}'\text{FeCl}$.^[28] Other unprecedented examples include the monomeric LAl containing aluminum in the oxidation state +I, that is rare,^[27] and stable Ge^{2+} hydride LGeH ,^[37] the selenols LAl(SeH)_2 , $[\text{LAl(SeH)}]_2\text{Se}$,^[26] and the terminal hydroxide of aluminum LAl(OH)_2 .^[38]

The recent resurgence of β -diketiminato ligands prompted us to investigate such ligands closely. Currently, there are various routes to obtain β -diketiminato ligands starting from metal alkyls and 2 eqv. of a nitrile or acylamide directly leading to metal complexes (Al, Li).^[14,39,40] The ligand, L can be prepared most effectively by the method of Feldman and co-workers following the route as shown in Scheme 1. It involves the direct condensation of 2,4-pentanedione, 2,6-di-*iso*-propylaniline, in the presence of HCl in boiling ethanol and subsequent neutralization of the ligand hydrochloride with Na_2CO_3 to yield free ligand (Scheme 1).^[34,35] Work described in this thesis will also include areas pertaining to related topics.



Scheme 1. Synthesis of a sterically encumbered β -diketiminato ligand

1.2. Group 13 chlorides

Inorganic mono- and trihalides are known for all Group 13 metals.^[41] The trihalides form a large number of addition compounds, especially those of aluminum are applicable in Friedel–Crafts catalysis,^[42] useful in transhalogen reaction to convert non-metal fluorides to the corresponding chlorides.^[43] The nature of formation of addition compounds (e.g, MX_3L , MX_3L_2 , MX_3L_3) depends on the relative influence of the underlying d^{10} electron configuration and also on the atom coordinated to the metal ($\text{L} = \text{Py}$, Me_2S , MeCO_2Et , PR_3 etc.).

A number of M(III) derivatives with the β -diketiminate ligand L have been previously reported and structurally characterized [$\text{L} = \text{HC}\{(\text{CMe})(2,6\text{-}i\text{Pr}_2\text{C}_6\text{H}_3\text{N})\}_2$]. These include the cation $[\text{LAlMe}]^+$,^[44] the dimethyl derivatives LMMe_2 ,^[44,45] the dichlorides LMCl_2 and the diiodides LMI_2 ($\text{M} = \text{Al}$, Ga , or In).^[46] Synthesis of LAlMe_2 was reported by Smith et al. whereas other complexes were reported by Power and co-workers. Preparation of LMCl_2 was accomplished by the reaction of $\text{LLi}\cdot\text{OEt}_2$ with MCl_3 . While the reaction of GaI with $\text{LLi}\cdot\text{OEt}_2$ yields LGaI_2 and LGa , whereas LInI_2 was prepared by the reaction of $\text{LLi}\cdot\text{OEt}_2$ with InI_3 . The LInCl_2 when treated with 2 eqv. of MeMgBr led to the formation of the indiumdimethyl, LInMe_2 .^[46] It is noticeable that all these complexes have symmetrical substituents around the metal atom. Presently, there is a growing interest in the chemistry of such complexes where the metal atom has at least two different substituents.

Based on long sustained interest in the synthesis of β -diketiminate complexes of Group 13 metals the Roesky group has contributed to a whole new range of novel species. While some of these are useful as catalysts,^[47,48] those with the metal in low oxidation state are also synthetically useful.^[27] Recently, the sterically encumbered neutral LAl(Me)Cl , which can be utilized as a starting material for the synthesis of the monohydroxide LAl(Me)OH , has been reported.^[49] This product can act as a synthon to assemble a range of homo- and heterobimetallic derivatives of

which some have found applications in ethylene polymerization^[47,50] and polymerization of ϵ -caprolactone.^[48] Therefore, it was our primary interest to prepare other derivatives of $\text{LAl}(\text{Me})\text{Cl}$ where the Al atom will have at least two different substituents, and also to extend it to the higher congeners of Group 13 elements.

1.3. Group 13 fluorides and hydrides

Group 13 fluorides

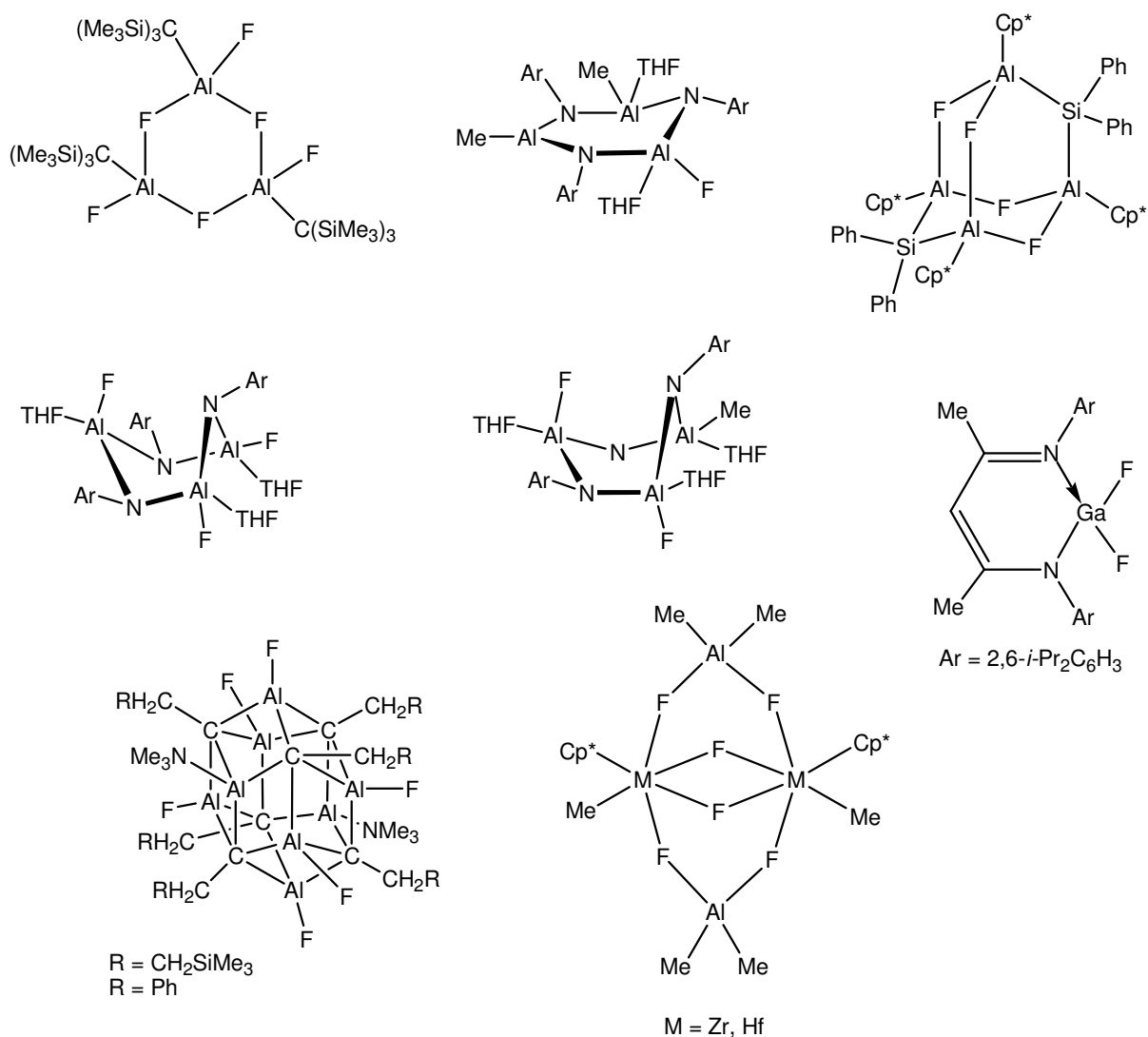
Organoaluminum fluorides constitute an interesting class of compounds applicable as catalyst activators for the metallocene halides and alkyls in homogeneous single-site polymerization catalysis.^[51-53] AlF_3 is one of the most stable substance whereas the organoaluminum fluorides contain very strong and highly polar Al–F bonds. They are also more covalent with weaker Al–C bond.^[54] Due to this behaviour they are widely employed as intermediates in the synthesis of trialkylalanes by Ziegler in his catalytic system for olefin polymerization.^[55] At present a wide variety of fluorinating agents is available. For example, $\text{BF}_3 \cdot \text{OEt}_2$, $\text{HBF}_4 \cdot \text{OEt}_2$, Me_3SnF , alkali-metal fluorides, ammonium fluorides, Olah's reagent etc. and a diverse range of organoaluminum fluorides are available.^[54,56,57] Roesky and co-workers have contributed to the preparation of main group and Groups 4-6 fluorides from their corresponding chlorides using trimethyltin fluoride as a fluorinating agent.^[54,56,57] Examples include *tris*(trimethylsilyl)methyl aluminum difluoride, functionalization of hydrides on the carbaalane cluster and many others (see Chart 1).^[52-54,57-60]

Almost all the chloride and iodide complexes of Group 13 elements supported by the β -diketiminato ligand have been synthesized and structurally characterized.^[40] Although no fluorides of aluminum have been reported, few β -diketiminato boron fluorides of the formula

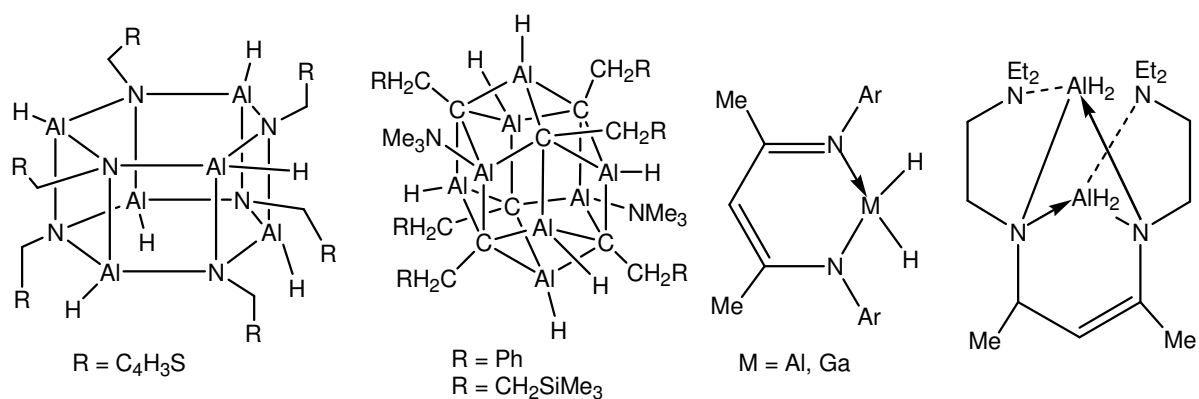
$[\text{HC}\{(\text{CMe})\text{RN}\}_2]\text{BF}_2$ ($\text{R} = \text{Me}, \text{Et}, n\text{Pr}, \text{C}_3\text{H}_5$)^[61,62] and only one gallium difluoride^[60] have been synthesized (Chart 1).

Group 13 Hydrides

Covalent chemistry of boron hydrides has been more extensively studied than the heavier elements of Group 13. Hydrides of Al (alanes) are easily accessible and more tractable among Group 13 metals.^[63-66] Simple hydrides of Group 13 metals in the form MH_3 , $\text{MH}_3 \cdot \text{NMe}_3$, LiMH_4 , are known for a long time.^[66,67] The recently isolated aluminum trihydride complex stabilized by *N*-heterocyclic carbenes or Arduengo–Carbene, add to new examples in this class of compounds.^[68] The trimethylamine adducts are crystalline solids and the metal atom adopts a five-coordinate trigonal bipyramidal structure.^[69,70] These have been utilized as reducing agent in a wide range of inorganic and organic transformations as well as precursor in chemical vapour deposition technique to generate highly active surface layers and conductors.^[71] In addition, they are excellent precursor in the synthesis of alumoxanes, galloxanes *via* the controlled hydrolysis,^[72] carbaalane clusters using acetylenes / substituted acetylenes,^[73,74] and amidoalanes clusters with organic nitriles.^[75] Subsequently, Roesky et al. isolated the first β -diketimate aluminum dihydride which has been a very versatile synthon in the synthesis of aluminumdithiol,^[76] aluminumdiselenol,^[26] pentacoordinated *tert*-butylperoxo aluminum compound,^[77] and planar dimeric six-membered spirane aluminum hydrazide.^[78] In order to investigate similar reaction chemistry with the corresponding gallium analogue Roesky et al. isolated the first β -diketimate galliumdihydride complex LGaH_2 ^[60] by reacting LGaI_2 with 2 eqv. of $\text{LiH} \cdot \text{BEt}_3$ (Chart 1). Representative examples of organometallic hydrides of aluminum and gallium supported by non β -diketimate ligands are shown in Chart 1.^[60,79]



Organoaluminum and gallium fluorides



Organoaluminum and gallium hydrides

Chart 1

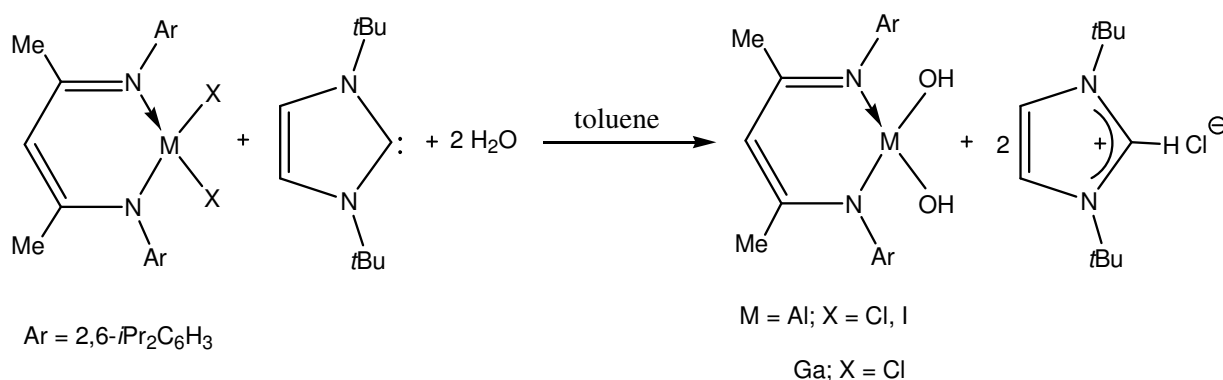
1.4. Organoaluminum hydroxides

The successful assembly of $[(2,6\text{-}i\text{Pr}_2\text{C}_6\text{H}_3)(\text{SiMe}_3)\text{NSi}(\text{OH})_3]$, $[(\text{Me}_3\text{Si})_2\text{CHSi}((\mu\text{-O})(\text{OH}))_3]$ ^[80,81] and $[(\text{Me}_3\text{Si})_3\text{CSn}((\mu\text{-O})(\text{OH}))_3]$ ^[82] prompted Roesky et al. to synthesize compounds containing Al–OH bonds from the controlled hydrolysis of alkyl- and arylaluminum compounds.^[83] This approach was possible due to the lability of the Al–C bond. The second motivation for the hydrolysis route arises from the discovery of Sinn and Kaminsky that the partial hydrolysis product of trimethyl aluminum *viz.*, methylalumoxane (MAO) was an extremely potent co-catalyst in the polymerization of ethylene and propylene.^[84,85] In order to explore the structure of MAO, Barron and co-workers had carried out numerous studies on the partial hydrolysis of alkylaluminum compounds such as $t\text{Bu}_3\text{Al}$. Many interesting products were isolated in these reactions and some of them such as $[t\text{Bu}_2\text{Al}(\mu\text{-OH})]_3$ could be thermolyzed to polyhedral alumoxane cages.^[86] A systematic study on the hydrolysis of $(\text{Me}_3\text{Si})_3\text{CMMe}_2$ ^[87] and Me_3M ^[88] (M = Al, Ga) was carried out by Roesky et al. in order to isolate hydroxylated aluminum (gallium, indium) compounds. Representative examples of these hydroxylated products are shown in Chart 2. Other examples include tetrameric $[(\text{Ph}_2\text{Si})_2\text{O}_3\text{Al}(\mu\text{-OH})]_4$ ^[89] and the $[\text{Al}_5(t\text{Bu})_5((\mu_3\text{-O})_2(\mu_3\text{-OH})_2(\mu\text{-OH})_2(\mu\text{-O}_2\text{CPh})_2)]$ ^[90] complexes. Although successful, the hydrolysis route has some drawbacks. (1) As can be seen from Chart 2, almost all the products contain $\mu\text{-OH}$ groups; preparation of terminal hydroxides by hydrolysis of alkyl- and arylaluminum (gallium and indium) compounds is synthetically formidable. (2) Control of the number of hydroxyl groups in the eventual products of hydrolysis of alkyl- and arylaluminum compounds appears to be difficult. Thus, preparation of *simple* hydroxides of the type $\text{L}_2\text{Al}(\text{OH})$ and $\text{LAl}(\text{OH})_2$ requires a paradigm change in the synthetic strategy.

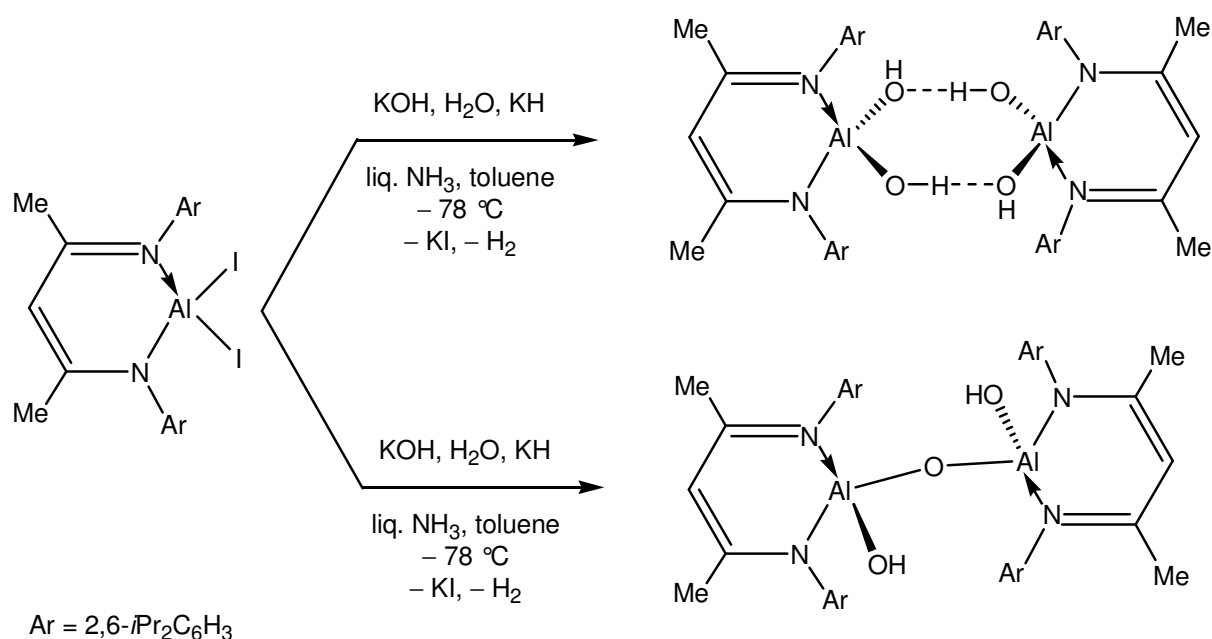


To overcome the principal synthetic challenges in preparing a molecular lipophilic terminal hydroxide of aluminum the following strategies can be adopted. (a) Prevention of condensation reactions which can lead to Al–O–Al bonds, (b) tuning the reactivity of the Al–OH groups so that they do not react (during the process of their synthesis) in an intra or intermolecular manner with other organic groups present on the aluminum center, and (c) designing substituents on aluminum that would be inert themselves, while allowing lipophilicity and preventing self-condensation that would not impede the reactivity of the hydroxyl groups entirely. The latter factor is also quite important since soluble aluminum hydroxides would be good starting materials for the preparation of a number of Al–O–M derivatives.

Based on the factors, as discussed above, Roesky and co-workers have recently reported terminal hydroxides of aluminum $\text{LAl}(\text{OH})_2$,^[38] $[\text{LAl}(\text{OH})]_2(\mu\text{-O})$ ^[91] and gallium $\text{LGa}(\text{OH})_2$.^[92] The latter was synthesized by the hydrolysis of LGaCl_2 in the presence of *N*-heterocyclic carbene as HCl acceptor, while the former was prepared with the same method as well as by the hydrolysis of LAlI_2 in liq. NH_3 /toluene two phase system in the presence of KH and KOH as outlined in Schemes 2 and 3, respectively.

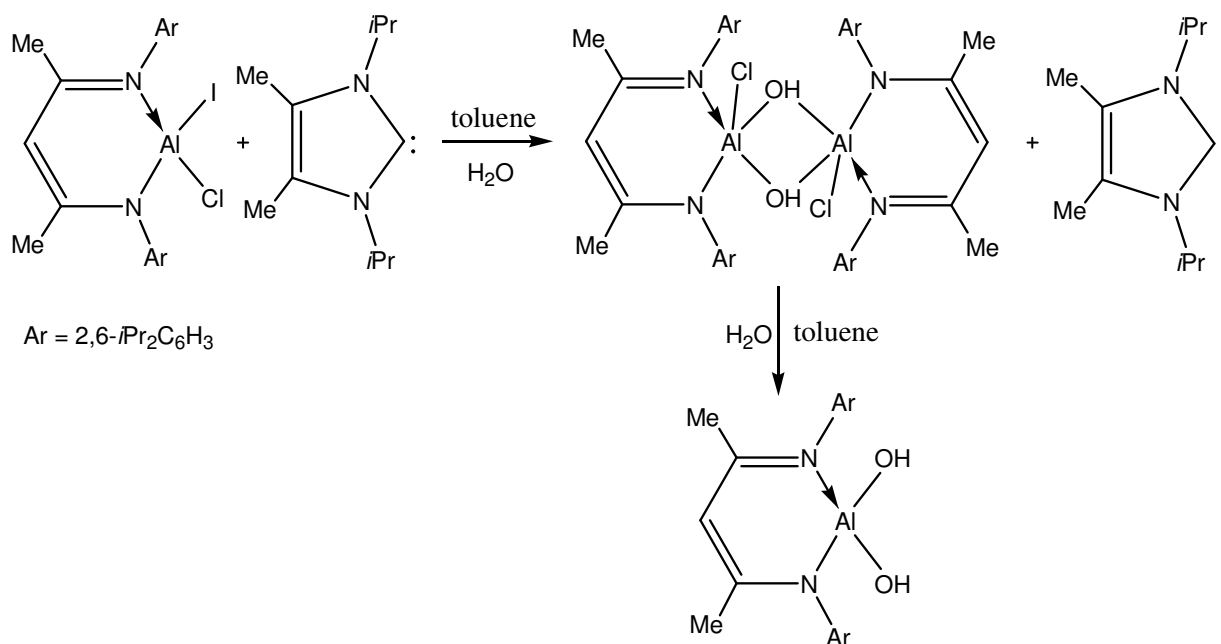


Scheme 2. Synthesis of aluminum and gallium dihydroxide



Scheme 3. Synthesis of aluminum hydroxide and alumoxane hydroxide

Scheme 4 depicts the stepwise hydrolysis of aluminum chloriodide in the presence of *N*-heterocyclic carbene. In this case the more labile Al–I bond is hydrolyzed preferentially to Al–Cl bond that leads to the formation of aluminum chlorohydroxide [LAl(Cl)OH]₂. The next step of hydrolysis generates aluminum dihydroxide LAl(OH)₂.^[49]



Scheme 4. Stepwise hydrolysis of aluminum chloriodide

1.5. Organogallium hydroxides

Presently, a wide range of terminal to bridging and from monomeric to oligomeric hydroxides of aluminum have been synthesized and structurally characterized.^[38,49,83-85,87-91] However, only a few hydroxides of gallium containing terminal –OH groups have been reported. In 1994 Atwood et al. reported the preparation of the first gallium dihydroxide stabilized by a bulky pincer type ligand, $\{[2,6-(\text{Me}_2\text{NCH}_2)\text{C}_6\text{H}_3]\text{Ga}(\text{OH})_2\}_3 \cdot 10\text{H}_2\text{O}$ (Chart 2), from the corresponding dihydride and water.^[93] Other examples of gallium hydroxide containing bridging and terminal OH groups have also been described. The compounds $[\text{R}_2\text{Ga}(\mu\text{-OH})]_2$ ($\text{R} = \text{Mes}$,^[28] $i\text{Pr}$,^[94] $(\text{Me}_3\text{Si})_2\text{CH}$),^[95] and $[\text{RR}'\text{Ga}(\mu\text{-OH})]_3$ ($\text{R} = \text{R}' = t\text{Bu}$,^[96,97] $\text{R} = \text{R}' = \text{Ph}$,^[98] $\text{R} = (\text{Me}_3\text{Si})_3\text{C}$ $\text{R}' = \text{Me}$ ^[87]) are representatives of bridged hydroxides, whereas $[(t\text{Bu}_3\text{Si})\text{Ga}(\text{OH})(\mu\text{-OH})]_4$ ^[99] contains both, bridging and terminal OH groups, respectively (Chart 2). The previously reported monohydroxides of gallium include hydroxygallium phthalocyanine,^[100] $(2,6\text{-Mes}_2\text{C}_6\text{H}_3)_2\text{GaOH}$ ^[101] and others contain hydroxy-bridged $[2,6\text{-Mes}_2\text{C}_6\text{H}_3\text{GaMe}(\mu\text{-OH})]_2$,^[101] and $[\text{Ga}(\text{OH})(\text{SO}_4)(\text{terpy})(\text{H}_2\text{O})] \cdot \text{H}_2\text{O}$.^[102] The continuous interest in Roesky's group has been the synthesis of Group 13 hydroxides containing a terminal –OH group which resulted in a series of compounds $\text{LAl}(\text{OH})_2$,^[38] $\text{LGa}(\text{OH})_2$,^[92] $\text{LAl}(\text{Me})\text{OH}$ ^[47] and $[\text{LAlOH}]_2(\mu\text{-O})$ ^[91] [$\text{L} = \text{HC}\{(\text{CMe})(2,6\text{-}i\text{Pr}_2\text{C}_6\text{H}_3\text{N})\}_2$]. As in the synthesis of terminal hydroxides of aluminum, a key factor has been the choice of an appropriate ligand environment about the metal atom in addition to the synthetic strategy that allows the product formation in a rational and predictable manner. The β -diketiminato ligand L not only offers steric protection to the metal center but also its chelating ability in forming a stable six-membered ring comprising the metal atom thereby offering the desired kinetic stability to the complexes.^[103]

1.6. Homo- and heterometallic oxides containing aluminum

Homo- and heterometallic compounds containing aluminum are considered important due to their potential application in catalysis and in the synthesis of metal modified zeolites with desirable properties.^[104] Alumoxanes constitute a very important class of homometallic compounds of aluminum primarily due to the discovery of MAO (methyl alumoxane) as an extremely potent co-catalyst for olefin polymerization.^[84,85] Analogous to MAO a number of other derivatives have also been synthesized with other alkyl and aryl groups.^[86-90] These efforts are mainly focused on controlled hydrolysis of aluminum alkyls and aryls. The major problem of this approach as a synthetic tool is the lack of predictability of the product *before* the reaction. The task of assembling gallalumoxanes meets similar synthetic challenges. Nöth and co-workers utilized the reaction of $\text{AlH}_3\cdot\text{NMe}_3$ with various alcohols to prepare alkoxyalanes.^[105] Use of aminoalcohols partially controls the aggregation where the amino group serves as an internal coordinating ligand.^[106] However such an approach was not available to control the composition of alumoxanes. Thus, instead of using Al-H or Al-C bonds as an entry point for the synthesis of Al-O-Al bonds it would be ideal to use organoaluminum hydroxides containing Al-O linkages. Recent isolation of a discrete aluminum dihydroxide $\text{LAl}(\text{OH})_2$ ^[38] and an alumoxane hydroxide (Scheme 3) and the reaction of the former in preparing an alumoxane with a three coordinated aluminum center,^[91] as demonstrated by Roesky and co-workers, prompted us to utilize aluminum monohydroxide $\text{LAl}(\text{Me})\text{OH}$ ^[47,50] to assemble different new kinds of alumoxanes and mixed metal aluminum oxides.^[47,48,105]

For the synthesis of heterometallic compounds of aluminum a variety of approaches are available and aluminum has been combined in the form of organometallic oxides and alkoxides with a range of metals across the periodic table. In the majority of these reactions aluminum alkoxides are involved. However, there is no direct control on metal nuclearity and on the final

composition of the resulting compound. In this part of the introduction, motivation for the syntheses of homometallic alumoxane hydride and its gallium congener, an oxide containing Al–O–Sb moiety, aluminum–tin oxide and a lithium aluminate containing Li–O–Al moiety have been discussed.

Only two compounds have been reported which contain Al and Sb atoms. The first compound is ionic aluminosilsesquioxane with the cation Me_4Sb^+ without any formal Al–O–Sb bonds.^[106] Whereas the second compound is an aluminum–antimony heterodinuclear porphyrin $[(\text{oep})(\text{Me})(\text{Sb–O–Al})(\text{oep})]\text{ClO}_4$ which was synthesized by the very sluggish reaction of $[(\text{oep})(\text{Me})\text{Sb}(\text{OH})]\text{ClO}_4$ with $(\text{oep})\text{AlMe}$ in only 7 % yield.^[107] Some aluminum compounds containing tin are known especially when tin is in its oxidation state (IV).^[108,109] However, only few tin(II) compounds with aluminum are reported. Heterobimetallic compounds of Al and Sn(II) reported earlier are the only bimetallic isopropoxides, e.g., $\text{Sn}[\text{Al}(\text{O-}i\text{Pr})_4]_2$ is prepared by the reaction of $\text{K}[\text{Al}(\text{O-}i\text{Pr})_4]$ with SnCl_2 in isopropanol.^[110] An alcohol metathesis technique leads to the formation of other bimetallic alkoxides. Reactions of $\text{Sn}[\text{Al}(\text{O-}i\text{Pr})_4]_2$ with acetylacetone (Hacac) give $\text{Sn}[\text{Al}(\text{O-}i\text{Pr})_2(\text{acac})_2]_2$ and $\text{Sn}[\text{Al}(\text{acac})_4]_2$, with alcohols ROH they give $\text{Sn}[\text{Al}(\text{OR})_4]_2$ (R = Me, Et, CH_2CF_3 , $\text{CH}(\text{CH}_2\text{Cl})_2$).^[110] The compound $\text{ClSn}\{\text{Al}(\text{O-}i\text{Pr})_4\}$ was prepared by the reaction of $\text{K}[\text{Al}(\text{O-}i\text{Pr})_4]$ with SnCl_2 in 1:1 molar ratio.^[111] Similarly, heteroleptic glycolates of tin(II) with Al were also reported.^[112] The only structurally characterized mixed Al and Sn(II) alkoxide chloride is $(t\text{BuO})_4\text{AlSnCl}$ prepared by the reaction of $\text{NaAl}(\text{O-}t\text{Bu})_4$ and SnCl_2 which is monomeric with the central AlO_2Sn four-membered ring. The corresponding $\text{NaAl}(\text{O-}i\text{Pr})_4$ derivative reacts with SnCl_2 to yield a coordination polymer $(i\text{PrO})_4\text{AlSn}_2\text{Cl}_3$ incorporating a trigonal bipyramidal Sn_2Cl_3^+ cation. When $(i\text{PrO})_4\text{AlSn}_2\text{Cl}_3$ reacts with moisture it leads to the formation of $[(i\text{PrO})_5\text{Cl}_2\text{Al}_2]_2\text{O}_2\text{Sn}_4\text{Cl}_2$ which has a central $\text{O}_2\text{Sn}_4\text{Cl}_2$ cluster with four-coordinated η^4 -bridging Cl atoms.^[113]

A number of lithium aluminates have been reported and structurally characterized. However, the majority of these contain the oxygen atom as alkoxide rather than oxide, and lithium atoms have the coordination number higher than two and are often coordinated to *N*-donor ligands e.g., pyridine,^[114] amines^[114] or amino alcohols^[115] or methylthio ethanol^[116] apart from O-coordinating sites. Chelated anionic aluminates, reported by Atwood and Hill, fall in this category.^[117] Nöth and co-workers prepared a new class of organyloxyhydridoaluminates by the reaction of lithium aluminum hydride with alcohols and phenols in ether solvents.^[118,119] These exist as mono-, di- and triorganyloxyhydridoaluminates $\text{MAIH}_{4-n}(\text{OR})_n$. Both Al–H–Li and Al–Li–O bridges were found for lithium cation. The stability of these compounds towards disproportionation strongly depends on the steric demand of the organic group and the solvent. Thus, $\text{LiAlH}_3(\text{OR})$ was stable only with $\text{R} = 2,6\text{-}i\text{Bu}_2\text{C}_6\text{H}_3$. The $\text{LiAlH}_2(\text{OR})_2$ was isolated when $\text{R} = i\text{Bu}_2\text{MeC}$ and $2,6\text{-}i\text{Bu}_2\text{C}_6\text{H}_3$. The triorganyloxyhydridoaluminates are the most stable compounds in the series and were isolated with $\text{R} = i\text{Bu}_2\text{MeC}$, Ph_3C and $2,6\text{-}i\text{Pr}_2\text{C}_6\text{H}_3$.^[118]

The lithium aluminates which are monomeric to trimeric and the oxygen atom present as an oxide ions comprising $[\text{Me}_2\text{AlN}(2\text{-C}_5\text{H}_4\text{NPh})_2(\text{O})\text{Li}_2 \cdot 2 \text{ THF}]$. This species can be synthesized by the oxygenation of $\text{Me}_2\text{Al}[\text{N}(\text{SiMe}_3)_2][\text{N}(2\text{-C}_5\text{H}_4\text{NPh})\text{Li}]$ in THF. This molecule has a butterfly-type Al_2Li_2 bimetallic core that stabilizes discrete, molecular lithium oxide.^[120] Roesky et al. reported the synthesis of monolithium salt of the trimesitylaluminum water adduct i.e., $[\text{Mes}_3\text{Al}(\mu\text{-OHLi})] \cdot 3 \text{ THF}$ and further deprotonation with $n\text{BuLi}$ affords $[\text{Mes}_2\text{Al}(\mu\text{-OLi})]_2 \cdot 4 \text{ THF}$.^[88]

1.7. Heterometallic oxides containing gallium

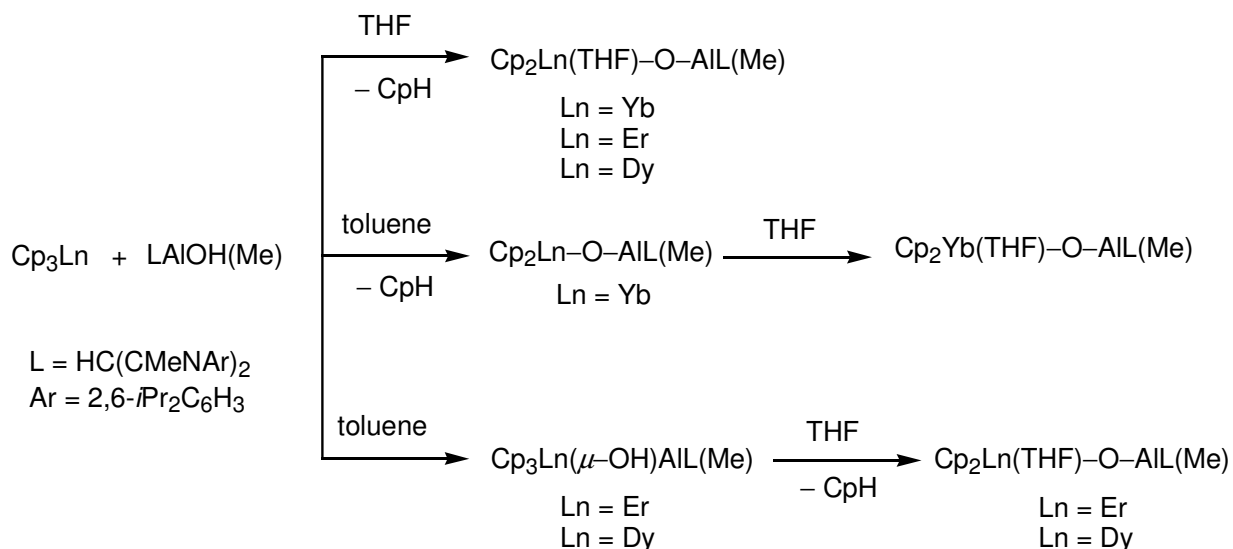
This section of the introduction gives an overview of the literature pertaining to the heterobimetallic compounds of gallium containing any of the following elements: lithium, zirconium, samarium, neodymium, and ytterbium where oxygen atom serves as a linker between two metal atoms.

Continued interest of Roesky group towards the synthesis of mixed metallic Group 13 element and lithium compound led to the discovery of $[\text{Mes}_3\text{Ga}(\mu\text{-OHLi})] \cdot 3 \text{ THF}$ by the treatment of Mes_3Ga with LiOH . When the complex $[\text{Mes}_3\text{Ga}(\mu\text{-OHLi})] \cdot 3 \text{ THF}$ was deprotonated with $n\text{BuLi}$ it generates the lithiumgallate $[\text{Mes}_2\text{Ga}(\mu\text{-OLi})]_2 \cdot 4 \text{ THF}$.^[88] Treatment of $[\text{Ga}_2(t\text{Bu})_4(\text{neol-H})_2]$ with LiOH in Et_2O results in the formation of the trimeric species $[\text{Ga}_3\text{Li}_4(t\text{Bu})_6(\text{neol})_3(\text{OH})(\text{THF})]$ (neol = 2,2-dimethylpropane-1,3-diol). This trimer consists of a $\text{Ga}_3\text{O}_6\text{C}_9$ macrocyclic core encompassing four lithium atoms in turn capped by a hydroxide group. However, when the same reaction was carried out in *n*hexane it led to the formation of $[\text{Ga}_2\text{Li}(t\text{Bu})_4(\text{OH})_2(\text{neol-H})]$. The core of this molecule consists of a Ga_2LiO_3 cycle where the Li atom is chelated by the neol-H ligand.^[121] Another lithium gallate was prepared by the reaction of two eqv. of 2,4,6-*tris*((dimethylamino)methyl)phenoxy lithium (Ar^nOLi) with GaCl_3 to yield $[(\text{Ar}^n\text{O})_2\text{GaCl}_2]\text{Li}$.^[122] The $\{\text{Li}(\text{THF})\}_2\{\text{Ga}((S)\text{-BINOLate})_3\}$ was prepared by the reaction of $\text{Li}_2(S)\text{-BINOLate}$ with GaCl_3 [$(S)\text{-BINOL}$ = $(S)\text{-}(-)\text{-}2,2'\text{-dihydroxy-1,1'-binaphthyl}$]. The same ligand reacts with $\text{PhCH}_2\text{GaCl}_2$, in THF to afford the gallate $[\{\text{Li}(\text{DME})\}_3\{\text{Ga}((S)\text{-Binolate})_3\}] \cdot 1.5 \text{ THF}$ after recrystallization from DME. In both compounds the oxygen atom bridges between Li and Ga atoms, the Li atom is also coordinated to THF and DME molecules, respectively.^[123] A self assembled dinuclear cryptand of a helicate-type of gallium assisted by a tetraketone ligand exhibits the lithium's binding to oxygen atoms of the cryptand. This cryptand was shown to act as cation (Li^+) receptor on addition of LiClO_4 .^[124] The dimer

$\{[\text{GaI}(\text{C}(\text{SiMe}_3))(\text{OCMe}_3)(\text{OH})]\text{Li}\}_2$ via the Li–O bridges was obtained as a second product in a disproportionation reaction of $\text{Ga}_2\text{I}_2\{\text{C}(\text{SiMe}_3)_3\}_2$ with lithium *tert*-butanolate.^[125]

Reaction of gallium alkoxide with zirconocene complexes of benzynes leads to the formation of the gallium–zirconium heterobimetallic compound $[\text{Me}_2\text{Ga}(\mu\text{-OMe})(\mu\text{-1,2-3-methoxyphenyl})\text{Zr}(\eta^5\text{-C}_5\text{H}_5)_2]$ the only heterobimetallic derivative of gallium–zirconium known without a single crystal X-ray structure.^[126]

Mehrotra and co-workers have reported the double isopropoxide of gallium and lanthanides $[\text{Ln}\{\text{Ga}(\text{O-}i\text{Pr})_4\}_3]$, (Ln = La, Pr, Nd, Sm, Gd, Ho and Er) by the reaction of either lanthanide chlorides with potassium gallium isopropoxides or of lanthanide isopropoxides with gallium isopropoxides. This is the beginning of the new area of research that combines both the main group and the lanthanide atom to constitute a novel class of heterobimetallic species.^[127] Subsequently bimetallic complexes containing Al–O–Ln moieties have been synthesized and their utility in the polymerization of ϵ -caprolactone has been explored.^[48] As shown in Scheme 5, the reaction of $\text{LAl}(\text{Me})\text{OH}$ with a suitable lanthanide precursor leads to the synthesis of aluminum lanthanide mixed oxides. As an extension of this study the reactivity of the corresponding gallium hydroxide $\text{LGa}(\text{Me})\text{OH}$ to assemble similar compounds with lanthanides has been explored.



Scheme 5. Synthesis of aluminum lanthanide mixed oxides

1.8. *N*-Heterocyclic carbene complexes of gold(I)

Recently there has been a resurgence of interest in the chemistry of gold compounds in general and that of gold(I) compounds in particular. A major driving force for this interest has been the utility of soluble gold compounds in various applications ranging from precursor for gold nanoparticles^[128,129] to drugs,^[130] and catalysts.^[131-133] Among Au(I) compounds, there has been considerable success in the preparation of alkynyl gold complexes. These are among the most stable organogold complexes.^[134] Although dinuclear complexes such as $\text{R}_3\text{PAuC}\equiv\text{CAuPR}_3$ have been known for some time,^[135,136] Schmidbaur and co-workers have recently isolated terminal acetylides of gold in the form of gold ethynyl complexes $\text{RAuC}\equiv\text{CH}$ ($\text{R} = \text{MePH}_2, \text{Me}_3\text{P}$).^[137] A key factor in this successful assembly is the utility of appropriate phosphane ligands in stabilizing such compounds. It has also been shown that these compounds can be used as reliable synthons in crystal engineering owing to strong and predictable aurophilic

[Au(I)–Au(I)] interactions.^[138] Another interesting aspect of these complexes has been the ability to exhibit rich photophysical and photochemical behaviour.^[139–142]

One of the key challenges in Au(I) chemistry remains the availability of reasonably stable synthons, which would allow *simple* substitution reactions. The use of sterically hindered *N*–heterocyclic carbenes^[143] for such a purpose was regarded as ideal.^[144,145] Accordingly, a facile one-step, high yield synthesis of a lipophilic gold(I)–*N*–heterocyclic carbene complex C_{*t*}BuAuCl was accomplished. Another motivation was to use such complexes to incorporate other functional groups on gold by simple substitution reaction. In 2005, Baker and co-workers reported the synthesis of C_{*t*}BuAuCl complex by transmetallation of C_{*t*}BuAgCl and (Me₂S)AuCl.^[146]

1.9. Aim and scope of the present work

The Sections 1.2–1.8 describe the importance of aluminum and gallium halides, hydroxides as useful precursor for material science and industry. New synthetic strategies starting from easily accessible precursor such as halides or hydrides leading to these species are therefore warranted. The work described here was aimed at achieving a facile and easy synthetic route for the preparation of terminal mono hydroxides of aluminum and gallium that is supported by the sterically encumbered β -diketiminato ligand and to synthesize novel compounds of gold(I) stabilized by *N*-heterocyclic carbenes. Based on these facts the objectives of the present work are

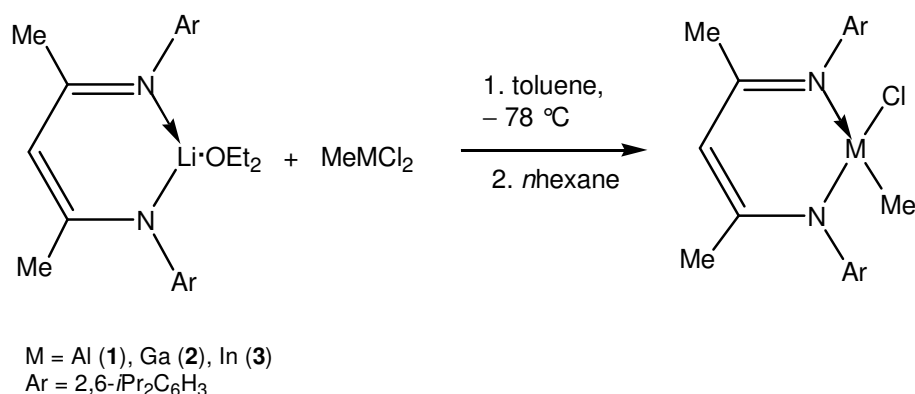
1. to develop new synthetic strategies for the preparation of mononuclear molecular hydroxides of aluminum and gallium supported by sterically encumbered β -diketiminato ligands.
2. to use these species as a synthon to assemble a variety of homo- and heterobimetallic systems of potential application.
3. to use spectral methods such as NMR spectroscopy, IR spectroscopy and X-ray structural analysis to unambiguously characterize the products obtained.
4. to develop a facile route to prepare *N*-heterocyclic carbene complexes of gold(I) chloride and to use it as a starting material in simple substitution reactions to incorporate new functionalities on gold(I).

2. Results and Discussion

2.1. Compounds containing Group 13 element–halogen bonds

2.1.1. Reaction of $LLi \cdot OEt_2$ with $MeMCl_2$ ($M = Al$ (**1**), Ga (**2**), In (**3**))

As reported earlier, the reaction between lithium salt of the β -diketiminato ligand and the metal chlorides leads to a clean reaction under the formation of LiCl as a driving force for the reaction. The formation of a single product was not realized in a reaction of LH with metal hydrides or metal alkyls, rather it leads to the formation of a mixture of products which are difficult to separate due to their similar solubilities in solvents like *n*hexane, *n*pentane, toluene, ether etc. Therefore, the synthesis of $LM(Me)Cl$ ($M = Al$ (**1**), Ga (**2**), In (**3**)) has been accomplished by the reaction of $LLi \cdot OEt_2$ with $MeMCl_2$ (Scheme 6). Compounds **1–3** are examples of novel β -diketiminato metal complexes with metals having two different substituents. Compounds **1–3** have been characterized by means of spectroscopic and spectrometric techniques. Compounds $LaI(Me)Cl$ (**1**), $LGa(Me)Cl$ (**2**), and $LIn(Me)Cl$ (**3**) are thermally stable solids with melting points of 192, 190 and 185 °C respectively, and are sensitive to moisture. 1H NMR of **1** reveals the $Al-Me$ to resonate at -0.65 ppm and two septets at 3.21 and 3.76 ppm, characteristics of an asymmetrically substituted metal center in complexes with β -diketiminato ligand. The corresponding protons of **2** appear at -0.31 ($Ga-Me$) and septets at 3.15 and 3.87 ppm whereas those of **3** appear at -0.28 ($In-Me$) and septets at 3.15 and 3.83 ppm. The most intense peak in the EI-MS spectrum of **1**, **2**, and **3** corresponds to the loss of the Me group from the molecular ion as $[M^+ - Me]$ and were observed at m/z 479, m/z 523 and m/z 567 respectively.



Scheme 6. Preparation of β -diketiminato supported Group 13 methylchlorides

2.1.2. Molecular crystal structures of $LM(\text{Me})\text{Cl}$ ($M = \text{Al (1), Ga (2), In (3)}$)

The unambiguous molecular geometry of **1–3** was determined by X-ray crystallography. Colorless crystals of **1–3** were obtained from *n*hexane solution. The three isostructural compounds crystallize in the monoclinic space group $P2_1/n$. Only one of the four independent molecules existing in an unit cell of complexes **1–3** are shown in Figures 1–3, respectively. The most common feature among the structures is that the four atoms of the C_3N_2 ring C(1), C(3), N(1) and N(2) are almost planar, and the metal lies significantly out of the C_2N_2 plane. The C(2) atom in this case also deviates from the C_2N_2 plane, but the deviation is not so large like in the case of the metal atom. This boat conformation can also be found in many other derivatives of these ligands from Group 13 metals and from elements of different groups of the periodic table. The ring C–C and C–N distances lie within the narrow ranges 1.395–1.410(3) and 1.324–1.347 Å, which are indicative of a considerable multiple bond character. It is noteworthy that within the $\text{C}_3\text{N}_2\text{M}$ ($M = \text{Al (1), Ga (2), In (3)}$) rings the N–M–N angle is invariably the narrowest, smallest for **3**, 90.9(1)°. Complexes **1–3** exist as tetrahedral structures with the metal atoms surrounded by the chlorine atom, methyl group and nitrogen atoms of the chelating β -diketiminato ligand. The

bite angle of the β -diketiminato ligand N(1)–M(1)–N(2) ranges from 97.6(1), 97.1(1) to 90.9(1)° for **1–3** respectively, they are smaller than the regular tetrahedral bond angle of 109.28°.

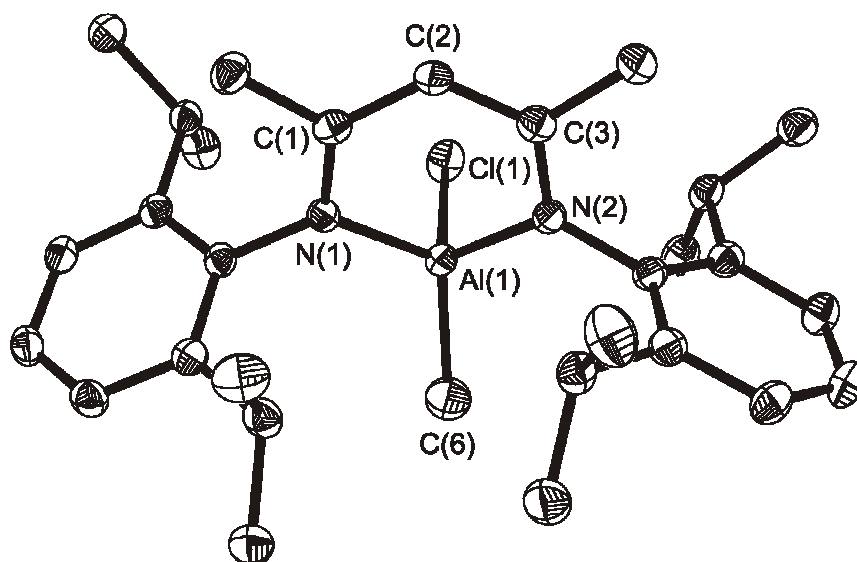


Figure 1. Molecular crystal structure of LAl(Me)Cl (**1**). Thermal ellipsoids are shown with 50 % probability. Hydrogen atoms are omitted for clarity. Selected bond lengths [Å] and angles[°]: Al(1)–C(6) 1.905(5), Al(1)–Cl(1) 2.158(1), Al(1)–N(1) 1.906(2), Al(1)–N(2) 1.887(2); C(6)–Al(1)–Cl(1) 114.9(4), N(1)–Al(1)–N(2) 97.6(1), N(1)–Al(1)–C(6) 117.2(4), N(2)–Al(1)–C(6) 113.2(4), N(2)–Al(1)–Cl(1) 106.8(1), N(1)–Al(1)–Cl(1) 105.4(1).

The Al(1)–C(6) bond length in LAl(Me)Cl (**1**) 1.905(5) Å is shorter than those of LAlMe₂ (1.958(3) and 1.970(3) Å, av 1.964 Å)^[45] reported earlier. The Al(1)–Cl(1) bond length of 2.158(1) Å in **1** is comparable to that of LAlCl₂ (2.134(1) and 2.119(1) Å, av 2.126 Å).^[46] The C(6)–Al(1)–Cl(1) bond angle of 114.9(4)° lies in between the angles of C(1)–Al(1)–C(2) 115.4(2)° in LAlMe₂^[45] and Cl(1)–Al(1)–Cl(2) 108.02(2)° in LAlCl₂.^[46]

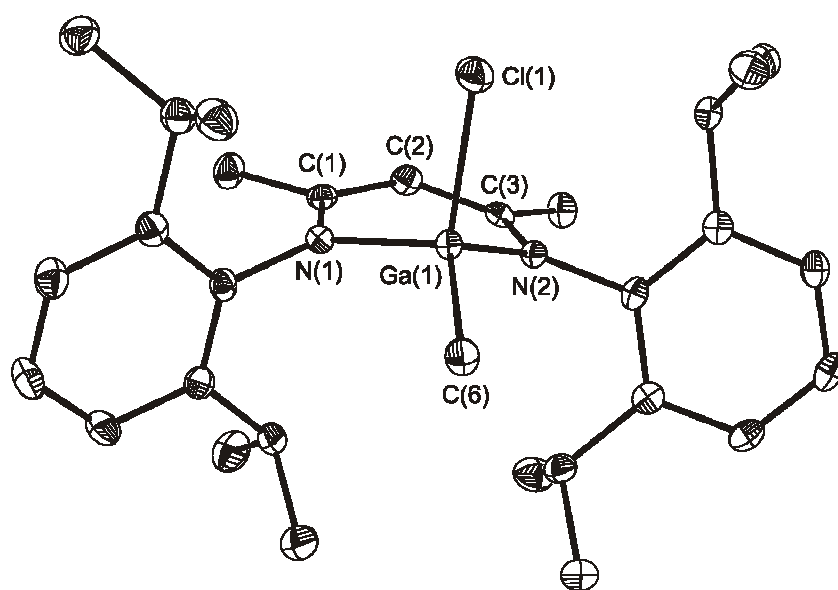


Figure 2. Molecular crystal structure of LGa(Me)Cl (**2**). Thermal ellipsoids are shown with 50 % probability. Hydrogen atoms are omitted for clarity. Selected bond lengths [\AA] and angles[$^\circ$]: Ga(1)–C(6) 1.956(2), Ga(1)–Cl(1) 2.223(1), Ga(1)–N(1) 1.949(1), Ga(1)–N(2) 1.936(1); C(6)–Ga(1)–Cl(1) 114.5(1), N(1)–Ga(1)–N(2) 97.1(1), N(1)–Ga(1)–C(6) 119.3(1), N(2)–Ga(1)–C(6) 116.3(1), N(1)–Ga(1)–Cl(1) 103.1(1), N(2)–Ga(1)–Cl(1) 104.0(1).

The Ga(1)–C(6) bond length in LGa(Me)Cl (**2**) of 1.956(2) \AA is comparable to those observed in LGaMe₂ (1.970(2) and 1.979(2) \AA , av 1.975 \AA).^[46] Similarly, the Ga(1)–Cl(1) bond length in **2** is 2.223(1) \AA which is the same like the average found in LGaCl₂ (2.228(1) and 2.218(1) \AA , av 2.223 \AA).^[46] The C(6)–Ga(1)–Cl(1) angle is 114.5(1) $^\circ$ that lies in between the angles of C(30)–Ga(1)–C(31) 122.44(9) $^\circ$ in LGaMe₂ and Cl(1)–Ga(1)–Cl(2) 110.20(4) $^\circ$ in LGaCl₂.^[46]

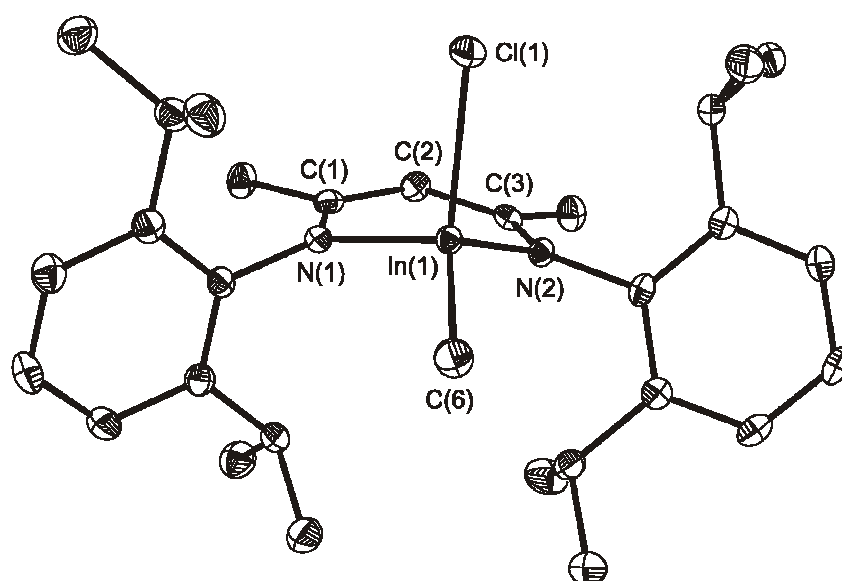
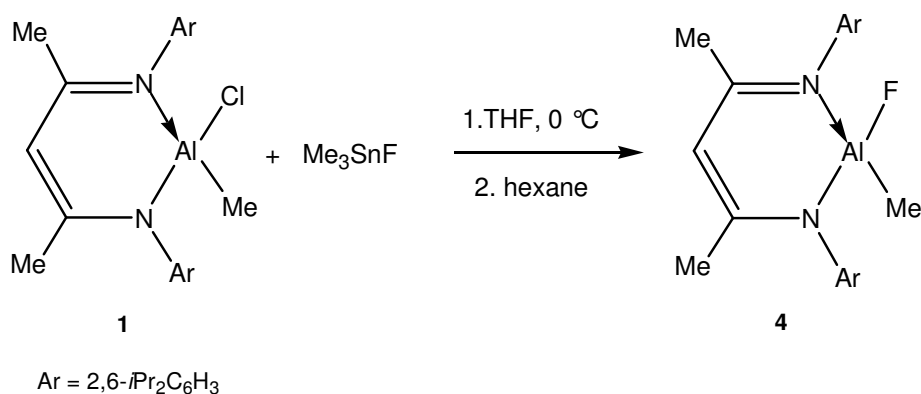


Figure 3. Molecular crystal structure of $\text{LIn}(\text{Me})\text{Cl}$ (**3**). Thermal ellipsoids are shown with 50 % probability. Hydrogen atoms are omitted for clarity. Selected bond lengths [\AA] and angles[$^\circ$]: $\text{In}(1)\text{--C}(6)$ 2.138(2), $\text{In}(1)\text{--Cl}(1)$ 2.402(1), $\text{In}(1)\text{--N}(1)$ 2.148(2), $\text{In}(1)\text{--N}(2)$ 2.133(2); $\text{C}(6)\text{--In}(1)\text{--Cl}(1)$ 119.1(1), $\text{N}(1)\text{--In}(1)\text{--N}(2)$ 90.9(1), $\text{N}(1)\text{--In}(1)\text{--C}(6)$ 122.4(1), $\text{N}(2)\text{--In}(1)\text{--C}(6)$ 117.0(1), $\text{N}(1)\text{--In}(1)\text{--Cl}(1)$ 100.9(1), $\text{N}(2)\text{--In}(1)\text{--Cl}(1)$ 101.3(1).

The $\text{In}(1)\text{--C}(6)$ bond length in $\text{LIn}(\text{Me})\text{Cl}$ (**3**) of 2.138(2) \AA is almost similar to those observed in $\text{LIn}(\text{Me})_2$ (2.148(1) and 2.168(1) \AA , av 2.158 \AA).^[46] The $\text{In}(1)\text{--Cl}(1)$ bond length of 2.402(1) \AA is comparable to those of LInCl_2 (2.3872(9) and 2.404(3) \AA , av 2.396 \AA).^[46] The $\text{C}(6)\text{--In}(1)\text{--Cl}(1)$ angle in **3** is 119.1(1) $^\circ$ that is wider than the $\text{Cl}(1)\text{--In}(1)\text{--Cl}(2)$ angle of 108.99(8) $^\circ$ in LInCl_2 ^[46] but narrower than the $\text{C}(30)\text{--In}(1)\text{--C}(31)$ angle of 130.94(6) $^\circ$ in LInMe_2 .^[46]

2.1.3. Reaction of LAl(Me)Cl (1**) with Me_3SnF and X-ray crystal structural characterization of LAl(Me)F (**4**)**

Trimethyltin fluoride has proved to be a versatile fluorinating agent particularly in the metathesis of main group chlorides and of Group 4–6 to the corresponding fluorides.^[54,58,147] Trimethyltin chloride generated during the metathesis is readily removed *in vacuo*. Thus, the reaction of LAl(Me)Cl (**1**) with Me_3SnF in THF results in the complete conversion of **1** to LAl(Me)F (**4**) (Scheme 7). Compound **4** was characterized by its ^{19}F NMR spectrum. The Al–F resonance appears at 8.6 ppm. Methyl protons of Al–Me are coupled to the F atom and are observed as a doublet at –0.82 ppm. EI–MS of **4** exhibits $[M^+ - \text{Me}]$ as the base peak at m/z 463.



Scheme 7. Preparation of the β -diketiminato methylaluminumfluoride

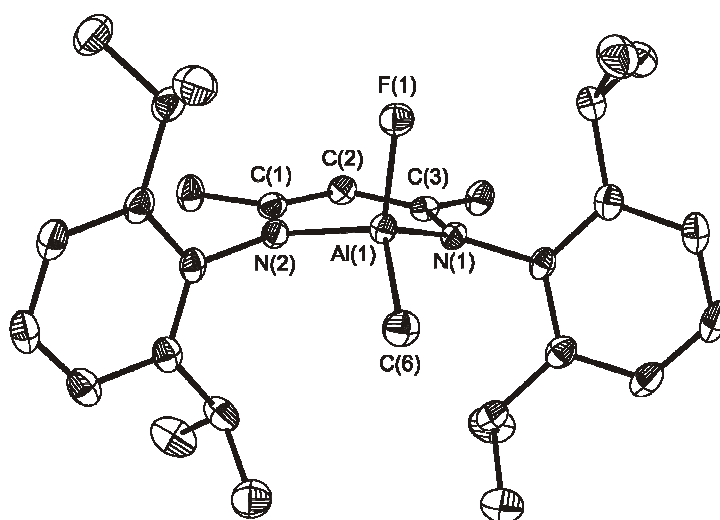
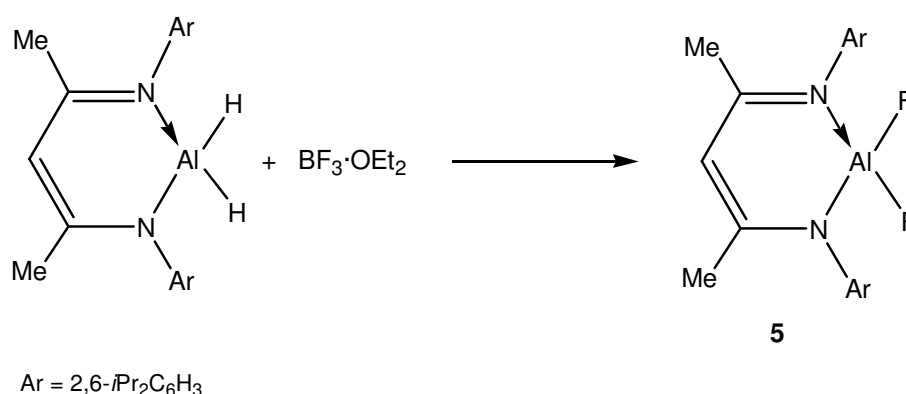


Figure 4. Molecular crystal structure of LAl(Me)F (**4**). Thermal ellipsoids are shown with 50 % probability. Hydrogen atoms are omitted for clarity. Selected bond lengths [\AA] and angles[$^\circ$]: Al(1)–C(6) 1.944(2), Al(1)–F(1) 1.679(1), Al(1)–N(1) 1.897(1), Al(1)–N(2) 1.885(1); F(1)–Al(1)–C(6) 144.7(1), F(1)–Al(1)–N(1) 105.7(1), F(1)–Al(1)–N(2) 107.8(1), N(1)–Al(1)–N(2) 97.1(1), N(1)–Al(1)–C(6) 115.8(1), N(2)–Al(1)–C(6) 114.1(1).

The Al atom in LAl(Me)F (**4**) is out of plane of the chelating β -diketimate MC_3N_2 six-membered ring. The F and Me are projecting above and below the AlC_3N_2 plane in **4**. Diisopropyl phenyl substituents on N atoms of the β -diketimate ligand are perpendicular to the MC_3N_2 ring. The Al(1)–C(6) bond distance in LAl(Me)F (**4**) of 1.944(2) \AA is slightly shorter than that found in LAl(Me)Cl (**1**) (1.905(5) \AA) and LAlMe₂ (av 1.964 \AA).^[46] The C(6)–Al(1)–F(1) bond angle is 144.7(1) $^\circ$ which is wider than the corresponding angle in the chlorine derivative LAl(Me)Cl (**1**) (114.9(4) $^\circ$).

2.1.4. Reaction of LAIH_2 with $\text{BF}_3 \cdot \text{OEt}_2$ and X-ray crystal structure of LAIF_2 (**5**)

When LAIH_2 was treated with $\text{BF}_3 \cdot \text{OEt}_2$ at low temperature and allowed to warm to room temperature the difluoride LAIF_2 (**5**) was isolated (Scheme 8). A singlet in the ^{19}F NMR of **5** at 6.8 ppm confirms the formation of Al-F bond and the Al atom resonates at 66.9 ppm in the ^{27}Al NMR spectrum. EI-MS spectrum of **5** shows $[M^+]$ as the base peak at m/z 482.



Scheme 8. Preparation of the β -diketiminato aluminumdifluoride

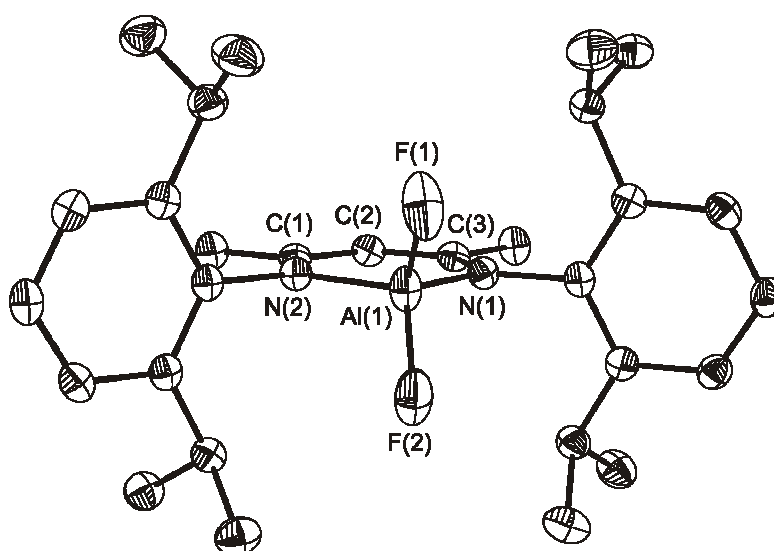


Figure 5. Molecular crystal structure of LAlF_2 (**5**). Thermal ellipsoids are shown with 50 % probability. Hydrogen atoms are omitted for clarity. Selected bond lengths [\AA] and angles[$^\circ$]: $\text{Al(1)}\text{--F(1)}$ 1.655(1), $\text{Al(1)}\text{--F(2)}$ 1.650(1), $\text{Al(1)}\text{--N(1)}$ 1.865(1), $\text{Al(1)}\text{--N(2)}$ 1.866(1); $\text{F(1)}\text{--Al(1)}\text{--F(2)}$ 107.8(1), $\text{N(1)}\text{--Al(1)}\text{--N(2)}$ 99.3(1), $\text{F(1)}\text{--Al(1)}\text{--N(2)}$ 112.8(1), $\text{F(2)}\text{--Al(1)}\text{--N(2)}$ 111.6(1), $\text{F(1)}\text{--Al(1)}\text{--N(1)}$ 112.1(1), $\text{F(2)}\text{--Al(1)}\text{--N(1)}$ 113.2(1).

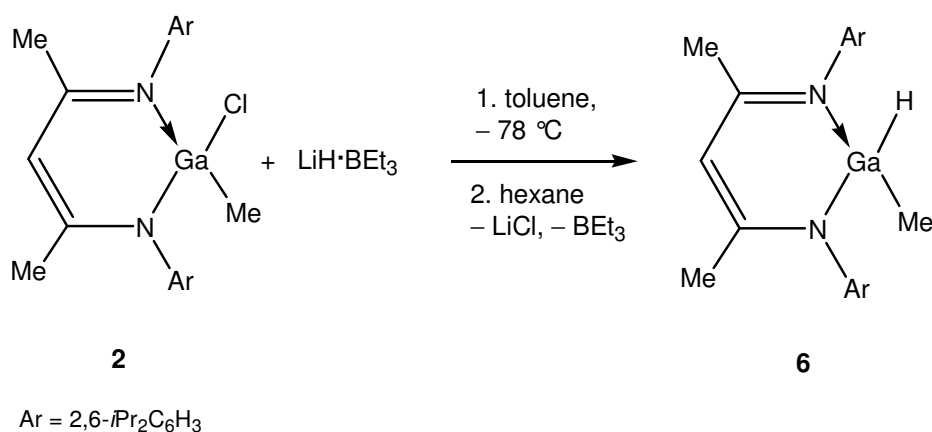
The Al–F bond distance of 1.679(1) \AA in LAl(Me)F (**4**) is slightly longer than those observed in LAlF_2 (**5**) (1.655(1) and 1.650(1) \AA) and that in $[\text{OCMeCHCMeN(2,6-}i\text{Pr}_2\text{C}_6\text{H}_3)]_2\text{AlF}$ (1.6775(14) \AA).^[148] However, the Al–F bond lengths in **4** and **5** are comparable to terminal Al–F bonds in $[(\text{Me}_3\text{Si})_3\text{CAIF}_2]_3$ (av 1.669 \AA) but are significantly shorter than the bridging ones (av 1.805 \AA).^[149] The $\text{F(1)}\text{--Al(1)}\text{--C(2)}$ angle in **4** is $144.66(6)^\circ$ which is wider than the $\text{F(1)}\text{--Al(1)}\text{--F(2)}$ angle of $107.80(7)^\circ$ in **5**, probably due to smaller size of the F atom compared to the Me group.

2.1.5. Reduction of LGa(Me)Cl (**2**) with LiBEt_3H and X-ray crystal structure of LGa(Me)H (**6**)

A number of hydrides of aluminum have been prepared ranging from mono-, di- and trihydrides.^[63-66] The latter has been a very strong and useful reducing agent. Although the corresponding gallium compounds^[66] are also known, their stability is lower than the aluminum compounds. Attempts have been devoted to increase the stability of these compounds by coordination of an ancillary ligand to the gallium atom. These are among the most easily accessible, more stable and usually, more malleable than the parent hydrides. Most common are the Lewis base adducts of Group 13 metal hydrides.^[66,67] Thus, $\text{GaH}_3\cdot\text{NMe}_3$ is stable below room temperature but its shelf life is considerably lower at room temperature. Therefore it is a synthetic

challenge to prepare stable mono- and dihydrides of gallium. An obvious route is the reduction of the corresponding chlorides with a suitable reducing agent.

The reduction of $\text{LGa}(\text{Me})\text{Cl}$ (**2**) with $\text{LiH}\cdot\text{BEt}_3$ in toluene smoothly affords $\text{LGa}(\text{Me})\text{H}$ (**6**) in good yield (Scheme 9). Compound **6** is a stable solid with a melting point of $177\text{ }^\circ\text{C}$. In the ^1H NMR spectrum of **6** the $\text{Ga}-\text{H}$ resonates at 5.49 ppm as a broad peak, whereas the $\text{Ga}-\text{Me}$ protons appear as doublet at -0.45 ppm indicating its coupling to the hydride group. The base peak in the EI-MS spectrum of **6** at m/z 487 corresponds to $[\text{M}^+ - \text{Me}]$. The IR spectrum of **6** shows a strong band at 1825 cm^{-1} which can be attributed to the $\text{Ga}-\text{H}$ stretch.



Scheme 9. Preparation of the β -diketiminato methylgalliumhydride

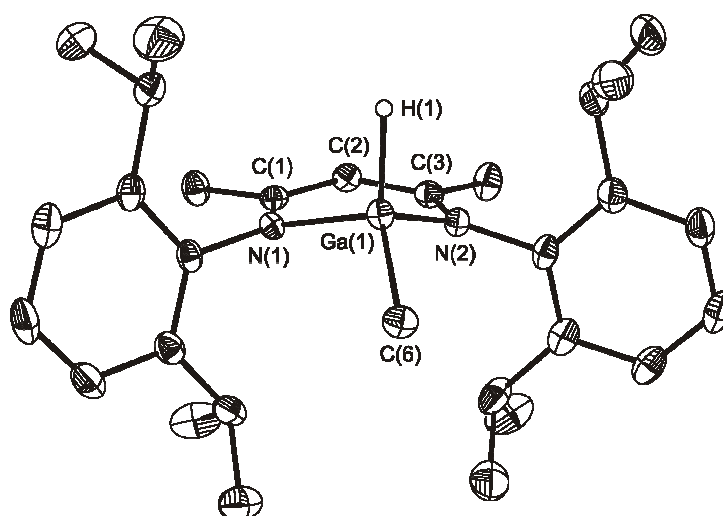


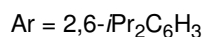
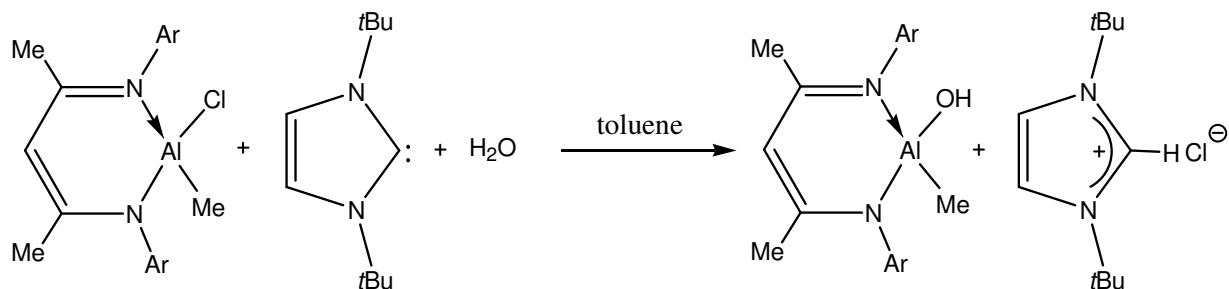
Figure 6. Molecular crystal structure of LGa(Me)H (**6**). Thermal ellipsoids are shown with 50 % probability. Hydrogen atoms except on Ga are omitted for clarity. Selected bond lengths [\AA] and angles [$^\circ$]: Ga(1)–C(6) 1.955(2), Ga(1)–H(1) 1.75(2), Ga(1)–N(1) 1.968(2), Ga(1)–N(2) 1.976(2); C(6)–Ga(1)–H(1) 118.3(6), N(1)–Ga(1)–N(2) 94.3(1), N(1)–Ga(1)–C(6) 111.2(1), N(2)–Ga(1)–C(6) 112.7(1), N(1)–Ga(1)–H(1) 109.5(6), N(2)–Ga(1)–H(1) 108.3(7).

The structure of the complex LGa(Me)H (**6**) is analogous to its parent compound LGa(Me)Cl (**2**). The arrangement of the hydride and methyl group around the Ga atom is above and below the GaC_3N_2 plane with the Ga atom out of the C_3N_2 plane in a distorted tetrahedral environment. The Ga(1)–C(6) bond length in LGa(Me)H (**6**) of 1.955(2) \AA was found to be identical with 1.956(2) \AA observed in LGa(Me)Cl (**2**). The Ga–H distance in **6** (1.75(2) \AA) is comparable to those in $[\text{tBuOGaH}_2]_2$ (1.61(10) and 1.60(12) \AA)^[150] but slightly longer than those observed in $[(\text{tBuO})_2\text{GaH}]_2$ (1.53(7) \AA).^[150] The C(6)–Ga(1)–H(1) bond angle in **6** (118.3(6) $^\circ$) is comparable to that observed in its parent compound LGa(Me)Cl (114.5(1) $^\circ$).

2.2. Hydrolysis of $\text{LAl}(\text{Me})\text{Cl}$ (1), $\text{LGa}(\text{Me})\text{Cl}$ (2) in the presence of *N*-heterocyclic carbene as HCl scavenger

2.2.1. Hydrolysis of $\text{LAl}(\text{Me})\text{Cl}$ (1) and molecular crystal structure of $\text{LAl}(\text{Me})\text{OH}$ (7)

Recently, Roesky and co-workers obtained the molecular aluminum dihydroxides $\text{LAl}(\text{OH})_2$ ^[38] and $[\text{LAl}(\text{OH})]_2(\mu\text{-O})$ ^[91] from LAlI_2 and $\text{LAl}(\text{Me})\text{OH}$ from $\text{LAl}(\text{Me})\text{Cl}$ in the two phase liquid ammonia/toluene system, at -78°C , containing a $\text{KOH}/\text{H}_2\text{O}/\text{KH}$ mixture.^[47] Successful employment of the imidazolium salts in the reactions with different chlorosilanes as well as in the hydrolysis and ammonolysis reactions encouraged us to use *N*-heterocyclic carbenes as HCl scavengers. This is contradictory to the use of amines as HCl acceptors which did not lead to the pure product.^[151] Addition of one eqv. H_2O to a toluene solution of $\text{LAl}(\text{Me})\text{Cl}$ and one eqv. 1,3-di-*tert*-butylimidazol-2-ylidene yields $\text{LAl}(\text{Me})\text{OH}$ (7) and insoluble 1,3-di-*tert*-butylimidazolium chloride (Scheme 10). Removal of the volatiles *in vacuo* and extraction with *n*hexane affords 7 as microcrystals in 86 % yield (compare with 68 % yield obtained from the two phase system liq. NH_3 /toluene after 4 h). The answer to the pertinent query to the successful use of *N*-heterocyclic carbenes is due to the following facts: (a) Use of amines leads to an equilibrium between the protonated amine and the free base, thus causing side reactions during the hydrolysis. On the other hand, with *N*-heterocyclic carbenes no such equilibrium is expected to exist due to the favored covalent C–H bond formation.^[143] (b) The resulting imidazolium chloride is only sparingly soluble in hydrocarbon solvents such as *n*hexane, toluene or THF, which allows its easy separation from the reaction mixture by filtration through Celite. In addition, the imidazolium chlorides can be easily recycled to the free carbenes using strong base such as KO^tBu or NaH .^[152] (c) The high reactivity of $\text{LAl}(\text{OH})_2$ and $\text{LAl}(\text{Me})\text{OH}$ toward protic reagents also hampers the use of amines as HCl acceptor.



Scheme 10. Synthesis of β -diketiminate supported methylaluminumhydroxide

Compound **7** is a colorless crystalline solid that melts at 192 °C. To our surprise no decomposition or polymerization was observed when **7** was kept in toluene solution or in the solid state under an inert atmosphere, even when a solid sample of **7** was heated above 190 °C. The most intense peak in the EI mass spectrum of **7** appeared at m/z 461 [$M^+ - \text{Me}$], and the peak at m/z 443 (20 %) was assigned to the fragment [$M^+ - \text{Me} - \text{H}_2\text{O}$]. The ^1H NMR spectrum of **7** shows two singlets at 0.53 and -0.88 ppm which can be attributed to the protons of O-*H* and Al-*Me* groups, respectively. The IR spectrum of **7** shows a sharp band (3728 cm^{-1}) which can be attributed to AlO-H stretch.

Molecular crystal structure of LAl(Me)OH (7)

Single crystals of **7**, suitable for X-ray structural analysis were obtained from the toluene solution at -20 °C in one week. The crystal data and the structure presented here is the one obtained by the hydrolysis of LAl(Me)Cl (**1**) in liq. NH₃/toluene two phase system as reported earlier.^[47] Compound **7** crystallizes in the monoclinic space group $P2(1)/c$. The X-ray structure reveals **7** as a monomeric aluminum hydroxide (Figure 7). The Al center exhibits a distorted tetrahedral geometry with two nitrogen atoms of the β -diketiminate ligand, one Me and an OH

group. The small N(1)–Al(1)–N(2) angle ($96.3(1)^\circ$) is the result of formation of the C_3N_2Al six-membered ring. The Al–OH bond length ($1.731(3) \text{ \AA}$) is slightly longer than those found in $La(OH)_2$ ($1.695(15)$ and $1.711(16) \text{ \AA}$),^[38] and comparable to those in $[La(OH)]_2(\mu-OH)$ ($1.738(3)$ and $1.741(3) \text{ \AA}$)^[91] but significantly shorter than those of Al–(μ -OH) bonds in $[(Ph_2Si)_2O_3]_4Al_4(\mu-OH)_4$ (av 1.800 \AA),^[89] $[Mes_2Al(\mu-OH)]_2 \cdot 2THF$ ($1.822(1) \text{ \AA}$; Mes = mesityl),^[153] and $Al_5(tBu)_5(\mu_3-O)_2(\mu_3-OH)_2(\mu-OH)_2(\mu-O_2CPh)_2$ (av 1.824 \AA).^[90] The Al–Me bond length ($1.961(3) \text{ \AA}$) is comparable to those found in $Al(Me)(mqp)_2$ ($1.964(6) \text{ \AA}$; mqp = 2-(4'-methylquinolinyl)-2-phenolato)^[154] and $(OCMeCHCMeNAr)_2AlMe$ ($1.975(2) \text{ \AA}$).^[148]

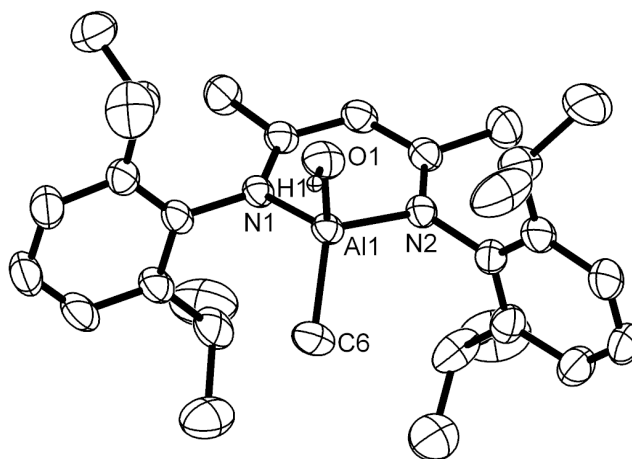


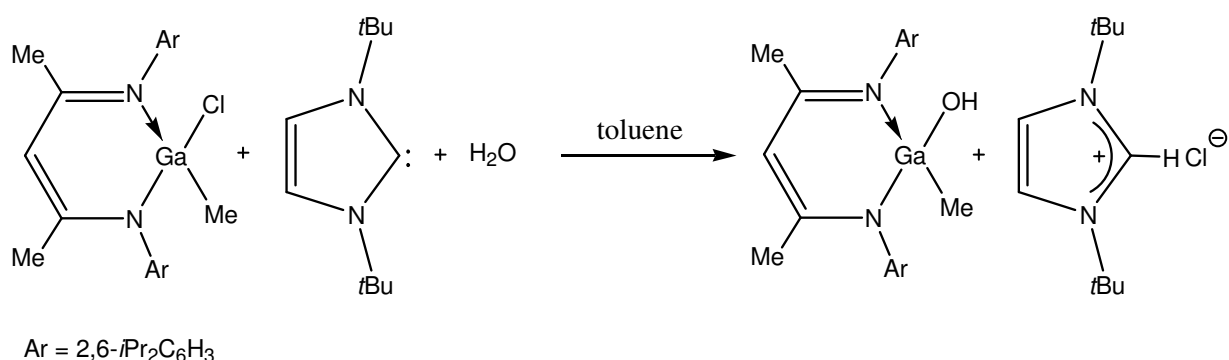
Figure 7. Molecular crystal structure of $LaAl(Me)OH$ (**7**). Thermal ellipsoids are shown with 50 % probability. The hydrogen atoms of the C–H bonds are omitted for clarity. Selected atomic distances [\AA] and angles [$^\circ$]: Al(1)–O(1) $1.731(3)$, Al(1)–N(1) $1.940(3)$, Al(1)–N(2) $1.907(3)$, Al(1)–C(6) $1.961(3)$; O(1)–Al(1)–N(1) $105.8(1)$, O(1)–Al(1)–N(2) $108.1(1)$, N(1)–Al(1)–N(2) $96.3(1)$, O(1)–Al(1)–C(6) $116.6(2)$, N(1)–Al(1)–C(6) $115.0(1)$, N(2)–Al(1)–C(6) $113.0(2)$.

Why does the hydrolysis of LAl(Me)Cl proceed in such a smooth manner leading to the isolation of LAl(Me)OH ? This is a pertinent query in view of the known decomposition of aluminum compounds (aluminum alkyls, aluminum aryls, aluminum amides) to aluminum oxides and hydroxides upon reaction with water. The answer seems to lie in a number of factors. (1) The Lewis acidity of the intermediates is considerably decreased on account of the *coordinatively saturated* aluminum centers. Further, the presence of a sufficient number of electron rich nitrogen ligands around aluminum also reduces the Lewis acidity of the aluminum. (2) *N*-heterocyclic carbenes facilitate a smooth transformation of the chloride LAl(Me)Cl into the hydroxide LAl(Me)OH . (3) The β -diketiminato ligand provides a crucial electronic role. Moreover, it acts as an efficient chelating ligand forming a stable six-membered ring with aluminum providing sufficient electronic relief to the Lewis acidic aluminum center which in turn retards the reactivity of the Al–OH unit.

2.2.2. Hydrolysis of LGa(Me)Cl (2) and molecular crystal structure of LGa(Me)OH (8)

The recent isolation of LGa(OH)_2 ^[92] and LAl(Me)OH prompted us to look for a similar gallium derivative. Another driving force was the compound $[(\text{LAlMe})(\text{Cp}_2\text{ZrMe})](\mu\text{-O})$ which was a very good catalyst for the polymerization of ethylene.^[47] Moreover, LAl(Me)OH has been utilized to prepare a series of aluminum lanthanide hetero-bimetallic complexes.^[48] A methylgallium hydroxide $\text{MeGa(OH)Pz}_2\text{BMe}_2$ ($\text{Pz}_2\text{BMe}_2 = \text{bis}(\text{pyrazolyl})\text{dimethylboron}$) was isolated by Rettig and co-workers as a by-product of the reaction between $\text{Na}[\text{Me}_2\text{BPz}_2]$ and $\text{Me}_2\text{GaCl}\cdot\text{OEt}_2$. The formation of $\text{MeGa(OH)Pz}_2\text{BMe}_2$ probably resulted from an accidental use of wet solvent.^[155] Therefore, it was of interest to prepare a molecule with similar functionalities with a much simpler procedure which rationally allows the assembly of such molecules. Similar to the synthesis of LAl(Me)OH (7), the hydrolysis of LGa(Me)Cl (2) with a stoichiometric

amount of water in the presence of 1,3-di-*tert*-butylimidazol-2-ylidene as hydrogen chloride acceptor results in the formation of LGa(Me)OH (**8**) in good yield (76 %) (Scheme 11). Recent measurements and theoretical calculations confirmed a high basicity of the *N*-heterocyclic carbenes in polar solvents such as DMSO or acetonitrile. The 1,3-di-*tert*-butylimidazol-2-ylidene, used in the present case as a HCl acceptor, reveals a pK_a of 24.0 (exp./theor. 24.5±0.2.) in DMSO and 33.7±0.1 (theor.) in acetonitrile.^[156] This clearly explains the almost irreversible bonding of the free protons to the carbene and high yields of products LAI(Me)OH (**7**) and LGa(Me)OH (**8**).



Scheme 11. Synthesis of β -diketiminato supported methylgalliumhydroxide

Compound **8** has been unambiguously characterized by means of spectroscopic, spectrometric and crystallographic techniques. Compound **8** is a colorless crystalline solid and thermally quite stable. Compound **8** melts at 200 °C. The EI mass spectrum of **8** revealed that the most intense peak appears at m/z 503 and corresponds to the loss of one methyl group from the molecular ion, $[M^+ - \text{Me}]$. The IR spectrum of **8** shows a sharp band at 3676 cm⁻¹ which can be attributed to the GaO–H stretch. The ¹H NMR spectrum for **8** shows two resonances (0.08 and –0.57 ppm) which can be attributed to the protons of GaO–H and Ga–Me groups, respectively. The other resonances for **8** are characteristic for the β -diketiminato ligand L.

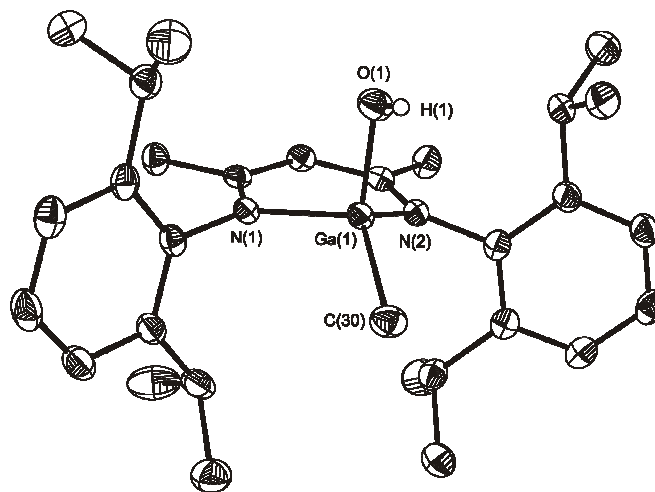
Molecular crystal structure of LGa(Me)OH (8)

Figure 8. Molecular crystal structure of LGa(Me)OH (**8**). Thermal ellipsoids are shown with 50 % probability. The hydrogen atoms of the C–H bonds are omitted for clarity. Selected atomic distances [\AA] and angles [$^\circ$]: Ga(1)–O(1) 1.831(1), Ga(1)–N(1) 1.957(1), Ga(1)–N(2) 1.953(1), Ga(1)–C(30) 1.949(2). O(1)–Ga(1)–N(1) 102.8(1), O(1)–Ga(1)–N(2) 105.4(1), N(1)–Ga(1)–N(2) 95.6(1), O(1)–Ga(1)–C(30) 119.5(1), N(1)–Ga(1)–C(30) 116.0(1), N(2)–Ga(1)–C(30) 114.3(1).

Single crystals of **8** suitable for X-ray structural analysis were obtained from *n*hexane solution. Compound **8** crystallizes in the monoclinic space groups $P2_1/c$. The X-ray crystal structure reveals **8** as a monomeric gallium hydroxide (Figure 8). The Ga center exhibits a distorted tetrahedral geometry with two nitrogen atoms of the β -diketimate ligand, one Me group and an OH group. The small N(1)–Ga(1)–N(2) angle $95.6(1)^\circ$ is the result of the formation of the $\text{C}_3\text{N}_2\text{Ga}$ six-membered ring. The Ga–OH bond length (1.831(1) \AA) in **8** is considerably shorter than that found in hydroxyl(methyl)galliumbis(pyrazolyl)dimethylboron (2.033(5) \AA) and in

$[(2,6\text{-Mes}_2\text{C}_6\text{H}_3\text{Ga}(\text{Me})(\mu\text{-OH}))_2]$ (av 1.914 Å)^[101] but slightly longer than that observed in $(2,6\text{-Mes}_2\text{C}_6\text{H}_3)_2\text{GaOH}$ (1.783(2) Å).^[101] The Ga–Me distance of 1.949(2) Å in **8** is comparable to 1.957(8) Å observed in hydroxy(methyl)galliumbis(pyrazolyl)dimethylboron^[155] and in $[(2,6\text{-Mes}_2\text{C}_6\text{H}_3\text{Ga}(\text{Me})(\mu\text{-OH}))_2]$ (av 1.947 Å).^[101]

2.2.3. The OH functional group of $\text{LAl}(\text{Me})\text{OH}$ (**7**) and $\text{LGa}(\text{Me})\text{OH}$ (**8**)

The OH groups are the most important functional groups for solid support as well as for the immobilization of catalytically active metal complexes and also for solid acid catalysts.

The IR spectrum (Nujol) of **7** and **8** exhibits a sharp band (3728 cm^{-1}) and (3676 cm^{-1}), respectively, for the terminal OH group which is in agreement with the solid state structures of **7** and **8**. The absorption frequency of the OH group in **7** and **8** is comparable to the terminal OH groups found in compounds $\text{LAl}(\text{OH})_2$ (3727 cm^{-1})^[38] and $[\text{LAl}(\text{OH})]_2(\mu\text{-O})$ (3716 cm^{-1}),^[91] but higher than those found in the Brönsted acids SAPO-34 (3600-3625 cm^{-1})^[157] and zeolite Chabazite (3603 cm^{-1}).^[158] Therefore, **7** and **8** contain a free Brönsted acidic OH group. The acidity of **7** can be anticipated due to the Lewis acidic Al(III) center and high bond strength of the Al–O bond. Furthermore, in the ^1H NMR spectrum the proton of the OH group in **7** resonates at δ 0.53 ppm whereas the corresponding resonance for **8** was observed at 0.08 ppm. This result is similar to that observed for $[\text{LAl}(\text{OH})]_2(\mu\text{-O})$ (– 0.30 ppm).^[91] It is noteworthy that on one hand the OH group of **7** is reactive enough to react with Cp_2ZrMe_2 and Cp_2ZrHCl on the other hand it does not impede the formation of **7** during the course of the reaction as it does not eliminate methane.^[47] Presumably kinetic stability disfavors intermolecular methane evolution due to the sterically encumbered β -diketiminato ligand. This is also observed in the formation of **8**.

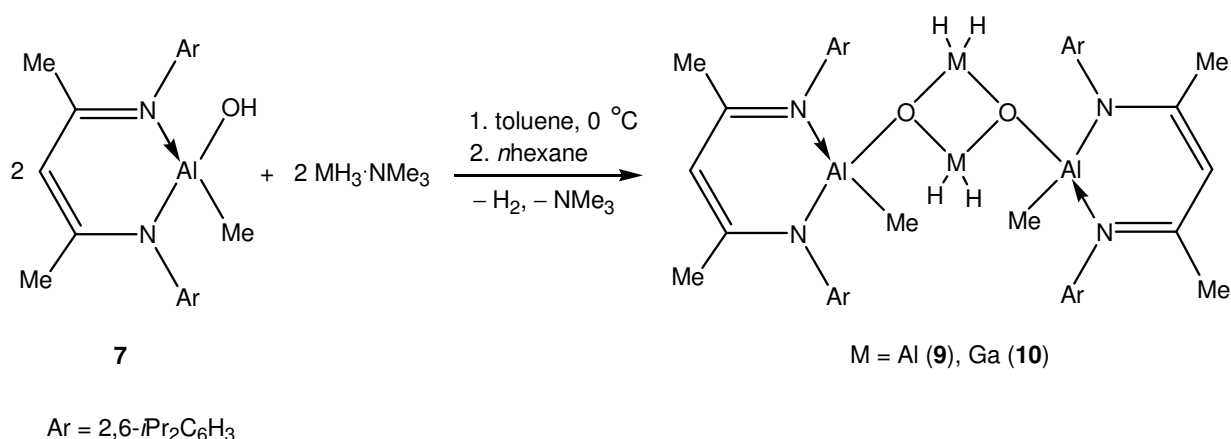
2.3. Reactions of LAl(Me)OH ; syntheses of homo–and heterobimetallic oxides

2.3.1. Reaction of LAl(Me)OH (**7**) with $\text{AlH}_3\cdot\text{NMe}_3$ and $\text{GaH}_3\cdot\text{NMe}_3$

The synthesis of alumoxanes via the controlled hydrolysis of alkyl and aryl aluminum compounds also leads to interesting compounds but it suffers from a major drawback in that the composition of the final product cannot be predicted *before* the reaction. Some trinuclear and a tetranuclear derivatives containing Al–O–Al moieties are known but they are either alkoxyalanes^[119,150] or aminoalkoxyalanes.^[159] Systematic study of the controlled hydrolysis of trimesitylgallium and –aluminum was monitored by Roesky and co-workers which shed more light on the hydrolysis process.^[88,153] The alumoxanes and hybrid alumoxanes were prepared by Barron and co-workers.^[86] In order to assemble soluble lipophilic organoalumoxanes in a predictable and rational manner a paradigm shift in the synthetic approach is required. Thus, instead of taking the Al–C or Al–H bonds as the starting point for making Al–O–Al bonds of alumoxanes and heteroalumoxanes, containing an Al–O linkage of organoaluminum hydroxides were explored. A second goal was to retain reactive groups on the metal centers in such compounds. This would allow a stepwise synthesis of cage structures.

Therefore, in the following section the synthesis of homo– and heteroalumoxane containing an oxide ion between metal centers will be described. The synthesis of these molecules was possible by preparing an unprecedented aluminum monohydroxide LAl(Me)OH (**7**). The reaction of LAl(OH)Me with a stoichiometric amount of $\text{MH}_3\cdot\text{NMe}_3$ ($\text{M} = \text{Al, Ga}$) in toluene at 0 °C results in a vigorous evolution of hydrogen and the formation of $[\{\text{LAl(Me)}\}(\mu\text{-O})(\text{AlH}_2)]_2$ (**9**) and $[\{\text{LAl(Me)}\}(\mu\text{-O})(\text{GaH}_2)]_2$ (**10**) in excellent yields (Scheme 12). Thus, this synthetic methodology represents a viable and rational route for the preparation of novel and interesting compounds. Compounds **9** and **10** represent the first examples of a tetranuclear alumoxane and a gallium congener respectively. Apart from being examples of simple building blocks (Al_2O_2 and

Ga₂O₂) these also contain a pair of reactive MH₂ (M = Al, Ga) groups in the central core and Al–Me groups as the terminal end groups.



Scheme 12. Preparation of the alumoxanehydride and its gallium congener

Compounds **9** and **10** have been unambiguously characterized by means of spectroscopic, spectrometric and crystallographic techniques. Both **9** and **10** are colorless crystalline solids and are thermally quite stable. They decompose with melting at 260 and 234 °C respectively. The EI mass spectrum of **9** revealed that the most intense peak appears at m/z 1007 and corresponds to the loss of a hydrogen from the molecular ion. Similarly an ion at m/z 1079 in **10** is due to $[M^+ - \text{Me}]$. The IR spectrum of **9** shows a sharp absorption (1833 and 1850 cm⁻¹) corresponding to the symmetric and antisymmetric stretch of the AlH₂ fragment. The corresponding stretching modes for **10** appear at 1901 and 1929 cm⁻¹. The ¹H NMR resonances for **9** and **10** are broad at room temperature. However, a variable temperature ¹H NMR study revealed that the room temperature spectra of **9** and **10** are simplified by a dynamic process and upon cooling the broad signals become sharp and eventually resolve into different resonances for the two halves of the molecules which are expected based on the solid state structures for **9** and **10**. For **9** (– 60 °C) and **10** (– 70 °C) two sharp singlets were observed for the methyl groups which are located on

the terminal aluminum atoms. This suggests that the local environment around the two aluminum centers is slightly different at least at lower temperatures. This feature is also reflected in the hydride resonances of the central Al_2O_2 and Ga_2O_2 units. Although the exact nature of the dynamic process involved has not been clearly established, it is possible that this may be due to the restricted rotation of $\text{Al}-\text{O}-\text{Al}(\text{Ga})$ bond at lower temperatures.

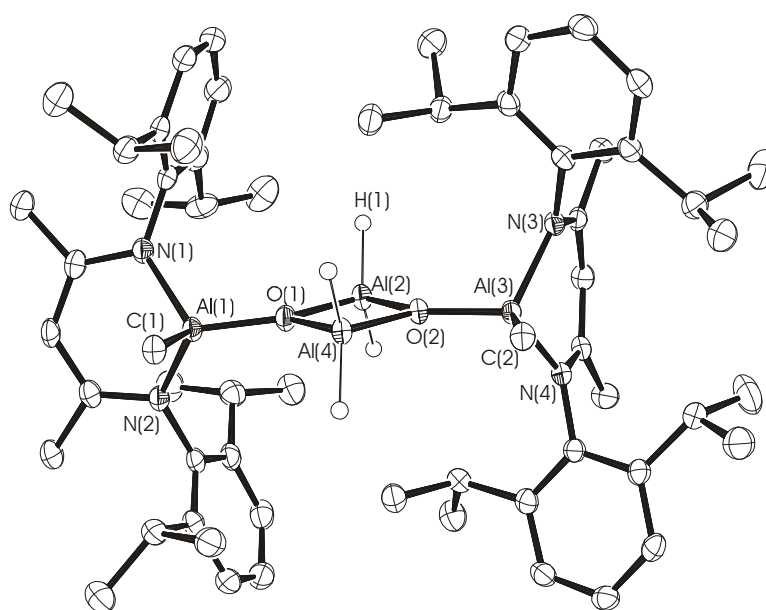


Figure 9. Molecular crystal structure of $[\{\text{LAl}(\text{Me})\}(\mu\text{-OAlH}_2)_2]$ (**9**). Thermal ellipsoids are shown with 50 % probability. The hydrogen atoms of the C–H bonds and hexane molecule are omitted for clarity. Selected bond lengths [\AA] and angles [$^\circ$]: $\text{Al}(1)\text{--O}(1)$ 1.748 (14), $\text{Al}(2)\text{--O}(1)$ 1.838 (14), $\text{Al}(2)\text{--O}(2)$ 1.828, $\text{Al}(4)\text{--O}(2)$ 1.824(14), $\text{Al}(4)\text{--O}(1)$ 1.842(14), $\text{Al}(2)\cdots\text{Al}(4)$ 2.679, $\text{Al}(3)\text{--O}(2)$ 1.772 (13), $\text{Al}(1)\text{--N}(1)$ 1.913(16), $\text{Al}(1)\text{--C}(1)$ 1.965(2); $\text{Al}(1)\text{--O}(1)\text{--Al}(2)$ 145.44 (8), $\text{Al}(1)\text{--O}(1)\text{--Al}(4)$ 121.13, $\text{O}(1)\text{--Al}(2)\text{--O}(2)$ 86.10(6), $\text{Al}(2)\text{--O}(2)\text{--Al}(4)$ 94.36(6), $\text{Al}(3)\text{--O}(2)\text{--Al}(2)$ 142.73(8), $\text{Al}(3)\text{--O}(2)\text{--Al}(4)$ 122.91(8), $\text{N}(1)\text{--Al}(1)\text{--N}(2)$ 96.51(7), $\text{N}(1)\text{--Al}(1)\text{--O}(1)$ 113.52(7).

Single crystals of **9** and **10** suitable for X-ray structural analysis were obtained from their *n*hexane solutions. Both compounds crystallize with a molecule of *n*hexane. The molecular structures of **9** and **10** are shown in Figures 9 and 10, respectively. Compounds **9** and **10** crystallize in the monoclinic space group, $P2_1/c$ and $P2_1/m$ respectively.

The X-ray crystal structure of **9** reveals that it is a dimer of the $[\{LAl(Me)\}(\mu-O)AlH_2]$ unit. The structure contains two terminal $LAlMe$ units that are linked to a central $[H_2AlO]_2$ core. The terminal aluminum centers are part of the six-membered C_3N_2Al rings. Each aluminum center of the central $[H_2AlO]_2$ four-membered ring contains two reactive hydrides. These are located above and below the plane of the Al_2O_2 ring. The two methyl groups on the terminal Al atoms are *cis* with respect to each other. The central four-membered ring is nearly planar. The terminal six-membered rings are displaced in an approximately perpendicular manner with respect to the central $[H_2AlO]_2$ ring. The metric parameters observed in **9** are not unusual. Thus, the Al–O distances in the Al_2O_2 ring (1.824(14) – 1.841(14) Å, av. 1.832 Å) are longer than the terminal Al–O distances (1.748(14) Å and 1.772(13) Å, av. 1.760 Å) and are similar to those found in aluminum alkoxides for example $[\{(tBu)_2(Me)COAlH_2\}_2]$ (Al–O 1.841 Å)^[119] and $[tBuOAlH_2]_2$ (Al–O 1.815 Å).^[150] The O–Al–O and Al–O–Al angles in the Al_2O_2 ring are 86.10 and 93.43° respectively, while the exocyclic Al–O–Al angles are 122.02 and 144.08°.

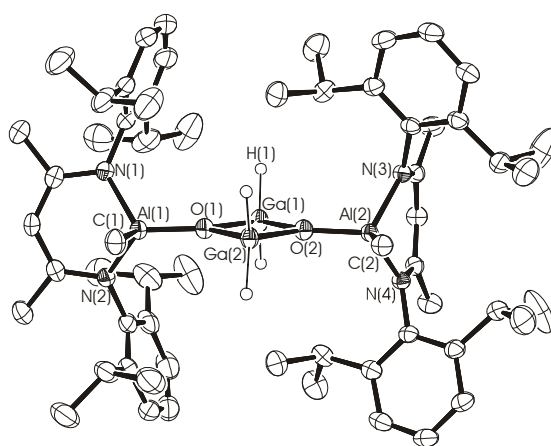
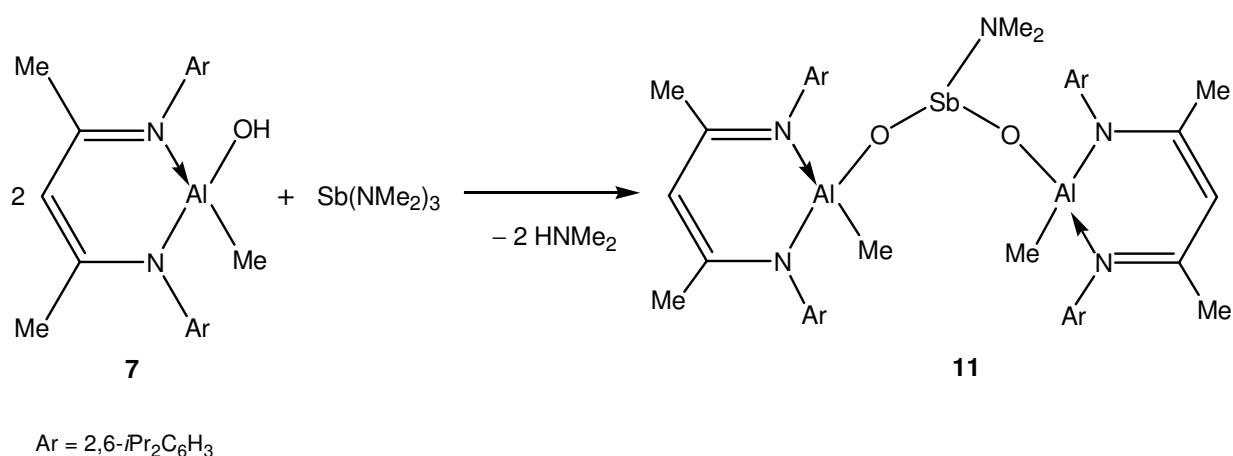


Figure 10. Molecular crystal structure of $[\{LAl(Me)\}(\mu-O)GaH_2]_2$ (**10**). Thermal ellipsoids are shown with 50 % probability. The hydrogen atoms of the C–H bonds and hexane molecule are omitted for clarity. Selected bond lengths [\AA] and angles $^\circ$: Al(1)–O(1) 1.733(2), Ga(1)–O(1) 1.933(2), Ga(1)–O(2) 1.924(2), Ga(2)–O(2) 1.917(2), Ga(2)–O(1) 1.939(2), Ga(1)–H(1) 1.516, Ga(1)···Ga(2) 2.849(7), Al(2)–O(2) 1.755(2), Al(1)–N(1) 1.920(19), Al(1)–C(1) 1.967(4); Al(1)–O(1)–Ga(1) 145.00(14), Al(1)–O(1)–Ga(2) 120.25(13), O(1)–Ga(1)–O(2) 84.73(9), Ga(1)–O(2)–Ga(2) 95.78(9), Ga(1)–O(2)–Al(2) 141.57(13), Ga(2)–O(2)–Al(2) 122.65(12), N(1)–Al(1)–N(2) 96.19(12), N(1)–Al(1)–O(1) 114.44(8).

The molecular structure of **10** is analogous to that of **9**. Thus, compound **10** also exists as a dimer and contains reactive hydride groups on the central gallium atoms of the planar Ga_2O_2 ring. The terminal C_3N_2Al rings are arranged in an approximately perpendicular manner with respect to the central Ga_2O_2 ring. Also, the methyl groups on the terminal aluminum centers are *cis* with respect to each other. The average O–Ga–O and Ga–O–Ga angles within the Ga_2O_2 ring are 84.73 and 95.27° respectively. This may be compared with those observed in $[tBuOGaH_2]_2$ (101.4°).^[150] The slightly wider angle in the latter is perhaps due to the bulky *t*Bu group that elongates the O–O diagonal in the four-membered ring. Exocyclic Al–O–Ga angles in **10** are 121.44 and 143.28° respectively. The terminal Al–O distance in **10** (1.746 \AA) is similar to that found in **9**. The Ga–O distance within the Ga_2O_2 ring (1.917(2) – 1.939(2) \AA , av. 1.928 \AA) is similar to those found in gallium alkoxides for example $[tBuOGaH_2]_2$ (Ga–O 1.908 \AA)^[150] and in $[Me_2NCH_2CH_2OGaH_2]_2$ (Ga–O 1.911 \AA).^[159]

2.3.2. Reaction of LAl(Me)OH (**7**) with $\text{Sb(NMe}_2)_3$

Antimony exists in nature as sulphide minerals stibnite Sb_2S_3 , ullmanite NiSbS , livingstonite HgSb_4S_8 , jamesonite $\text{FePb}_4\text{Sb}_6\text{S}_{14}$ etc. Small amounts of oxide minerals are also known, e.g. valentinite Sb_2O_3 , cervantite Sb_2O_4 and stibiconite $\text{Sb}_2\text{O}_4 \cdot \text{H}_2\text{O}$, formed by weathering.^[41] Organometallic oxides of antimony containing aluminum as a second metal are limited only to $[(\text{oep})(\text{Me})\text{Sb}-\text{O}-\text{Al}(\text{oep})]\text{ClO}_4$.^[107] The reaction of LAl(Me)OH (**7**) with $\text{Sb(NMe}_2)_3$ leads to the deprotonation of **7** and formation of **11**, a mixed metal oxide of aluminum and antimony containing $(\text{Al}-\text{O})_2\text{Sb}-\text{N}$ framework (Scheme 13).



Scheme 13. Preparation of the β -diketiminate aluminum–antimony oxide

The ^1H NMR spectrum of **11** shows that two halves of the molecule resonate at slightly different frequencies. The $\text{Al}-\text{Me}$ resonances are observed at -0.57 and -0.34 ppm which is expected based on the solid state structure of **11**. The SbNMe_2 protons resonate at 2.51 ppm. The EI mass spectrum of **11** shows the peaks assignable only to the ligand and its fragments.

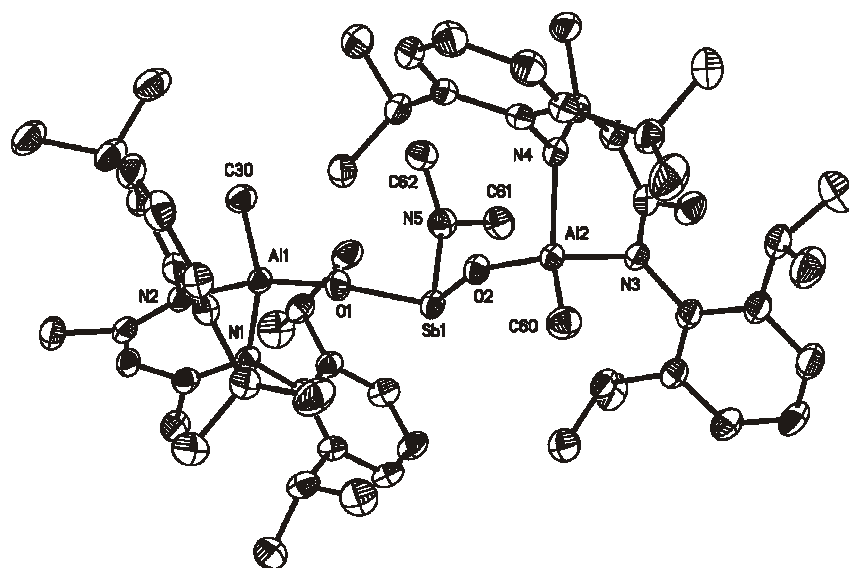


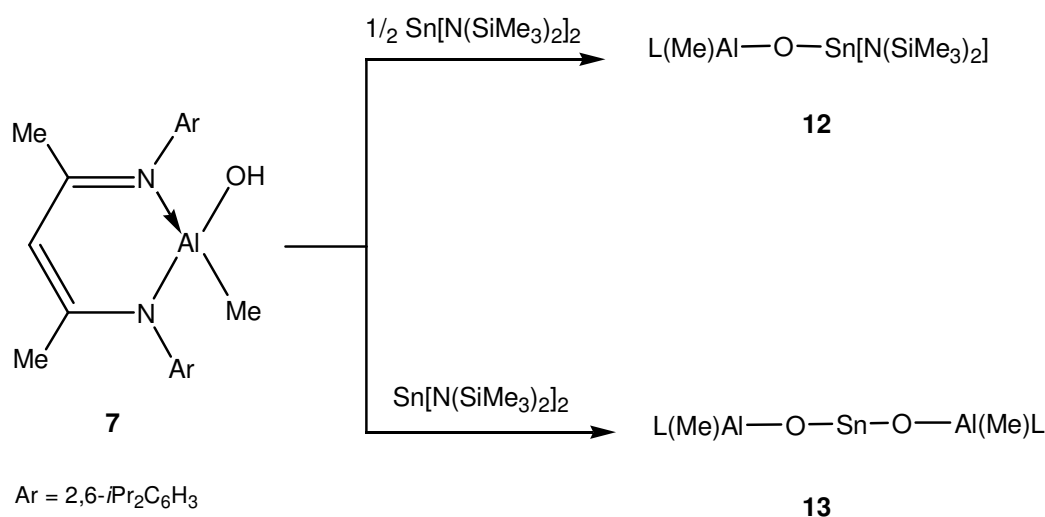
Figure 11. Molecular crystal structure of $[\text{LAl}(\text{Me})(\mu\text{-O})]_2\text{Sb}(\text{NMe}_2)$ (**11**). Thermal ellipsoids are shown with 50 % probability. The hydrogen atoms of the C–H bonds are omitted for clarity. Selected bond lengths [\AA] and angles $^\circ$]: Al(1)–O(1) 1.709(2), Al(2)–O(2) 1.714(2), Sb(1)–O(1) 1.925(2), Sb(1)–O(2) 1.928(2), Sb(1)–N(5) 2.017(3), Al(1)–N(1) 1.911(2), Al(1)–N(2) 1.928(3), Al(2)–N(3) 1.916(2), Al(2)–N(4) 1.929(3), Al(1)–C(30) 1.965(3), Al(2)–C(60) 1.953(3); O(1)–Sb(1)–O(2) 95.99(8), C(30)–Al(1)–O(1) 117.29(2), C(60)–Al(2)–O(2) 116.39(2), N(1)–Al(1)–N(2) 96.40(2), N(3)–Al(2)–N(4) 95.51(1), O(1)–Sb(1)–N(5) 96.00(2), O(2)–Sb(1)–N(5) 100.54(2), Al(1)–O(1)–Sb(1) 138.83(1), Al(2)–O(2)–Sb(1) 151.83(1), N(1)–Al(1)–C(30) 100.66(2), N(2)–Al(1)–C(30) 108.63(1), N(3)–Al(2)–C(60) 111.76(2), N(4)–Al(2)–C(60) 113.70(2).

Single crystals of **11** suitable for single crystal X-ray analysis were obtained from a *n*hexane solution. Compound **11** crystallizes in space group $P\bar{1}$. The X-ray structure of **11** supports the composition expected based on ^1H NMR spectral measurement that 2 eqv. of $\text{LAl}(\text{Me})\text{OH}$ (**7**) reacts with 1 eqv. of $\text{Sb}(\text{NMe}_2)_3$. The terminal aluminum atoms in **11** form highly distorted tetrahedron and the Sb atom resides in a bent conformation of the O(1)–Sb(1)–O(2) framework

with a bond angle of $95.99(8)^\circ$. The Sb(1)–N(5) bond length is $2.017(3)$ Å whereas the Sb–O bond lengths are $(1.928(2)$ and $1.925(2)$ Å, av. 1.926 Å) which is shorter than that observed in the inorganic cluster $\text{CaCu}_3\text{Cr}_2\text{Sb}_2\text{O}_{12}$ (Sb–O $2.048(6)$ Å).^[160] The Al(1)–O(1) ($1.709(2)$ Å) and Al(2)–O(2) ($1.714(2)$ Å) distances are slightly shorter compared to that of $\text{LAl}(\text{Me})\text{OH}$ (**7**) $1.731(3)$ Å.

2.3.3. Reaction of $\text{LAl}(\text{Me})\text{OH}$ (**7**) with $\text{Sn}[\text{N}(\text{SiMe}_3)_2]_2$

The majority of aluminum and tin bimetallic compounds belong to the metal alkoxide category. Aluminum and tin(II) mixed oxides are very rare compounds.^[108-112] The reaction between $\text{LAl}(\text{Me})\text{OH}$ (**7**) and $\text{Sn}[\text{N}(\text{SiMe}_3)_2]_2$ proceeds in a very controlled way. Thus, the treatment of $\text{Sn}[\text{N}(\text{SiMe}_3)_2]_2$ with 1 eqv. of **7** leads to the formation of **12**, a compound with Al–O–Sn–N framework. Formation of **12** proceeds with the elimination of 1 eqv. of $\text{HN}(\text{SiMe}_3)_2$ (Scheme 14).

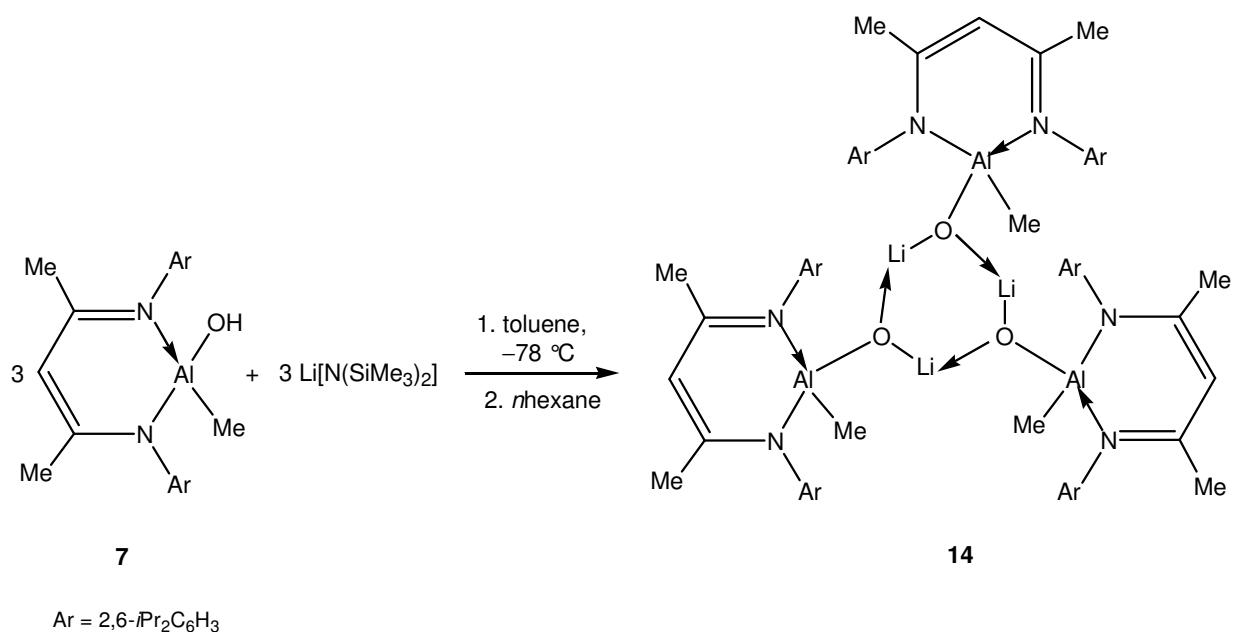


Scheme 14. Preparation of aluminum–tin(II) oxides

When $\text{Sn}[\text{N}(\text{SiMe}_3)_2]_2$ is treated with 2 eqv. of **7**, it affords compound **13**, with a Al–O–Sn–O–Al framework that proceeds with the elimination of 2 eqv. of $\text{HN}(\text{SiMe}_3)_2$ (Scheme 14). Formation of **12** and **13** was monitored by ^1H NMR spectroscopy. ^1H NMR spectra of **12** exhibits the Al–Me to resonate at -0.72 ppm and the amide protons of $\text{Sn}[\text{N}(\text{SiMe}_3)_2]$ resonate at 0.34 ppm. Other resonances are typical for the β -diketiminato ligand. In the ^1H NMR spectrum of **13**, Al–Me protons resonate at -0.80 ppm and amide protons were not detected. This indicates the complete conversion of the tin amide to the corresponding tin–aluminum oxide. The EI mass spectrum of **12** and **13** exhibit the peaks corresponding to the free ligand, L and its fragments.

2.3.4. Lithiation of $\text{LAl}(\text{Me})\text{OH}$ (**7**) and X-ray crystal structure of $[\text{LAl}(\text{Me})\text{OLi}]_3$ (**14**)

The reaction of $\text{LAl}(\text{Me})\text{OH}$ (**7**) with $\text{LiN}(\text{SiMe}_3)_2$ leads to complete deprotonation of the aluminum hydroxide to afford the lithium aluminate $[\text{LAl}(\text{Me})\text{OLi}]_3$ (**14**) as depicted in Scheme 15. Compound **14** is an off-white solid that melts at 250°C . In the IR spectrum of **14** no band corresponding to the AlO–H stretching mode was found, indicating complete deprotonation of the aluminum hydroxide. The EI mass spectrum of **14** exhibits the base peak at m/z 459 attributed to $[\text{M}^+ - \text{Me} - \text{Li}]$. The ^7Li NMR exhibits the lithium atom to resonate at 1.97 ppm, and ^1H NMR spectrum of **14** shows the Al–Me to resonate at -1.70 ppm and the γ -CH at 4.98 ppm.



Scheme 15. Preparation of the lithium aluminate

The unambiguous molecular structure of **14** was determined by single crystal X-ray structural analysis. Single crystals of **14** suitable for X-ray structural analysis were obtained from a *n*hexane solution. Compound **14** crystallizes in the hexagonal system, space group $P6(3)$ with a *n*hexane molecule as solvent of crystallization. Compound **14** exists as a trimer in the solid state. The molecular structure of **14** is shown in Figure 12 and the perspective view of the packing in the asymmetric unit of **14** and *n*hexane molecules filling the channels is shown in Figure 13.

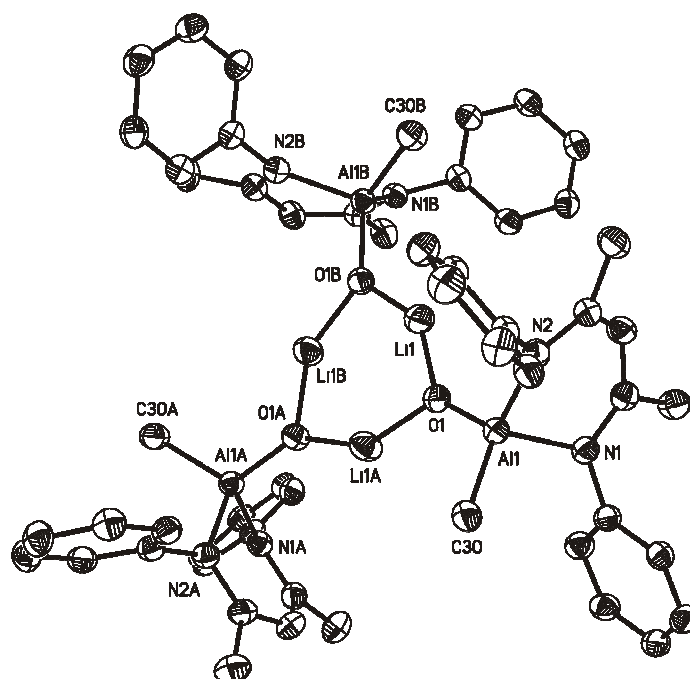


Figure 12. Molecular crystal structure of $[\text{LiAl}(\text{Me})\text{OLi}]_3$ (**14**). Thermal ellipsoids are shown with 50 % probability. The hydrogen atoms of the C–H bonds and hexane molecule are omitted for clarity. Selected bond lengths [\AA] and angles[$^\circ$]: Al(1)–O(1) 1.699(2), Al(1)–C(30) 1.972(2), Li(1)–O(1) 1.795(3), Li(1A)–O(1) 1.804(3), Li(1)–O(1B) 1.804(3), Al(1)–N(1) 1.983(2), Al(1)–N(2) 1.953(2), Li(1)···Li(1A) 2.716(5), Li(1)···Li(1B) 2.716(5); N(1)–Al(1)–N(2) 93.48(7), Al(1)–O(1)–Li(1) 137.34(2), C(30)–Al(1)–O(1) 117.09(8), N(2)–Al(1)–C(30) 115.57(8), N(1)–Al(1)–O(1) 112.05(7), N(2)–Al(1)–O(1) 111.30(6), Li(1A)–O(1)–Li(1) 98.00(2), O(1)–Li(1)–O(1B) 142.01(2).

Compound **14** forms a trimer of the $\text{LiAl}(\text{Me})\text{OLi}$ unit with a central six-membered Li_3O_3 ring, the terminal Al atoms in the chelated ligand rings are arranged in a perpendicular manner with respect to the central Li_3O_3 ring. The Al(1)–O(1) distance of 1.699(2) \AA is shorter than the distance in its parent compound $\text{LiAl}(\text{Me})\text{OH}$ (**7**) (1.731(3) \AA). The Li(1)–O(1) distance (1.795(3) and 1.804(3) \AA) observed in the central Li_3O_3 ring are in general considerably shorter than those

found in $[\text{Me}_2\text{AlN}(\text{2-C}_5\text{H}_4\text{N})\text{Ph}]_2(\text{O})\text{Li}_2 \cdot 2 \text{ THF}$ (1.89 Å),^[120] $[\text{Li}(\text{THF})_2(\mu\text{-O}(\text{---})\text{Menthol})_2\text{Al}(\text{H})_2] \cdot \text{THF}$ (av. 1.944 Å),^[118] $(\text{2,6-}i\text{Bu}_2\text{C}_6\text{H}_3\text{O})_2\text{Al}(\text{O-}i\text{nBu})_2\text{Li} \cdot 2 \text{ THF}$ (av. 1.960 Å),^[118] $[(\text{2,6-}i\text{Pr}_2\text{C}_6\text{H}_3\text{O})\text{Al}(\text{H})(\mu\text{-OC}_6\text{H}_3\text{-2,6-}i\text{Pr}_2)_2\text{Li}(\text{Et}_2\text{O})]$ (1.912 Å),^[118] $[\{ \text{2,4-}(\text{H})_2\text{-6-(CH}_2\text{NH-(2,6-}i\text{Pr}_2\text{C}_6\text{H}_3))\text{C}_6\text{H}_2\text{O} \}_2\text{Al}]\text{Li} \cdot \text{THF}$ (1.962 Å),^[117] and $[\{ (\text{2,4-}i\text{Bu})_2\text{-6-(CH}_2\text{NH-}i\text{Bu})\text{C}_6\text{H}_2\text{O} \}_2\text{Al}]\text{Li} \cdot \text{THF}$ (1.98 Å).^[117] The Li...Li separation within the ring is 2.716(5) Å. The exocyclic Al(1)–O(1)–Li(1) and C(30)–Al(1)–O(1) bond angle is 137.34(2) and 117.09(8)° respectively, whereas the endocyclic Li(1A)–O(1)–Li(1) bond angle is 98.00(2)°. The *n*hexane molecules in the crystal lattice of **14** occupy six symmetrically equivalent positions due to the *P*6(3) space group. The *n*hexane molecules pack the channels generated by the arrangement of the peripheral β -diketiminato ligands in the crystal lattice of **14**.

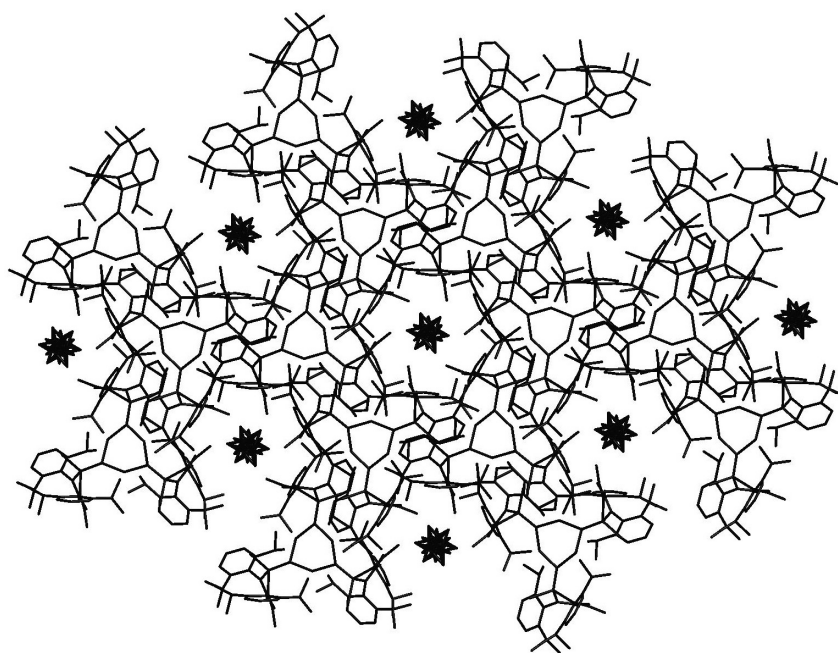
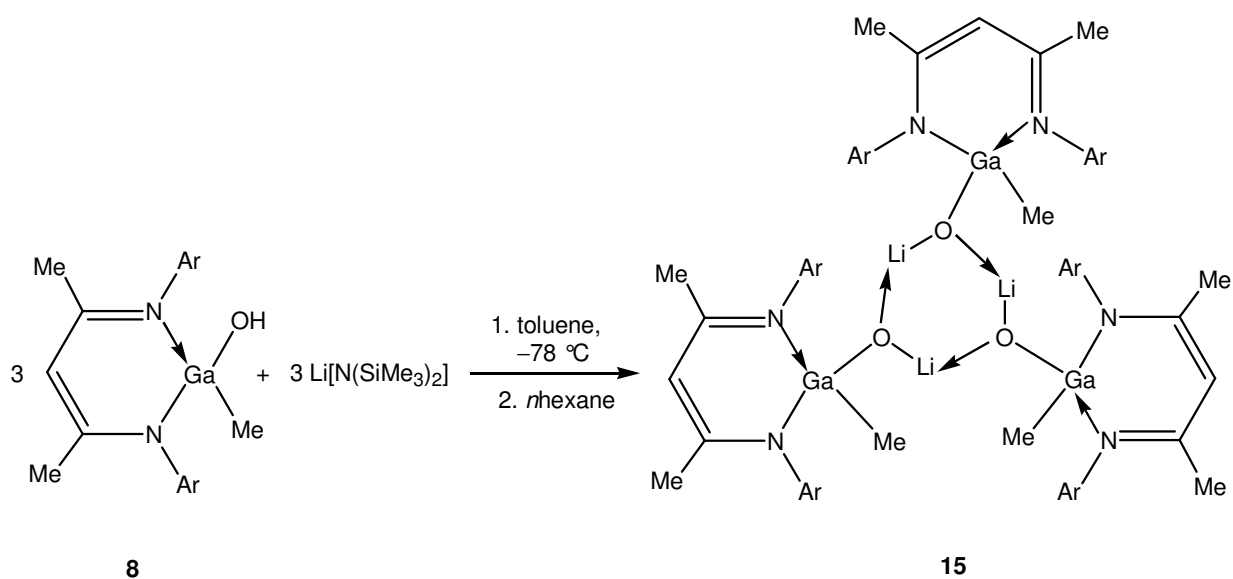


Figure 13. Perspective view of the packing in the asymmetric unit of $[\text{LaI}(\text{Me})\text{OLi}]_3$ (**14**). The *n*hexane molecules fill the channels between the molecules of **14** and are disordered in six symmetrically equivalent positions.

2.4. Reaction of LGa(Me)OH (**8**); syntheses of heterobimetallic derivatives

2.4.1. Lithiation of LGa(Me)OH (**8**) and X-ray crystal structure of [LGa(Me)OLi]₃ (**15**)

The reaction of LGa(Me)OH (**8**) with LiN(SiMe₃)₂ leads to complete deprotonation of the gallium hydroxide to afford the lithium gallate [LGa(Me)OLi]₃ (**15**) as depicted in Scheme 16. Compound **15** is an off-white solid that melts with decomposition at 280 °C. In the IR spectrum of **15** no band corresponding to the GaO–H stretching mode was found. The EI mass spectrum of **15** exhibits the base peak at *m/z* 503 which can be assigned to [*M*⁺ – Me – Li]. The ⁷Li NMR exhibits the lithium atom to resonate at 1.92 ppm, and the ¹H NMR spectrum of **15** shows the Ga–Me to resonate at –0.60 ppm and the γ-CH at 4.82 ppm.



Ar = 2,6-*i*Pr₂C₆H₃

Scheme 16. Preparation of the lithium gallate

The molecular geometry of **15** was determined by the aid of single crystal X-ray structural analysis. Single crystals of **15** suitable for X-ray structural analysis were obtained from its

*n*hexane solution. Compound **15** crystallizes in the hexagonal system in space group $P6(3)$, therefore **15** is isomorphous to its aluminum analogue **14**. Thus, compound **15** exists as a trimer in the solid state. Perspective view of the molecular structure of **15** is shown in Figure 14.

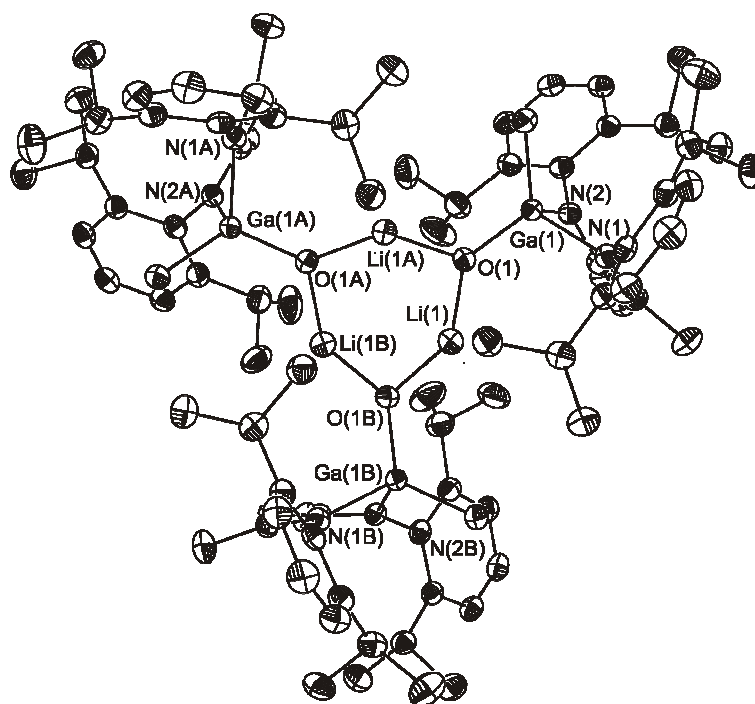
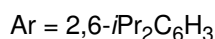
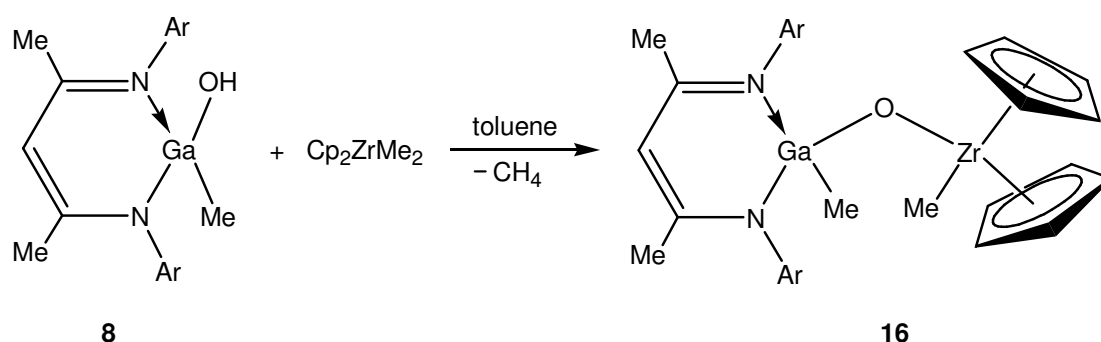


Figure 14. Molecular crystal structure of $[LGa(Me)OLi]_3$ (**15**). Thermal ellipsoids are shown with 50 % probability. The hydrogen atoms of the C–H bonds and hexane molecule are omitted for clarity. Selected bond lengths [Å] and angles[°]: Ga(1)–O(1) 1.783(2), Ga(1)–C(6) 1.973(2), Li(1)–O(1) 1.776(3), Ga(1)–N(1) 2.017(2), Ga(1)–N(2) 1.998(2), Li(1)···Li(1A) 2.734(5), Li(1)···Li(1B) 2.734(5), Li(1A)–O(1) 1.806(3), Li(1)–O(1B) 1.806(3); N(1)–Ga(1)–N(2) 92.24(6), Ga(1)–O(1)–Li(1) 135.32(2), C(6)–Ga(1)–O(1) 119.41(7), N(1)–Ga(1)–C(6) 112.79(8), N(2)–Ga(1)–C(6) 110.49(8), N(1)–Ga(1)–O(1) 109.50(6), N(2)–Ga(1)–O(1) 109.02(7), Li(1A)–O(1)–Li(1) 99.52(2), O(1)–Li(1)–O(1B) 140.47(2).

The Li(1)–O(1) bond length observed in **15** (1.776(3) Å) is slightly shorter than that of the aluminum analogue **14** (1.795(3) Å) but significantly shorter than those found in [Ga₃Li₄(*t*Bu)₆(neol)₃(OH)(THF)] (1.80(4) to 1.99(4) Å),^[121] [Ga₂Li(*t*Bu)₄(OH)₂(neol-H)] (1.82(1) to 1.90(1) Å),^[121] and {[SiMe₃)₃CGa(OH)(I)(OCMe₃)]Li}₂ (1.923(7) to 1.956(7) Å).^[125] The Ga(1)–O(1) bond length (1.783(2) Å) in **15** is shorter than that in the corresponding hydroxide LGa(Me)OH (1.831(1) Å). The exocyclic Ga(1)–O(1)–Li(1) and C(6)–Ga(1)–O(1) bond angle is 135.32(2) and 119.41(7)° respectively, whereas the endocyclic Li(1A)–O(1)–Li(1) bond angle is 99.52(2)°.

2.4.2. Reaction of LGa(Me)OH (**8**) with Cp₂ZrMe₂

The reaction of LGa(Me)OH (**8**) with Cp₂ZrMe₂ in toluene leads to methane evolution and the formation of LGa(Me)(μ-O)Zr(Me)Cp₂ (**16**) (Scheme 17). Compound **16** represents the first example of an X-ray characterized molecule with a Ga–O–Zr core. Compound **16** has been unambiguously characterized by means of spectroscopic, spectrometric and crystallographic techniques.



Scheme 17. Preparation of β-diketiminato gallium–zirconium oxide

Compound **16** is a colorless crystalline solid and melts with decomposition at 318 °C. The EI mass spectrum of **16** reveals a peak at m/z 739 due to $[M^+-Me]$. The 1H NMR resonances (-0.12 and -0.32 ppm) for **16** correspond to $Zr-Me$ and $Ga-Me$, respectively. The other resonances for **16** are characteristic for the β -diketiminate ligand, L and protons of the cyclopentadienyl rings. Single crystals of **16** suitable for X-ray structural analysis were obtained from its toluene solution. The molecular structure of **16** is shown in Figure 15. Compound **16** crystallizes in the monoclinic space group $P2_1/n$.

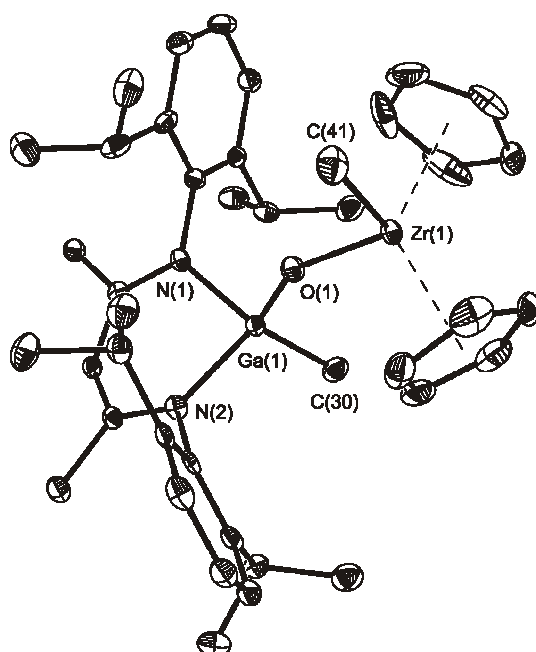


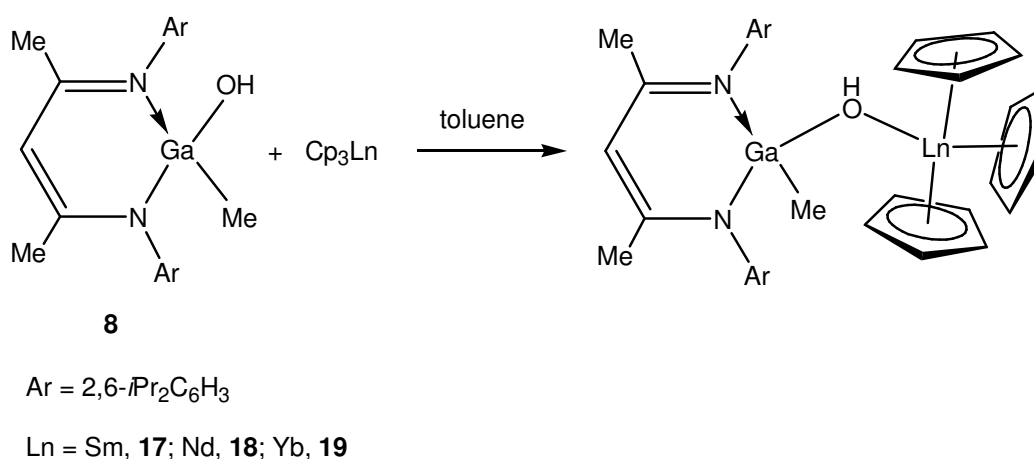
Figure 15. Molecular crystal structure of $LGa(Me)(\mu-O)Zr(Me)Cp_2$ (**16**). Thermal ellipsoids are shown with 50 % probability. The hydrogen atoms of the C–H bonds are omitted for clarity. Selected bond lengths [\AA] and angles[$^\circ$]: Ga(1)–O(1) 1.815(1), Ga(1)–N(1) 1.975(2), Ga(1)–N(2) 1.967(2), Ga(1)–C(30) 1.971(2), Zr(1)–O(1) 1.926(1), Zr(1)–C(41) 2.301(3); O(1)–Ga(1)–N(1) 109.0(1), O(1)–Ga(1)–N(2) 109.8(1), N(1)–Ga(1)–N(2) 96.1(1), O(1)–Ga(1)–C(30) 116.2(1), N(1)–Ga(1)–C(30) 112.3(1), N(2)–Ga(1)–C(30) 111.7(1), Ga(1)–O(1)–Zr(1) 146.7(1), O(1)–Zr(1)–C(41) 102.0(1).

The Ga atom exhibits a highly distorted tetrahedral geometry with two nitrogen atoms of the β -diketimate ligand, one Me group and an (μ -O) unit. The coordination sphere of Zr is completed by two Cp ligands and one Me group and an oxide group. The Me groups in **16** are bent out of the Ga–O–Zr plane in a *trans* manner. The Ga–(μ -O) bond length (1.815(1) Å) in **16** is slightly shorter than the Ga–O distance in LGa(Me)OH (**8**) (1.831(1) Å) and is shorter in other Ga–(μ -O) derivatives for example 1.910 Å in (MesGaO)₉^[161] and 1.898 Å in (Mes₂GaOLi)₂·4 THF.^[88] The Ga–O–Zr angle (146.7(1)°) lies between Ga–O–Ga angle (91.9(1)° in (Mes₂GaOLi)₂·4 THF^[88] and 100.6(2)° in [(*t* BuO)₂GaH]₂)^[150] and Zr–O–Zr angle (174.1(3)° in [Cp₂Zr(Me)]₂(μ -O)).^[162] The Zr(μ -O) bond length (1.926(1) Å) is slightly shorter than those exhibited by compounds [(Cp₂ZrCl)₂(μ -O)] (1.945(3) Å),^[163] [(Cp₂ZrMe)]₂(μ -O) (1.948(1) Å)^[162] and [{(Cp₂Zr)(μ -O)₃}] (1.959(3) Å),^[164] but significantly shorter than the Zr–(μ -O) or Zr–(μ -OH) bond lengths observed in the clusters [(Cp*Zr)₆(μ_4 -O)(μ -O)₄(μ -OH)₈]·2 (C₇H₈) (~ 2.106 Å)^[165] and [{(Cp*ZrCl)(μ -OH)}₃(μ_3 -OH)(μ_3 -O)]·2 THF (2.160(2) Å).^[166] The Zr–Me bond length (2.301(3) Å) in **16** is longer than that found in (Cp₂ZrMe)₂(μ -O) (2.276(9) Å).^[162]

2.4.3. Reaction of LGa(Me)OH (**8**) with Cp₃Ln (Ln = Sm (**17**), Nd (**18**), Yb (**19**))

Heterobimetallic compounds of gallium containing lanthanide atoms are extremely rare and so far no structural investigations have been carried out. The only known compounds to this category are those double isopropoxides of gallium and lanthanides reported by Mehrotra and co-workers.^[127]

Reaction of LGa(Me)OH (**8**) with 1 eqv. of Cp₃Ln was carried out in toluene at room temperature to afford the adducts LGa(Me)(μ -OH)LnCp₃ (Ln = Sm (**17**), Nd (**18**), Yb (**19**)) as shown in Scheme 18 in good yields accompanied by color change and precipitate formation.



Scheme 18. Preparation of β -diketiminate methylgalliumhydroxide lanthanide adducts

Compounds **17** and **19** are stable yellow solids, **17** melts at 275 °C and **19** melts with decomposition at 275 °C. Compound **18** is blue–green in color that melts with decomposition at 254 °C. As observed in the IR spectrum of these adducts, elimination of CpH did not occur and the (μ -OH) stretching frequency was observed at 3592, 3591, and 3609 cm⁻¹ respectively, for **17**, **18** and **19**. These frequencies are shifted to lower wave numbers when compared to that of LGa(Me)OH (**8**) observed at 3676 cm⁻¹ which also confirms that the hydroxide group bridges between Ga and Ln atoms. This is contrary to the reaction of the corresponding aluminum hydroxide LAl(Me)OH (**7**) with Cp₃Ln where the elimination of CpH occurred. This indicates that the LGa(Me)OH (**8**) is less acidic than LAl(Me)OH (**7**).

2.4.4. Molecular crystal structure of LGa(Me)(μ -OH)LnCp₃ (Ln = Sm (**17**), Nd (**18**))

Single crystals of **17**, and **18** were obtained from a toluene solution, Figures 16 and 17 show the molecular structures of **17** and **18** respectively. Compounds **17** and **18** are isomorphous and crystallize in the space group *P2₁/m*. The data of **17** and **18** are merohedrally twinned. The twin operation in both cases is a two-fold axis along the reciprocal axis 001. The hydrogen atom

on the bridging hydroxo group i.e., O(1) in compound **17** can not be located in the electron density map probably due to the refinement against non merohedrally twinned data. However, its presence was confirmed by the infrared spectrum and also due to the presence of three cyclopentadienyl rings connected to the samarium atom. Lanthanide ion possesses a pseudotetrahedral geometry surrounded by three cyclopentadienyl rings and an oxygen atom. The Ga atom forms a distorted tetrahedron with two nitrogen atoms of the β -diketiminato ligand, one carbon atom and an oxygen atom.

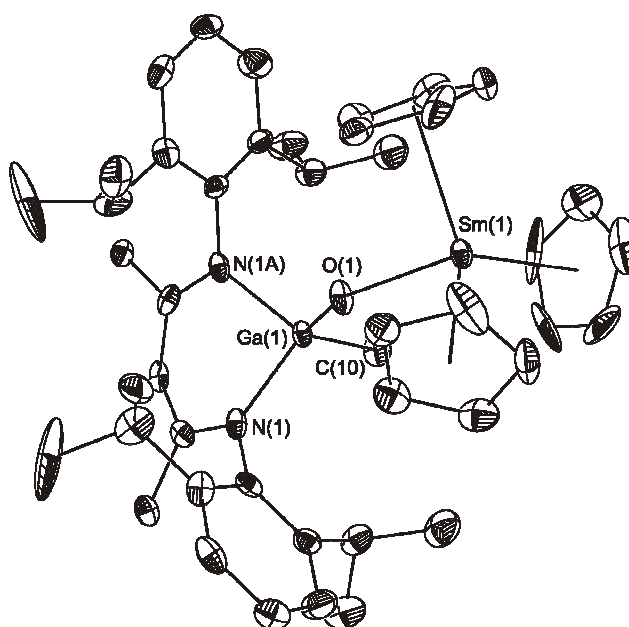


Figure 16. Molecular crystal structure of $\text{LGa(Me)}(\mu\text{-OH})\text{SmCp}_3$ (**17**). Thermal ellipsoids are shown with 50 % probability. Hydrogen atoms are omitted for clarity. Selected bond lengths [Å] and angles[°]: Ga(1)–C(10) 1.971(2), Ga(1)–O(1) 1.862(7), Ga(1)–N(1) 1.963(7), Ga(1)–N(2) 1.963(7), Sm(1)–O(1) 2.465(7); Ga(1)–O(1)–Sm(1) 149.3(4), O(1)–Ga(1)–N(1) 108.1(2), O(1)–Ga(1)–N(2) 108.1(2), N(1)–Ga(1)–N(2) 95.4(4), N(1)–Ga(1)–C(10) 114.0(3), N(2)–Ga(1)–C(10) 114.0(3).

The Ga(1)–O(1) bond length in compound **17** (1.862(7) Å) is longer than that found in LGa(Me)OH (1.831(1) Å). The Sm(1)–O(1) bond length of 2.465(7) Å is significantly shorter than the corresponding aluminum compound $\text{LAl(Me)}(\mu\text{-OH})\text{SmCp}_3$ (2.500(4) Å)^[48] but longer than that of $[\text{Cp}^*_2\text{Sm}(\mu\text{-O}_2\text{CSPh})]_2$ (2.328(2) Å).^[167] The Ga(1)–O(1)–Sm(1) core is bent with an angle of 149.3(4)° which is comparable to that of $\text{LAl(Me)}(\mu\text{-OH})\text{SmCp}_3$ (151.9(2)°).

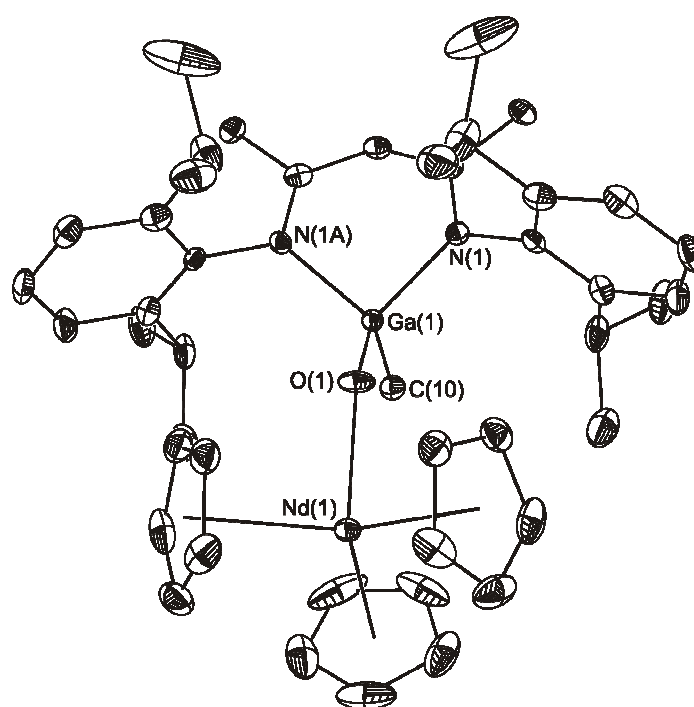


Figure 17. Molecular crystal structure of $\text{LGa(Me)}(\mu\text{-OH})\text{NdCp}_3$ (**18**). Thermal ellipsoids are shown with 50 % probability. Hydrogen atoms are omitted for clarity. Selected bond lengths [Å] and angles[°]: Ga(1)–C(10) 1.961(5), Ga(1)–O(1) 1.851(3), Ga(1)–N(1) 1.956(3), Ga(1)–N(2) 1.956(3), Nd(1)–O(1) 2.479(3); Ga(1)–O(1)–Nd(1) 149.71(2), O(1)–Ga(1)–N(1) 108.40(2), O(1)–Ga(1)–N(2) 108.40(2), N(1)–Ga(1)–N(2) 95.68(2), N(1)–Ga(1)–C(10) 114.13(2), N(2)–Ga(1)–C(10) 114.13(2).

Single crystals of **18** suitable for X-ray structural analysis were obtained from its toluene solution. Compound **18** crystallizes in space group $P2_1/m$ and is isomorphous to its samarium analogue **17**. Both the Ga atom and the Nd atom form a distorted tetrahedron and are connected through a bridging hydroxo group. The Ga(1)–O(1) bond length (1.851(3) Å) in **18** is longer than that found in its parent compound LGa(Me)OH (1.831(1) Å). This elongation is expected due to coordination of the oxygen atom to the other metal atom in **17** and **18**. The Nd(1)–O(1) bond length of 2.479(3) Å is longer as compared to the bridging Nd–O bond lengths in Nd₅O(O-*i*Pr)₁₃ (2.304(12) to 2.345(11) Å) but significantly shorter than the terminal Nd–O bond lengths (2.082(11) to 2.123(11) Å).^[168] The Ga(1)–O(1)–Nd(1) core is bent with an angle of 149.71(2)° which is comparable to its samarium analogue **17** (149.3(4)°).

2.5. N-Heterocyclic carbene complexes of gold(I)

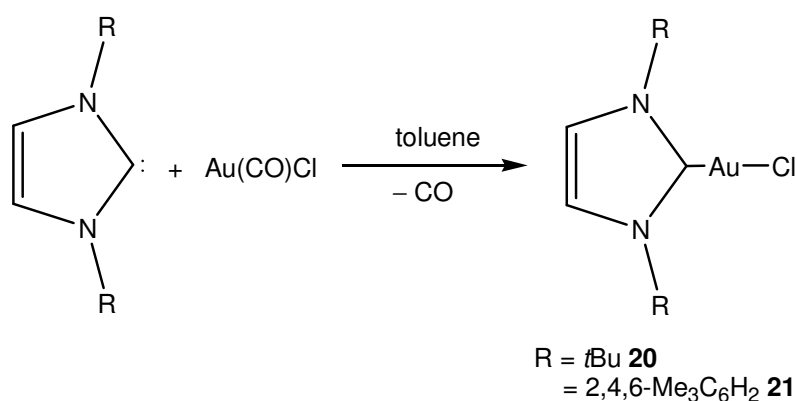
2.5.1. Synthesis and X-ray crystal structure of *C*_{tBu}AuCl (**20**) and *C*_{Mes}AuCl (**21**)

The first metal carbene complexes of *N*-heterocyclic carbenes were reported independently in 1968 by Wanzlick and Schönherr,^[169] and Öfele.^[170] It was not until the isolation of free carbenes in 1991 by Arduengo *et al.* that generated significant interest in *N*-heterocyclic carbenes and their complexes.^[171] *N*-heterocyclic carbene complexes of gold are relatively uncommon, the majority of these being linear two-coordinate gold(I) complexes.^[172-178] Linear complexes are useful models for theoretical studies and are also practically suitable for determining the electronic characteristics of metal ligand bonding through structural studies, since in linear systems steric factors are expected to play a less significant role than in complexes with other geometries.^[172,173,179-181]

The reported methods involve either tedious synthesis and generate *bis* carbene complexes, or the cleavage of polynuclear derivative which is always not a simple process, especially with

gold(I) derivatives and often results in oxidative addition reactions and mixed valence or gold(III) derivatives.^[135,144,145,181,182] The advantage of the present method lies in the fact that it leads to the formation of monocarbene gold(I) complexes as a sole product rather than the known ligand substitution reactions of RAuCl ($\text{R} = \text{PPh}_3$ or Me_2S) to prepare *biscarbene* gold(I) complexes.

The reaction of $\text{Au}(\text{CO})\text{Cl}$ with a stoichiometric amount of *N*-heterocyclic carbene (1,3-di-*tert*-butylimidazol-2-ylidene or 1,3-di-mesitylimidazol-2-ylidene) in toluene at room temperature results in a vigorous evolution of carbon monoxide and the formation of the corresponding carbene adducts **20** and **21** respectively (Scheme 19). Thus this synthetic method represents a viable and rational route for the preparation of *N*-heterocyclic carbene adducts of $\text{Au}(\text{I})$.



Scheme 19. Synthesis of *N*-heterocyclic carbene complexes of $\text{Au}(\text{I})$

Compounds **20** and **21** have been unambiguously characterized by means of spectroscopic, spectrometric, and crystallographic techniques. Both **20** and **21** are colorless crystalline solids and are thermally stable. They decompose with melting at 170 °C and 210 °C respectively. The EI mass spectrum of **20** revealed that the most intense peak appears at m/z 320 and corresponds to the loss of one *tert*-butyl group and the chlorine atom from the molecular ion. A similar fragment

at m/z 303 in **21** is due to $[M^+ - Cl - Au - H]$. The 1H NMR spectrum of **20** exhibits two singlets (1.83 and 7.26 ppm) for the protons of the *tert*-butyl groups and ($HC=CH$) of the carbene. They are shifted downfield relative to the 1,3-di-*tert*-butylimidazol-2-ylidene (1.51 and 7.06 ppm). The resonances of *o*-Me and *p*-Me in **21** (1.75 and 2.13 ppm) are observed upfield relative to the carbene (2.08 and 2.31 ppm) whereas the ($HC=CH$) protons in **21** (7.46 ppm) are found downfield relative to the carbene (7.07 ppm). A weak ^{13}C NMR resonance (167.6 ppm for **20**) can be assigned to the carbene carbon atom. However, in case of **21** no resonance downfield to 150 ppm was detected which could be assigned to the carbene carbon.

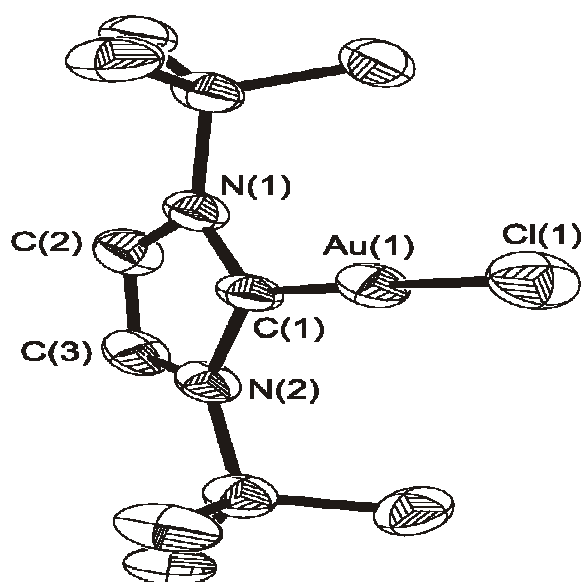


Figure 18. Molecular crystal structure of $C_{tBu}AuCl$ (**20**). Thermal ellipsoids are shown with 50% probability. Toluene molecule and hydrogen atoms are omitted for clarity. Selected bond lengths [\AA] and angles[$^\circ$]: Au(1)—C(1) 1.983(8), Au(1)—Cl(1) 2.290(2), N(1)—C(1) 1.376(9), N(2)—C(1) 1.362(1), C(2)—C(3) 1.315(1); C(1)—Au(1)—Cl(1) 178.9(2), N(2)—C(1)—N(1) 104.5(7), N(1)—C(1)—Au(1) 128.4(5), N(2)—C(1)—Au(1) 127.1(5).

Single crystals of **20** and **21** suitable for X-ray structural analysis were obtained from their toluene solutions. Compound **20** crystallizes with one molecule of toluene. The molecular structures of **20** and **21** are shown in Figures 18 and 20, respectively. Compound **20** crystallizes in the monoclinic space group $P2_1/c$ whereas compound **21** crystallizes in the orthorhombic space group $Fdd2$. The X-ray crystal structures of **20** and **21** reveal that the compounds are monomeric adducts of the *N*-heterocyclic carbene Au(I) chloride, no Au(I)–Au(I) interactions were observed.

The Au–Cl distances 2.290(2) Å in **20** and 2.281(4) Å in **21** are shorter than the Au–Cl distance in $[\text{Au}(\text{Me}_2\text{-bimy})\text{Cl}]^{[144]}$ (2.338(2) Å) but comparable to that in $\{\text{PhCH}_2\text{N}(\text{CH})_2\text{N}(\text{COPh})\text{C}\}\text{AuCl}^{[145]}$ (2.286(2) Å) and $[\text{Au}(\text{Me}_2\text{-imyl})\text{Cl}]$ (2.288(3) Å).^[183] The Au–C bond lengths 1.983(8) Å in **20** and 1.933(1) Å in **21** are similar to those found in $[\text{Au}(\text{Me}_2\text{-bimy})\text{Cl}]$ (1.985(1) Å),^[144] $\{\text{PhCH}_2\text{N}(\text{CH})_2\text{N}(\text{COPh})\text{C}\}\text{AuCl}^{[145]}$ (1.970(1) Å) and in $[\text{Au}(\text{Me}_2\text{-imyl})\text{Cl}]^{[183]}$ (1.98(1) Å). The average N–C distances of the ligand in **20** 1.369 Å and 1.377 Å in **21** are similar to those observed in $[\text{Au}(\text{Me}_2\text{-bimy})\text{Cl}]^{[144]}$ (1.371 Å) and in $\{\text{PhCH}_2\text{N}(\text{CH})_2\text{N}(\text{COPh})\text{C}\}\text{AuCl}^{[145]}$ (1.355 Å). The N(1)–C(1)–N(2) angles within the N_2C_3 five-membered ring of the carbene ligand in **20** 104.5(7)° and 102.6(9)° in **21** are similar to that in $\{\text{PhCH}_2\text{N}(\text{CH})_2\text{N}(\text{COPh})\text{C}\}\text{AuCl}$ 104.4(1)° but are slightly smaller than those in $[\text{Au}(\text{Me}_2\text{-bimy})\text{Cl}]$ 108(1)° and in $[\text{Au}(\text{Me}_2\text{-imyl})\text{Cl}]$ (106(10)°).^[183] In the crystal lattice **20** forms an extended network through agostic interaction of Au with one proton of the *t*Bu group from a neighbouring molecule (2.96 Å) and also interacts with one *o*-H of the solvating toluene molecule (3.06 Å) present in the crystal lattice, as shown in Figure 19. These are in the range 1.95–3.20 Å reported for similar $\text{H}\cdots\text{Au}$ interactions.^[184] In the case of **21** all aromatic hydrogens are involved in hydrogen bonds. Hydrogen atoms on C(7) and C(7A) are bonded by agostic interactions to Au from two different neighbouring molecules with a $\text{H}\cdots\text{Au}$ distance of 3.18 Å, (Figure 21) which is comparable to the values in the range 1.95–3.20 Å reported for

similar H \cdots Au interactions but slightly longer than those in **20**. Hydrogen atoms present on C(5), C(5A), C(2) and C(2A) are hydrogen bonded to Cl atoms of another molecule in a symmetrical manner as shown in Figure 21. The corresponding H \cdots Cl distances are 2.88 Å and 2.90 Å which agrees with the reported values of intermediate to long range intermolecular interactions.^[184,185]

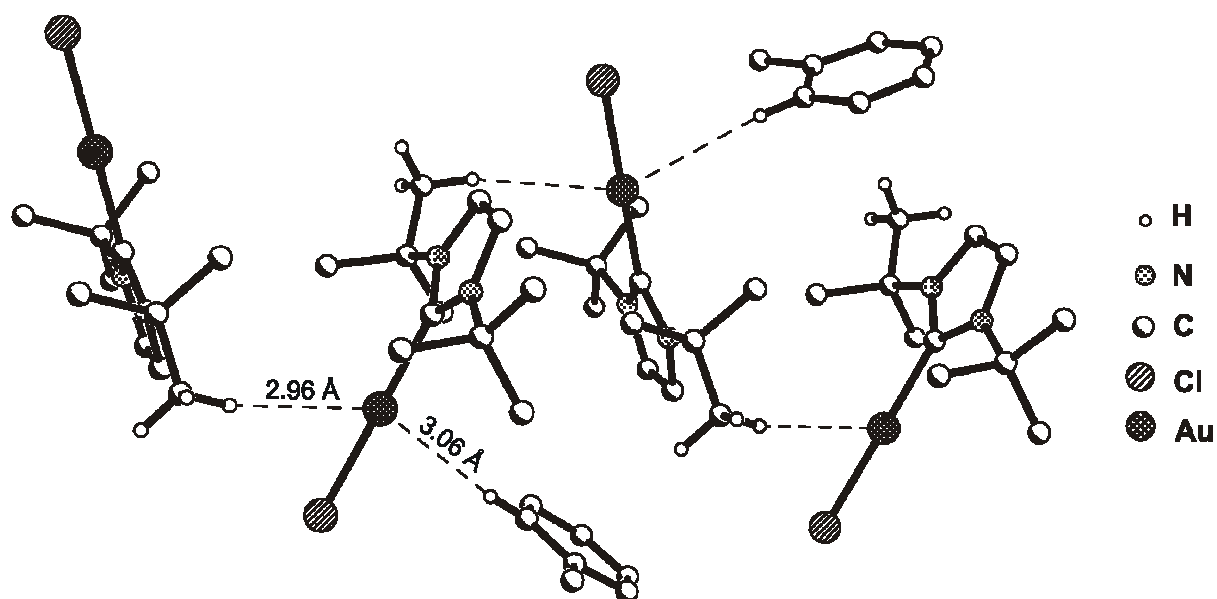


Figure 19. Perspective view of the agostic interactions of Au with *o*-H of the toluene molecule and with H atom of *t*Bu of the carbene ligand in the crystal state of C_{*t*Bu}AuCl (**20**), forming a zig-zag chain.

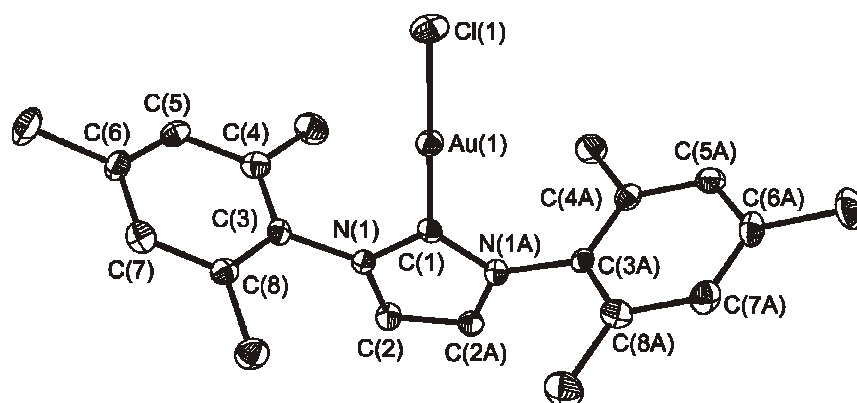


Figure 20. Molecular crystal structure of $C_{Mes}AuCl$ (**21**). Thermal ellipsoids are shown with 50% probability. Hydrogen atoms are omitted for clarity. Selected bond lengths [\AA] and angles [$^\circ$]: Au(1)—C(1) 1.933(1), Au(1)—Cl(1) 2.281(4), N(1)—C(1) 1.377(9), N(1A)—C(1) 1.377(9), C(2)—C(2A) 1.372(8); C(1)—Au(1)—Cl(1) 180.0(1), N(1A)—C(1)—N(1) 102.6(9), N(1)—C(1)—Au(1) 128.7(4), N(1A)—C(1)—Au(1) 128.7(4).

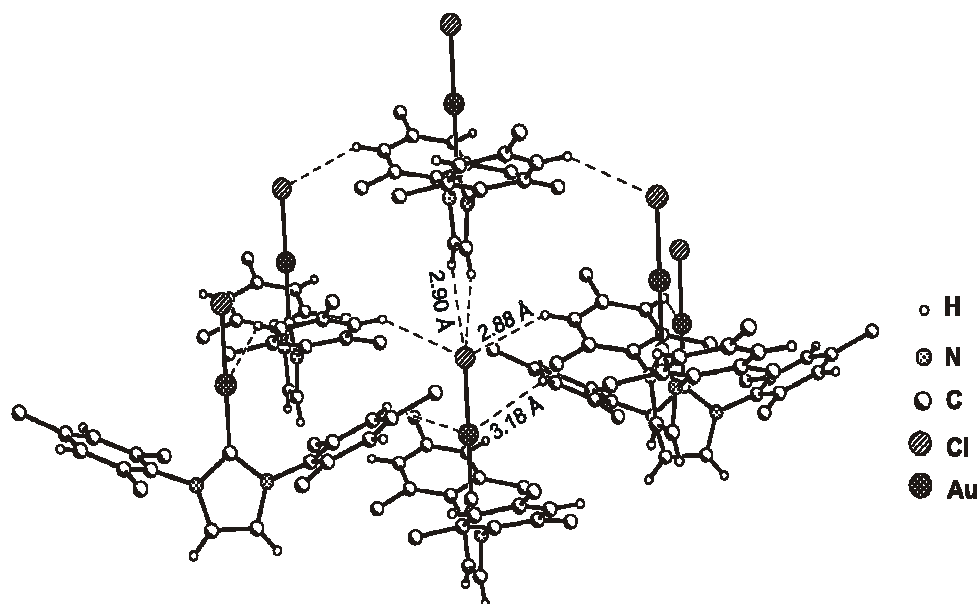


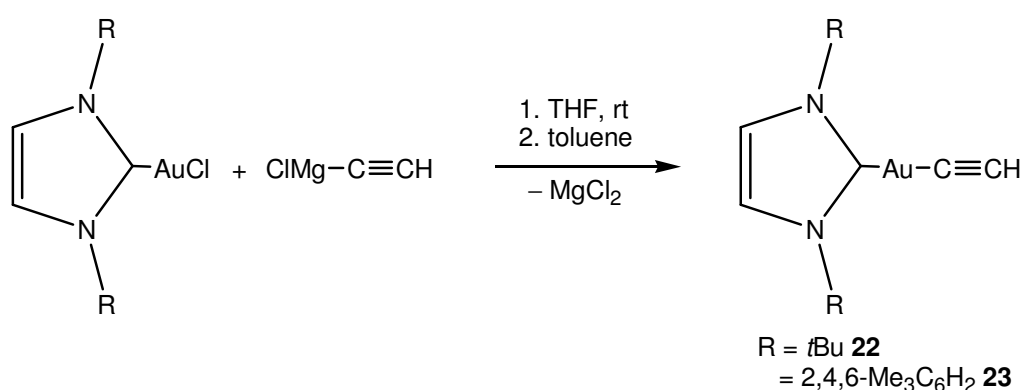
Figure 21. Perspective view of the chain formation through the agostic interaction of the aromatic protons of the carbene ligand with Au and Cl atoms in $C_{Mes}AuCl$ (**21**).

2.5.2. Preparation of $C_{tBu}AuC\equiv CH$ (22**) and $C_{Mes}AuC\equiv CH$ (**23**) and molecular crystal structure of $C_{tBu}AuC\equiv CH$ (**22**)**

Extensive research has been done on the alkynyl gold complexes, which are the most stable among all organogold complexes^[134] and often generate a variety of structural types owing to strong Au(I)-Au(I) aurophilic interaction.^[138] Ethynyl gold complexes of the type $R_3PAuC\equiv CAuPR_3$ are widely known,^[135,136] but Schmidbaur et al. isolated mononuclear $RAuC\equiv CH$ ($R = MePH_2, Me_3P$) from a mixture of mono- and dinuclear gold(I) ethynyl complexes.^[137] This shows that the nature of phosphine plays a predominant role in the synthesis of mono- and dinuclear gold(I) ethynyl complexes. Since *N*-heterocyclic carbenes are known to be better σ donor ligands compared to alkyl or aryl phosphines and thus are able to stabilize organometallic fragments, it was envisaged that gold(I) ethynyl complexes of the type $RAuC\equiv CH$ could be even more stable than the corresponding phosphine adducts.

Reaction of the adducts $C_{tBu}AuCl$ (**20**) and $C_{Mes}AuCl$ (**21**) with ethynylmagnesium chloride in THF smoothly affords the corresponding gold(I) ethynyls $C_{tBu}AuC\equiv CH$ (**22**) and $C_{Mes}AuC\equiv CH$ (**23**) in good yields (Scheme 20). Compounds **22** and **23** decompose with melting at 155 °C and 240 °C respectively. The EI mass spectrum of **22** revealed the molecular ion peak as the most intense one (m/z 402), whereas the ion at m/z 303 in **23** is the most intense peak and corresponds to the loss of Au and C_2H_2 units from the molecular ion. The IR spectrum of **22** shows a sharp band (1979 cm^{-1}) which can be attributed to the ethynyl stretching frequency. The corresponding stretching mode for **23** appears at 1982 cm^{-1} . The 1H NMR spectrum of **22** shows the ethylene proton to resonate at 1.22 ppm whereas the same proton in **23** resonates at 0.86 ppm. The resonances of the carbene ligand in **22** and **23** are shifted downfield relative to the free carbenes. The 1H NMR spectrum of **22** shows two singlets (1.84 and 7.29 ppm) for the protons of the *tert*-butyl groups and ($HC=CH$) of the carbene. They are shifted downfield relative to the free

carbene, (1.51 and 7.06 ppm). The resonances of *o*-Me and *p*-Me in **23** (2.13 and 2.34 ppm) are observed downfield (2.08 and 2.31 ppm) as well as the (*HC=CH*) protons in **23** (7.38 ppm) relative to the free carbene (7.07 ppm). A weak ^{13}C NMR resonance (187.9 ppm for **22**) can be assigned to the N–C–N carbon atom and it is shifted downfield relative to **20** (167.6 ppm).



Scheme 20. Synthesis of the monomeric terminal ethynyl Au(I) complexes

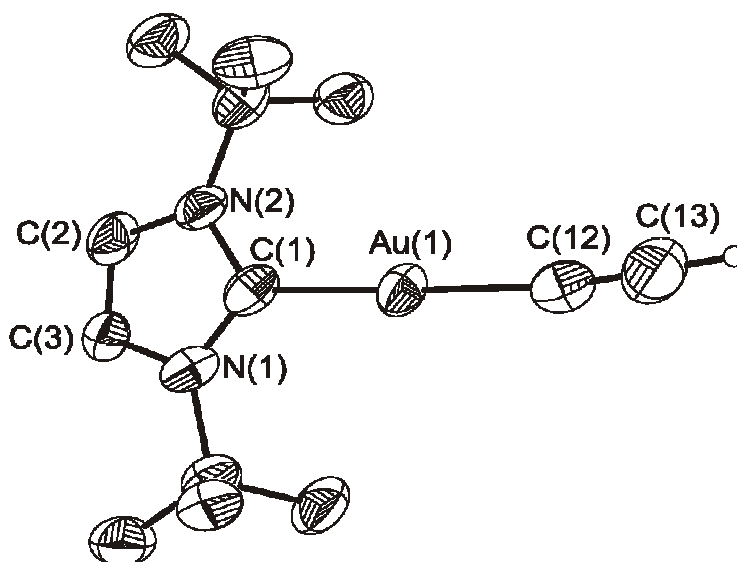


Figure 22. Molecular crystal structure for $\text{C}_{t\text{Bu}}\text{AuC}\equiv\text{CH}$ (**22**). Thermal ellipsoids are shown with 50% probability. Only the hydrogen atom on the ethynyl group is shown. The toluene molecule is omitted for clarity. Selected bond lengths [\AA] and angles[$^\circ$]: Au(1)–C(1) 2.05(1), N(1)–C(1)

1.37(2), N(2)—C(1) 1.34(2), C(2)—C(3) 1.34(2); Au(1)—C(12) 2.04(2), C(12)—C(13) 1.11(2); N(2)—C(1)—N(1) 107(1), N(1)—C(1)—Au(1) 125(2), N(2)—C(1)—Au(1) 128(1) C(1)—Au(1)—C(12) 178.7(6), Au(1)—C(12)—C(13) 171.3(2).

Single crystals of **22** suitable for X-ray structural analysis were obtained from its toluene solution. Repeated efforts to obtain a better data set for **22** were not successful due to the fast crystal decomposition caused by liberation of the solvating toluene molecules. The most optimistic data set is reported here. The molecular structure of **22** is shown in Figure 22. Compound **22** is isomorphous to **20**. The X-ray crystal structure of **22** reveals that the compound is a monomeric adduct of the *N*-heterocyclic carbene Au(I) acetylide with no Au(I)—Au(I) interactions. The Au(1)—C(2) distance of 2.05(2) Å in **22** is similar to that of [(MePh₂P)AuC≡CH]^[137] 2.008(4) Å. The C(12)—C(13) distance of the ethynyl moiety in **22** (1.11(2) Å) is comparable to that in [(MePh₂P)AuC≡CH]^[137] (1.187(6) Å). The Au(1)—C(2)—C(3) angle of 171(2)° in **22** is comparable to that in [(MePh₂P)AuC≡CH]^[137] (178.9(4)°). The C(1)—Au(1)—C(12) angle in **22** is close to linearity. The N(1)—C(1)—N(2) angle (107(1)°) is slightly wider than that of the parent compound **20** (104.5(7)°). The H···Au agostic interactions observed in the crystal of **22** are analogous to that of **20**. Thus, the contacts are 2.97 Å and 3.12 Å corresponding to the *o*-H of toluene and H atom of *t*Bu group of the carbene (Figure 23). Due to the disordered toluene molecule in **22** in two positions with occupancy ratio 87/13 the 2.97 Å distance is attributed to the major 87% part and 3.04 Å distance is attributed to the minor 13% part.

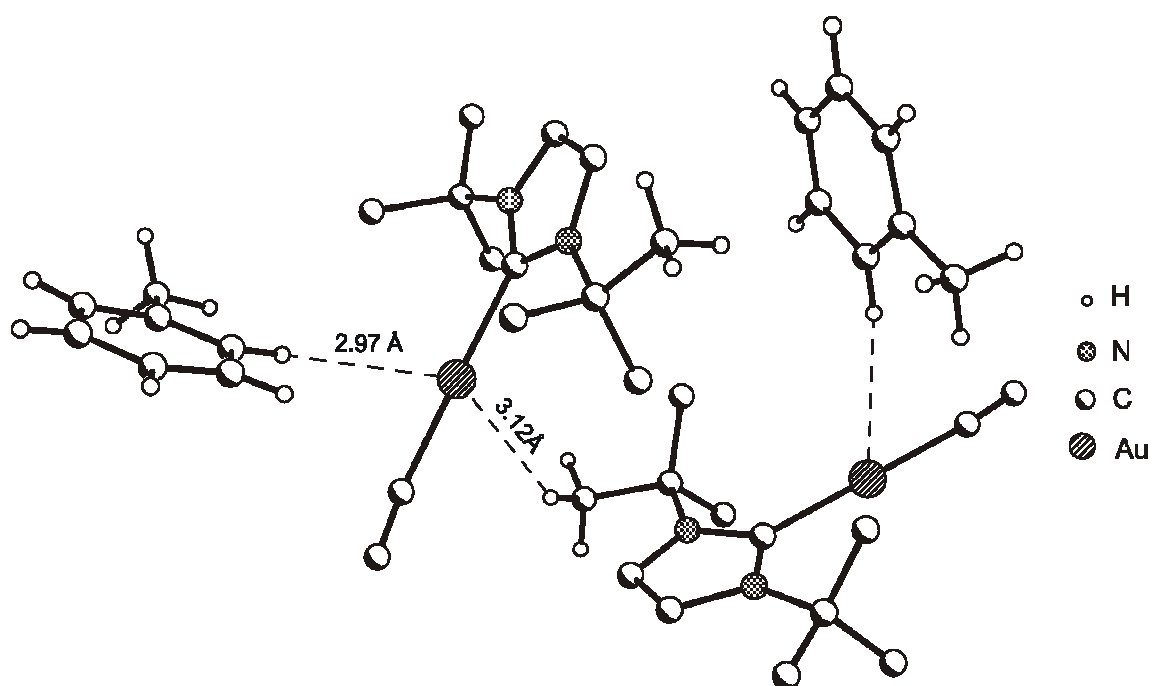


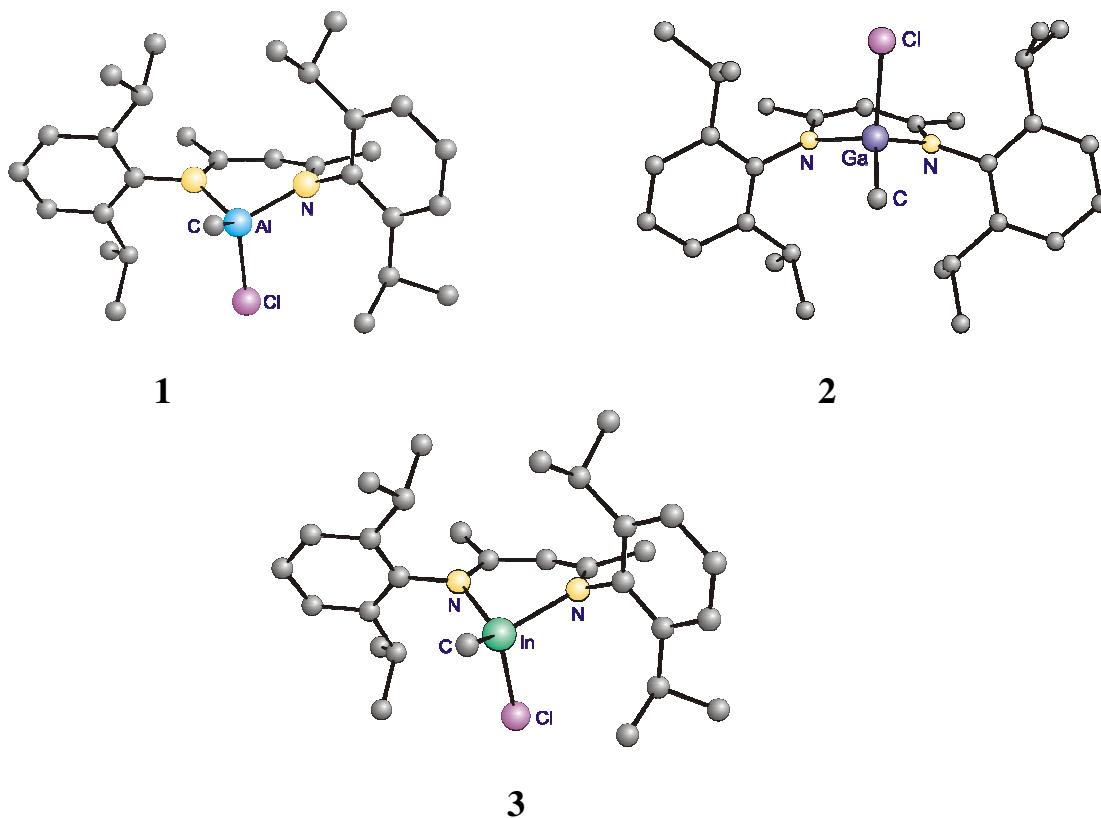
Figure 23. Perspective view of the agostic interactions of Au with *o*-H of the toluene molecule and with H atom of *t*-Bu of the carbene ligand in the crystal leading to the formation of a zig-zag chain in the crystal lattice in $C_{tBu}AuC\equiv CH$ (**22**).

3. Summary and Future Directions

3.1. Summary

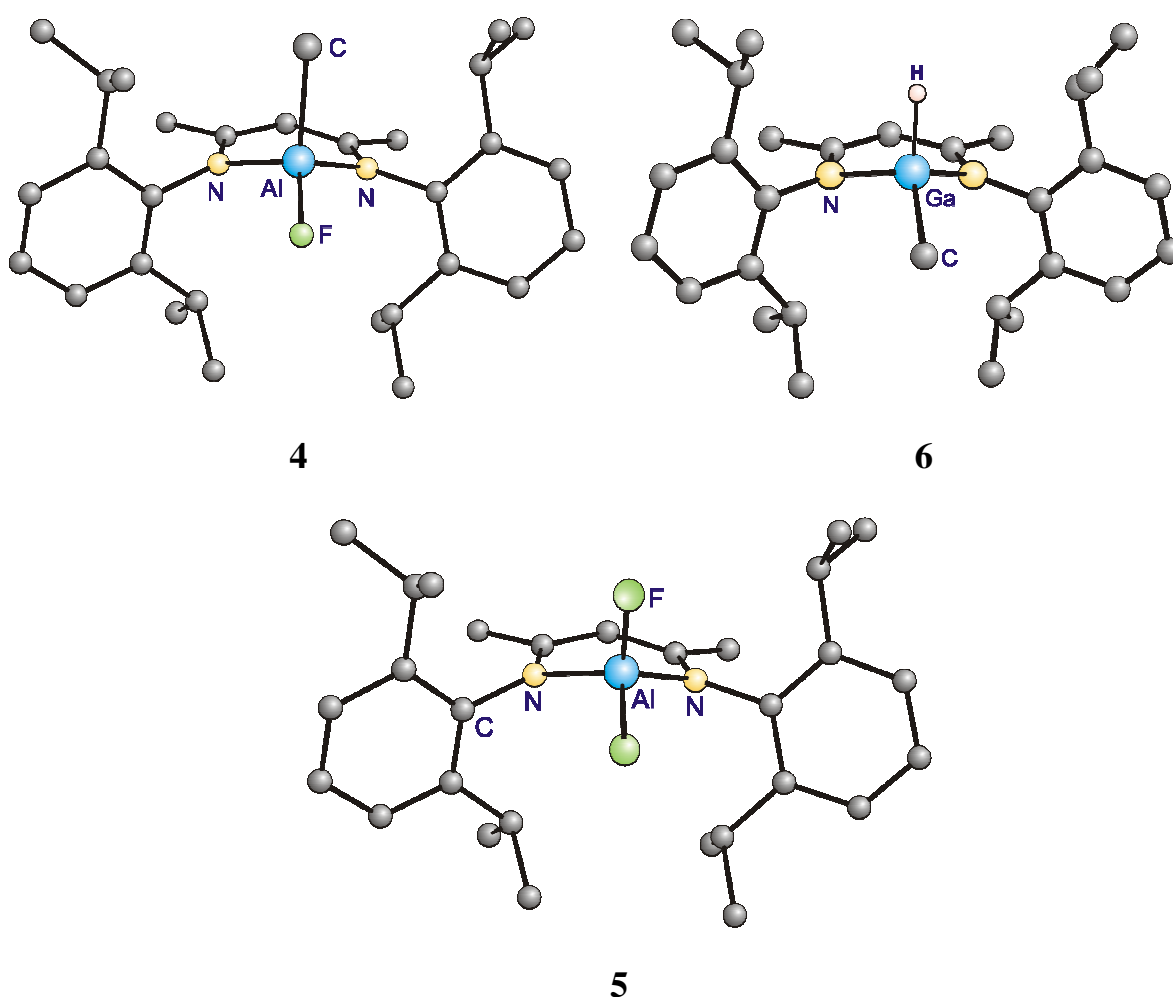
Organometallic molecules with useful functionalities have gained tremendous attention. These molecules sometimes act as models for the naturally occurring metal compounds and mimic their properties very closely.^[186] Substitution of functionalities leads to the synthesis of a variety of other new derivatives, and condensation in a controlled manner with suitable metal synthons affords a route to homo- and heterobimetallic complexes which are mostly useful as catalysts.^[47,50,187,188]

The first part of the thesis deals with the syntheses of β -diketiminato Group 13 methyl chlorides of the general formula LM(Me)Cl (M = Al (**1**), Ga (**2**), In (**3**)). These compounds represent examples of complexes where the metal atom is asymmetrically substituted to carry two different functional groups. Under given reaction conditions one of these two groups can be



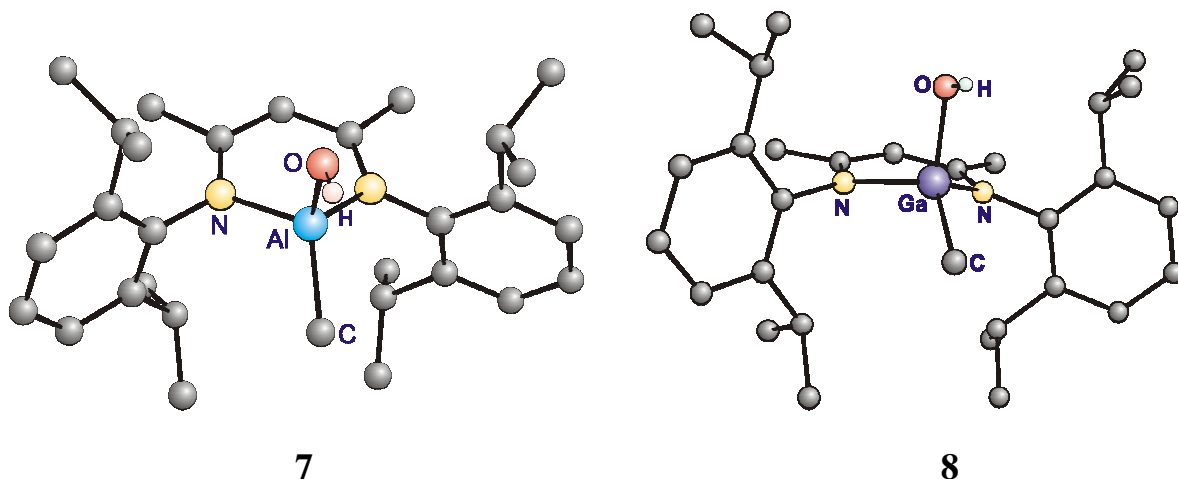
selectively substituted or replaced by another similar or different functional group.

Thus, the reaction of $\text{LAl}(\text{Me})\text{Cl}$ (**1**) with Me_3SnF smoothly yields the corresponding fluoride $\text{LAl}(\text{Me})\text{F}$ (**4**). Similarly, the reaction of $\text{LGa}(\text{Me})\text{Cl}$ (**2**) with $\text{LiH}\cdot\text{BEt}_3$ leads to the formation of $\text{LGa}(\text{Me})\text{H}$ (**6**). Compounds **4** and **6** also contain the metal center in an asymmetrically substituted environment. The aluminum difluoride LAlF_2 (**5**) was prepared by the reaction of LAlH_2 with $\text{BF}_3\cdot\text{OEt}_2$.

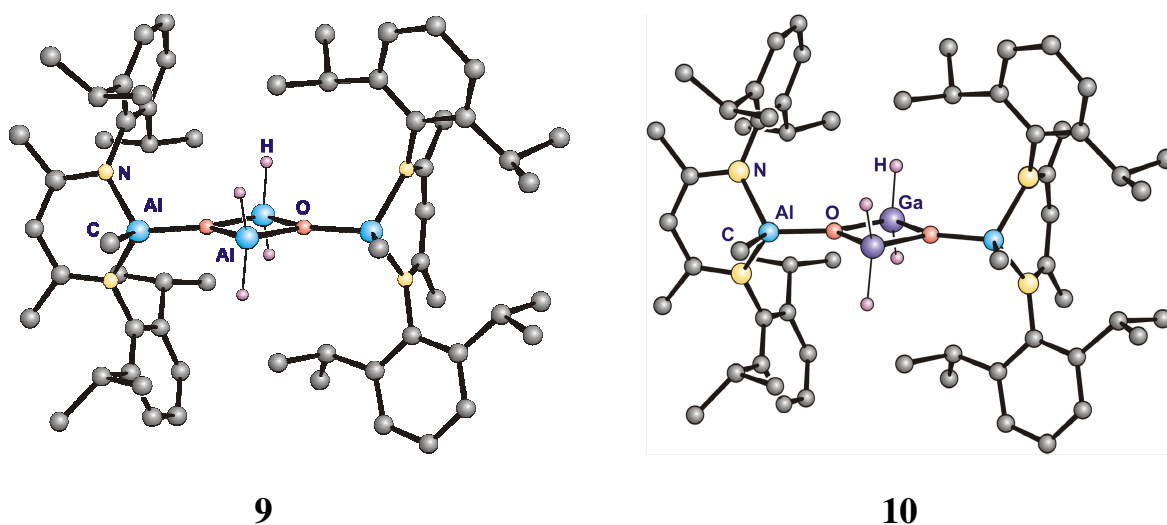


Furthermore, hydrolysis of the complexes $\text{LM}(\text{Me})\text{Cl}$ ($\text{M} = \text{Al}$ (**1**), Ga (**2**)) in the presence of *N*-heterocyclic carbene leads to the formation of the corresponding hydroxides $\text{LM}(\text{Me})\text{OH}$. *N*-heterocyclic carbene, acts as proton/ HCl scavenger, which is formed during the hydrolysis. The

imidazolium salt generated during the hydrolysis is easily separated, owing to its low solubility in *n*hexane and toluene, by filtration through Celite. After its purification the corresponding carbene is regenerated by deprotonation with a strong base such as KO^tBu or NaH.

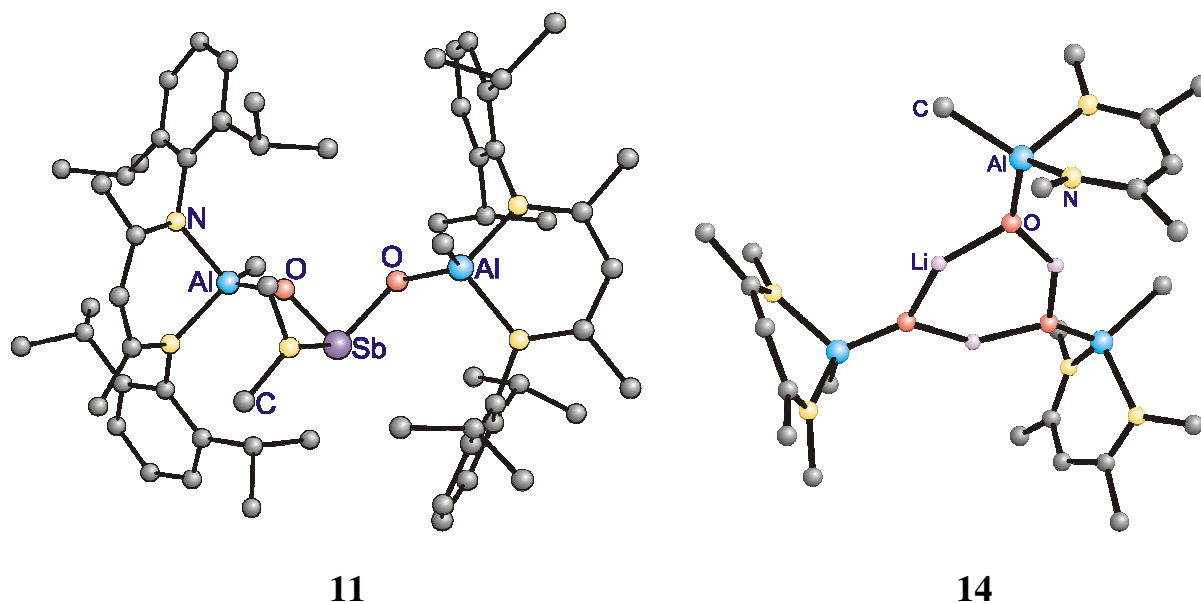


Due to strong Al–O and Ga–O bonds, compounds **7** and **8** were utilized to prepare a series of bimetallic oxides. Second part of the thesis involves the efforts to synthesize homo- and heterometallic oxides. Thus, the reaction of [Al(Me)OH] (**7**) with $\text{AlH}_3\cdot\text{NMe}_3$ and $\text{GaH}_3\cdot\text{NMe}_3$ smoothly affords the first tetranuclear alumoxane hydride containing an $\{\text{Al}_4\text{O}_2\}$ core in $\text{[Al(Me)OAlH}_2\text{]}_2$ (**9**) and the gallium congener with an $\{\text{Al}_2\text{Ga}_2\text{O}_2\}$ core in $\text{[Al(Me)OGaH}_2\text{]}_2$ (**10**). These compounds contain reactive hydride groups on the central M_2O_2 rings and methyl

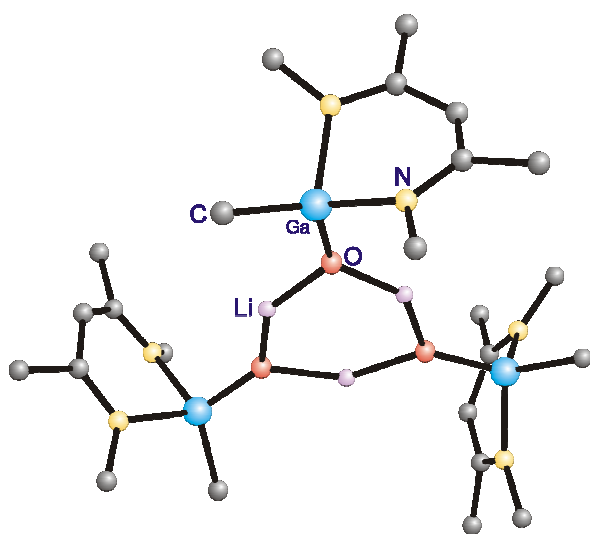


groups on the terminal aluminum atoms.

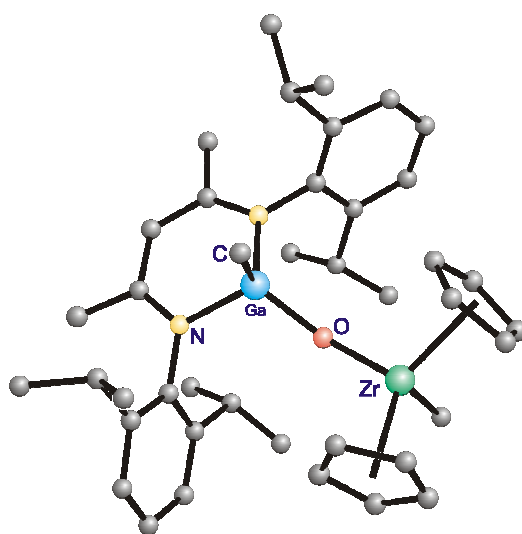
Deprotonation of **7** in the presence of strong bases such as $\text{Sb}(\text{NMe}_2)_3$ and $\text{Sn}\{\text{N}(\text{SiMe}_3)_2\}_2$ generates the heterobimetallic complexes containing Al–O–Sb, Al–O–Sn framework with the elimination of the corresponding amines.



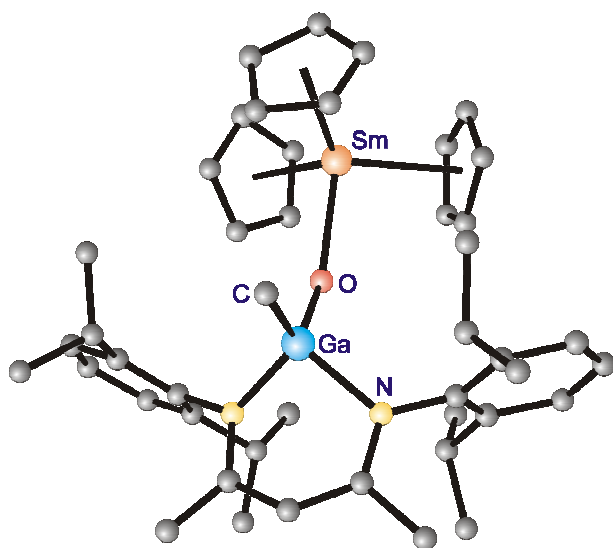
Furthermore, deprotonation of **7** and **8** with $\text{LiN}(\text{SiMe}_3)_2$ gave the corresponding lithium salts containing M–O–Li linkage $[\text{LAl}(\text{Me})\text{OLi}]_3 \cdot \text{C}_6\text{H}_{14}$ (**14**) and $[\text{LGa}(\text{Me})\text{OLi}]_3 \cdot \text{C}_6\text{H}_{14}$ (**15**). Compounds **14** and **15** are isomorphous and exist as trimers in the solid state due to $\text{Li} \cdots \text{O}$ interaction contrary to the solid state structures of **7** and **8** that exist as monomers, and no intermolecular hydrogen bonding was observed. Reaction of $\text{LGa}(\text{Me})\text{OH}$ (**8**) with Cp_2ZrMe_2 affords the heterobimetallic $\text{LGa}(\text{Me})(\mu\text{-O})\text{Zr}(\text{Me})\text{Cp}_2$ (**16**) with methane evolution. However, when **8** was treated with LnCp_3 ($\text{Ln} = \text{Sm}$ (**17**), Dy (**18**), Yb (**19**)) 1:1 adducts of the composition $\text{LGa}(\text{Me})(\mu\text{-OH})\text{LnCp}_3$ were generated and no deprotonation of $\text{LGa}(\text{Me})\text{OH}$ (**8**) was observed.



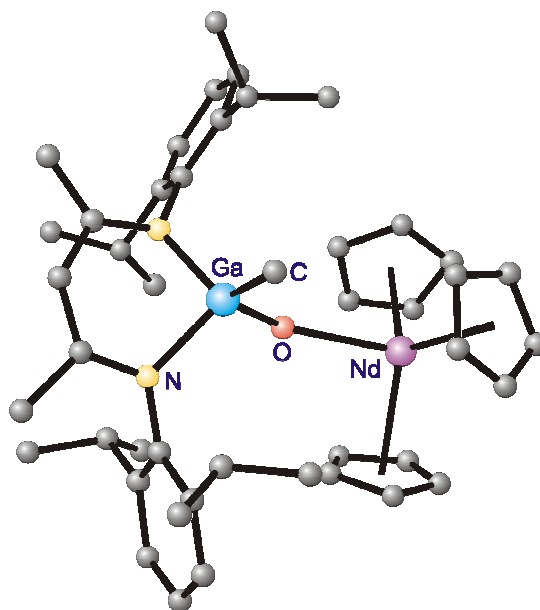
15



16



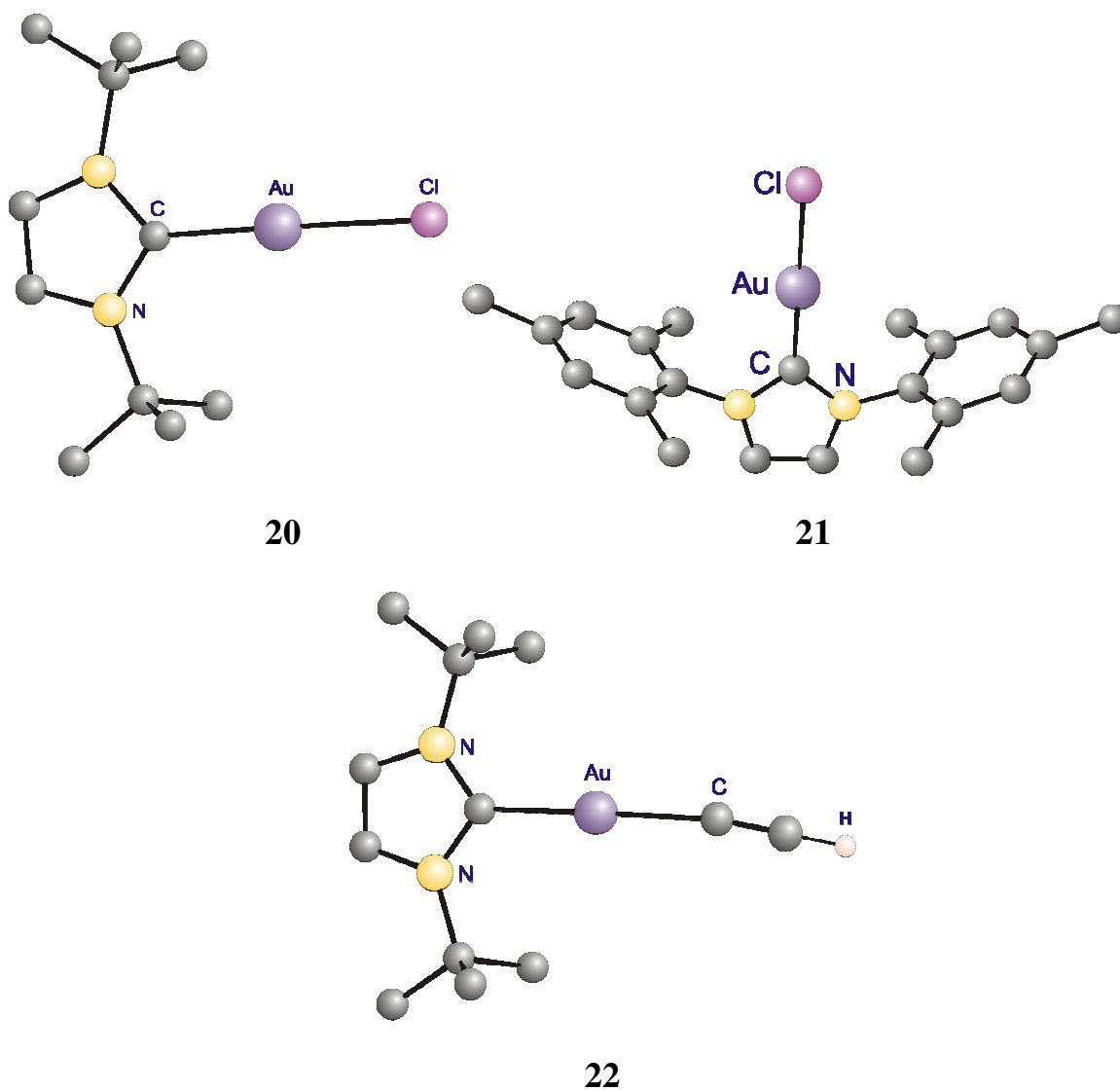
17



18

The last part of the thesis deals with the single-step synthesis of *N*-heterocyclic carbene complexes of gold(I) chloride. Treatment of Au(CO)Cl with 1,3-di-*tert*-butylimidazol-2-ylidene (C_{tBu}) or 1,3-di-mesitylimidazol-2-ylidene (C_{Mes}) substitutes the CO and generates the corresponding carbene gold chloride adducts, $C_{tBu}AuCl$ (**20**) and $C_{Mes}AuCl$ (**21**). Surprisingly, no Au(I)–Au(I) interaction was observed in **20** and **21**. However, *o*-hydrogen of the solvating

toluene molecule and hydrogen atom of the *t*Bu of the carbene ligand are involved in agostic interaction with the gold atoms forming a zig-zag chain in **21**. Similarly the aromatic hydrogens of the carbene ligand are involved in agostic interaction with the gold atom in **21**. Further reaction of **20** and **21** with ethynylmagnesium chloride leads to the formation of $C_{tBu}AuC\equiv CH\cdot C_7H_8$ (**22**) and $C_{Mes}AuC\equiv CH$ (**23**). Compounds **22** and **23** represent the first example of *N*-heterocyclic carbene gold(I) ethynyl complexes that contains a terminal $-C\equiv CH$ group. Solid state structure of **22** was determined and agostic interactions similar to that of **20** were observed resulting in the formation of a zig-zag chain in the crystal lattice of **22**.



3.2. Future directions

The work represented in the thesis has been carried out to construct the molecular hydroxides of aluminum and gallium to mimic the naturally occurring minerals to prepare their soluble analogues with a vision to be useful moieties for immobilization of catalytically active metal complexes and for solid-state acid catalysis. This task essentially entails the synthesis of suitable precursor to achieve these hydroxides which in this case were the corresponding chlorides. A future direction is to utilize the same metal chlorides to prepare the corresponding amides and thiols. In order to achieve this goal, similar methods should be applied (a) use of *N*-heterocyclic carbene as HCl scavenger, (b) using condensed NH_3 to prepare metal amides and (c) use of H_2S to prepare metal thiols. As with metal hydroxides, the amides and thiols should also be utilized to synthesize heterobimetallic amides and sulfides. Similar to the preparation of *N*-heterocyclic carbene complexes of Au(I), the chemistry of Au(I) hydroxides can be explored. In order to stabilize the complex formed, *N*-heterocyclic carbenes can be used with the judicious choice of the substituents on N atoms and the backbone carbon atoms of the *N*-heterocyclic carbenes.

4. Experimental Section

4.1. General procedure

All manipulations and handling of reagents were carried out under an atmosphere of purified nitrogen or argon using standard Schlenk techniques^[189] or a glovebox where O₂ and H₂O level is maintained usually below 1 ppm. All glassware was dried at 150 °C in an oven for at least 20 h and assembled hot and cooled *in vacuo* prior to use. Toluene (Na/benzophenone ketyl), benzene (Na/benzophenone ketyl), tetrahydrofuran (Na/benzophenone ketyl), diethylether (Na/benzophenone ketyl), *n*hexane (Na/benzophenone ketyl and diphenyl ether), pentane (Na/benzophenone ketyl and diphenyl ether), dichloromethane (calcium dihydride) were dried and distilled under nitrogen and degassed prior to use.

4.2. Physical measurements

NMR spectra were recorded on Bruker Avance 200, Bruker Avance 300, Bruker Avance 500 spectrometers with SiMe₄ as external standard (for ¹H and ¹³C), C₆F₆ for ¹⁹F nuclei, 1.0 M LiCl in D₂O (external) for ⁷Li nuclei, [Al(H₂O)₆]³⁺ (external) for ²⁷Al nuclei, and chemical shifts are reported in ppm. Downfield shifts relative to the reference are quoted positive, upfield shifts are assigned negative values. Heteroatom NMR spectra were recorded ¹H decoupled. Deuterated NMR solvents C₆D₆, C₇H₈, and THF-D₈ were dried by stirring for 2 days over Na/K alloy followed by distillation *in vacuo* and degassed.

Mass spectra were recorded on a Finnigan MAT 8230 or a Varian MAT CH5 spectrometer (70 eV) by EI-MS method. The most intense peak of an isotopic distribution is tabulated.

IR spectra were recorded on Bio-Rad Digilab FTS-7 spectrometer as nujol mull between KBr plates. The absorptions of characteristic functional groups (–OH, Al–H, Ga–H) are assigned and other absorptions (moderate to very strong) are only listed.

Melting points were obtained in sealed capillaries on a Büchi B-540 melting point instrument.

Elemental analyses were performed at the Analytical Laboratory of the Institute of Inorganic Chemistry, University of Göttingen.

Crystal structure determination: Intensity data for compounds **7**, **10**, **20**, **22** were collected on an STOE-AED2 four circle diffractometer using graphite monochromated Mo-K α radiation ($\lambda = 0.71073$ Å). Diffraction data for compounds **1–6**, **8**, **9**, **11**, **14–18**, **21** were measured on a Bruker three-circle diffractometer equipped with a SMART 6000 CCD detector using mirror monochromated Cu-K α radiation ($\lambda = 1.54178$ Å). Data for all compounds were collected at low temperature. The structures were solved by direct methods (SHELXS-97)^[190] and refined with all data by full-matrix least squares method on F^2 using SHELXL-97.^[191] The restraints and constraints are AFIX, DELU, EADP, FLAT, SAME, SADI, SIMU were used to treat disordered groups, lattice solvents such as toluene, *n*hexane and hydrogen atoms. The non-hydrogen atoms were refined anisotropically. The crystal data for all compounds along with the final residuals and other pertaining details are tabulated in Section 6, Tables 1–19.

4.3. Starting materials

MeLi (1.6 M in Et₂O, Acros Organics), MeAlCl₂ (1.0 M solution in hexane, Aldrich), AlMe₃ (2.0 M solution in toluene, Acros), GaMe₃ (Aldrich), GaCl₃ (Fluka), InCl₃ (Aldrich), InMe₃ (Aldrich), LiH·BEt₃ (1.0 M solution in THF), LiN(SiMe₃)₂ (Aldrich), Cp₂ZrMe₂ (Fluka), Cp₃Sm (Aldrich), CpNa (2.0 M solution in THF, Aldrich), ethynylmagnesium chloride (0.5 M solution in THF, Aldrich) were used as received. The BF₃·OEt₂ was freshly distilled prior to use. L,^[20] MeGaCl₂,^[192] MeInCl₂,^[193] Me₃SnF,^[194] AlH₃·NMe₃,^[195] GaH₃·NMe₃,^[196] Sb(NMe₃)₃,^[197]

$\text{Sn}\{\text{N}(\text{SiMe}_3)_2\}_2$,^[198,199] NdCp_3 ,^[200,201] YbCp_3 ,^[200,201] $\text{C}_{t\text{Bu}}$,^[202] C_{Mes} ^[152] were prepared by literature procedures. Demineralized, degassed H_2O was used for hydrolysis experiments.

4.4. Synthesis of compounds 1–23

4.4.1. Synthesis of $\text{LAl}(\text{Me})\text{Cl}$ (**1**)

$\text{LLi}\cdot\text{OEt}_2$ (2.49 g, 5.00 mmol) in toluene (30 mL) was added dropwise at $-60\text{ }^\circ\text{C}$ to MeAlCl_2 (5.00 mL, 1.0 M in *n*hexane, 5.00 mmol) in toluene (15 mL). The mixture was allowed to warm to room temperature and stirred for 12 h. Volatile components were removed *in vacuo* and the crude product was extracted with *n*hexane (100 mL). The final solution was concentrated to 50 mL and kept at $-32\text{ }^\circ\text{C}$ overnight to afford colorless crystals. An additional crop of $\text{LAl}(\text{Me})\text{Cl}$ was obtained from the mother liquor. Total yield (2.05 g, 83 %). Mp: $190\text{ }^\circ\text{C}$. Anal. Calcd. for $\text{C}_{30}\text{H}_{44}\text{AlClN}_2$ (494.30): C 72.9, H 8.9, N 5.6; found: C 72.8, H 9.0, N 5.6. ^1H NMR (500 MHz, C_6D_6): δ – 0.65 (s, 3 H, AlMe), 1.02 (d, $^3J_{\text{H-H}} = 6.8\text{ Hz}$, 6 H, CHMe_2), 1.19 (d, $^3J_{\text{H-H}} = 6.8\text{ Hz}$, 6 H, CHMe_2), 1.28 (d, $^3J_{\text{H-H}} = 6.8\text{ Hz}$, 6 H, CHMe_2), 1.46 (d, $^3J_{\text{H-H}} = 6.6\text{ Hz}$, 6 H, CHMe_2), 1.52 (s, 6H, CMe), 3.21 (sept, $^3J_{\text{H-H}} = 6.8\text{ Hz}$, 2 H, CHMe_2), 3.76 (sept, $^3J_{\text{H-H}} = 6.7\text{ Hz}$, 2 H, CHMe_2), 4.98 (s, 1 H, $\gamma\text{-CH}$), 7.15–7.05 (m, *Ar*). EI-MS: m/z (%): 479 (100) [$M^+ - \text{Me}$]. IR (Nujol, cm^{-1}) $\tilde{\nu}$: 1534, 1462, 1440, 1383, 1319, 1257, 1191, 1177, 1109, 1099, 1023, 935, 890, 799, 780, 759, 718, 660, 535, 456.

4.4.2. Synthesis of LGa(Me)Cl (2)

LLi·OEt₂ (1.49 g, 3.00 mmol) dissolved in toluene (30 mL) was cooled to – 78 °C. MeGaCl₂ (0.47 g, 3.00 mmol) dissolved in toluene (20 mL) was added to it with continuous stirring. The solution was allowed to warm to room temperature and stirred overnight. After removal of all volatiles the residue was extracted with *n*hexane (50 mL). Partial removal of the solvent and storage at – 26 °C afforded colorless crystals of LGa(Me)Cl. Additional crop of LGa(Me)Cl was obtained from the mother liquor. Total yield: (1.26 g, 78%). Mp: 190 ° C. Anal. Calcd. for C₃₀H₄₄ClGa₂N₂ (537.86): C 66.99, H 8.25, N 5.21; found: C 66.87, H 8.32, N 5.18. ¹H NMR (C₆D₆, 200 MHz): δ – 0.31 (s, 3 H, GaMe), 1.04 (d, ³J_{H-H} = 6.8 Hz, 6 H, CHMe₂), 1.19 (two overlapped d, ³J_{H-H} = 6.8 Hz, 12 H, CHMe₂), 1.48 (d, ³J_{H-H} = 6.8 Hz, 6 H, CHMe₂), 1.57 (s, 6 H, CMe), 3.15 (sept, ³J_{H-H} = 6.8 Hz, 2 H, CHMe₂), 3.87 (sept, ³J_{H-H} = 6.8 Hz, 2 H, CHMe₂), 4.90 (s, 1 H, γ-CH), 7.01–7.14 (m, 6 H, Ar). EI-MS: *m/z* (%): 538 (12) [*M*⁺], 523 (100) [*M*⁺ – Me], 501 (34) [*M*⁺ – Cl], 485 (14) [*M*⁺ – Me – Cl]. IR (Nujol, cm^{–1}) $\tilde{\nu}$: 1532, 1468, 1441, 1385, 1302, 1262, 1179, 1100, 1056, 1023, 934, 872, 797, 778, 759, 726, 646, 584, 532, 450.

4.4.3. Synthesis of LIn(Me)Cl (3)

To a cooled solution of MeInCl₂ (0.40 g, 2.00 mmol) in toluene (20 mL) at –78 °C, a solution of LLi·OEt₂ (1.00 g, 2.00 mmol) in toluene (25 mL) was added dropwise with continuous stirring. The solution was allowed to warm to room temperature and stirred overnight. After removal of all volatiles *in vacuo* the crude product was extracted with *n*hexane. Partial removal of solvent afforded colorless crystals of LIn(Me)Cl at 0 °C in two days. Yield: (0.75 g, 65%). Mp: 185 ° C. Anal. Calcd. for C₃₀H₄₄ClInN₂ (582.95): C 61.81, H 7.61, N 4.81; found: C

61.79, H 7.58, N 4.82. ^1H NMR (C_6D_6 , 200 MHz): δ – 0.28 (s, 3 H, InMe), 1.09 (d, $^3J_{\text{H-H}} = 6.8$ Hz, 6 H, CHMe_2), 1.23 (two overlapped d, $^3J_{\text{H-H}} = 6.8$ Hz, 12 H, CHMe_2), 1.46 (d, $^3J_{\text{H-H}} = 6.8$ Hz, 6 H, CHMe_2), 1.58 (s, 6 H, CMe), 3.15 (sept, $^3J_{\text{H-H}} = 6.8$ Hz, 2 H, CHMe_2), 3.83 (sept, $^3J_{\text{H-H}} = 6.8$ Hz, 2 H, CHMe_2), 4.80 (s, 1 H, $\gamma\text{-CH}$), 7.10–7.14 (m, 6 H, Ar). EI-MS: m/z (%): 582 (12) [M^+], 567 (100) [$M^+ - \text{Me}$]. IR (Nujol, cm^{-1}) $\tilde{\nu}$: 1526, 1383, 1317, 1268, 1254, 1177, 1163, 1107, 1099, 1055, 1043, 1021, 933, 859, 796, 778, 758, 720, 635, 518, 446.

4.4.4. Synthesis of $\text{LAl}(\text{Me})\text{F}$ (**4**)

THF (40 mL) was added to a mixture of $\text{LAl}(\text{Me})\text{Cl}$ (0.99 g, 2.00 mmol) and Me_3SnF (0.37 g, 2.00 mmol). The mixture was then stirred at room temperature until a clear solution was obtained (ca 24 h). After removal of all the volatiles, $\text{LAl}(\text{Me})\text{F}$ was extracted with *n*hexane (50 mL). Partial removal of the solvent and storage at 0 °C for 2 days afforded colorless crystals of $\text{LAl}(\text{Me})\text{Cl}$. Yield: (0.81 g, 85%). Mp: 202 °C. Anal. Calcd. for $\text{C}_{30}\text{H}_{44}\text{AlFN}_2$ (478.66): C 75.28, H 9.27, N 5.85; found: C 75.32, H 9.31, N 5.83. ^1H NMR (200 MHz, C_6D_6) δ – 0.82 (d, $^3J_{\text{H-F}} = 2.0$ Hz, 3 H, AlMe), 1.08 (d, $^3J_{\text{H-H}} = 6.8$ Hz, 6 H, CHMe_2), 1.19 (two overlapped d, $^3J_{\text{H-H}} = 6.8$ Hz, 6 H, CHMe_2), 1.29 (d, $^3J_{\text{H-H}} = 6.8$ Hz, 6 H, CHMe_2), 1.44 (d, $^3J_{\text{H-H}} = 6.8$ Hz, 6 H, CHMe_2), 1.56 (s, 6 H, CMe), 3.16 (sept, $^3J_{\text{H-H}} = 6.8$ Hz, 2 H, CHMe_2), 3.64 (sept, $^3J_{\text{H-H}} = 6.8$ Hz, 2 H, CHMe_2), 4.98 (s, 1 H, $\gamma\text{-CH}$), 7.05–7.12 (m, 6 H, Ar). ^{19}F NMR (188.28 MHz, C_6D_6): δ 8.6 (s, Al-F). EI-MS: m/z (%): 478 (10) [M^+], 463 (100) [$M^+ - \text{Me}$], 444 (8) [$M^+ - \text{Me} - \text{F}$]. IR (Nujol, cm^{-1}) $\tilde{\nu}$: 1624, 1550, 1531, 1444, 1384, 1318, 1256, 1191, 1177, 1105, 1055, 1023, 941, 879, 806, 797, 757, 720, 663, 629, 448.

4.4.5. Synthesis of LAlF_2 (**5**)

$\text{BF}_3 \cdot \text{OEt}_2$ (0.43 g, 0.38 mL, 3.0 mmol, 1.34 eq) was added dropwise to a cooled (-78°C) solution of LAIH_2 (1.00 g, 2.24 mmol) in toluene (10 mL). The solution was stirred at this temperature for 10 min, slowly warmed to room temperature and stirred overnight. All volatiles were removed *in vacuo* and the residue was crystallized from *n*hexane/toluene (1:1) to give large colorless crystals of LAlF_2 . Yield: (0.88 g, 82 %). Mp: 235°C . Anal. Calcd. for $\text{C}_{29}\text{H}_{41}\text{AlF}_2\text{N}_2$ (482.63): C 72.17, H 8.56, N 5.80; found: C 72.20, H 8.58, N 5.85. ^1H NMR (300 MHz, C_6D_6): δ 1.10 (d, $^3J_{\text{H-H}} = 6.9$ Hz, 12 H, CHMe_2), 1.41 (d, $^3J_{\text{H-H}} = 6.9$ Hz, 12 H, CHMe_2), 1.53 (s, 6 H, CMe), 3.30 (sept, $^3J_{\text{H-H}} = 6.9$ Hz, 4 H, CHMe_2), 4.94 (s, 1 H, $\gamma\text{-CH}$), 7.03–7.18 (m, 6 H, ArH). ^{19}F NMR (188 MHz, C_6D_6): δ 173.1 (s, AlF). ^{27}Al NMR (78.2 MHz, C_6D_6 , TMS): δ 66.9 (s, $W_{1/2} = 1350$ Hz). EI-MS: m/z (%): 482 (100) [M^+], 467 (41) [$M^+ - \text{Me}$], 447 (18) [$M^+ - \text{MeH} - \text{F}$]. IR (Nujol, cm^{-1}) $\tilde{\nu}$: 1539, 1318, 1255, 1177, 1102, 1030, 937, 900, 817, 803, 758, 719, 448, 412.

4.4.6. Synthesis of $\text{LGa}(\text{Me})\text{H}$ (**6**)

$\text{LGa}(\text{Me})\text{Cl}$ (1.07 g, 2.00 mmol) dissolved in toluene (20 mL) was cooled to -78°C . 1.0 M solution of super hydride LiBEt_3H (2.0 mL, 2.00 mmol, 1 equiv.) was added to it drop wise. The solution was allowed to warm to room temperature and stirred overnight. After removal of all volatiles the residue was extracted with *n*hexane (40 mL). Partial removal of the solvent and storage at -26°C afforded colorless crystals of $\text{LGa}(\text{Me})\text{H}$. Additional crop of $\text{LGa}(\text{Me})\text{H}$ was obtained from the mother liquor. Total yield: (0.72 g, 72 %). Mp: 177°C . Anal. Calcd. for $\text{C}_{30}\text{H}_{45}\text{GaN}_2$ (503.41): C 71.58, H 9.01, N 5.56; found: C 71.60, H 9.03, N 5.60. ^1H NMR (200 MHz, C_6D_6): δ -0.45 (d, 3 H, $^3J_{\text{H-H}} = 0.8$ Hz, GaMe), 1.16 (two overlapped d, $^3J_{\text{H-H}} = 7.2$ Hz, 12

H, CHMe_2), 1.30 (two overlapped d, $^3J_{\text{H-H}} = 6.8$ Hz, 12 H, CHMe_2), 1.57 (s, 6 H, CMe), 3.43 (sept, $^3J_{\text{H-H}} = 6.8$ Hz, 4 H, CHMe_2), 4.81 (s, 1 H, $\gamma\text{-CH}$), 5.49 (s broad, 1 H, GaH), 7.04–7.13 (m, 6 H, Ar). EI-MS: m/z (%): 502 (28) [M^+], 487 (100) [$M^+ - \text{Me}$]. IR (Nujol, cm^{-1}) $\tilde{\nu}$: 1825 (Ga-H), 1559, 1523, 1495, 1442, 1404, 1388, 1319, 1261, 1232, 1196, 1178, 1104, 1055, 1022, 935, 865, 796, 766, 644, 608, 590, 564, 523, 440.

4.4.7. Synthesis of $\text{LAl}(\text{Me})\text{OH}$ (7)

1,3-Di-*tert*butylimidazol-2-ylidene (1.08 g, 6.00 mmol) in toluene (50 mL) was added to $\text{LAl}(\text{Me})\text{Cl}$ (2.97 g, 6.00 mmol) in toluene (80 mL). The solution was stirred at room temperature for 10 minutes. Degassed and distilled water (108 μL , 6.00 mmol) was added slowly with vigorous stirring over a period of 30 minutes. The mixture was stirred for another 1 h. Volatile components were removed *in vacuo* and the crude product was extracted with *n*hexane (150 mL), where 1,3-di-*tert*-butylimidazolium chloride was filtered through celite. The final solution was concentrated (60 mL) and stored at -20 °C for two days to afford colorless crystals. Yield (2.45 g, 86 %). Mp: 192 °C. Anal. Calcd. for $\text{C}_{30}\text{H}_{45}\text{AlN}_2\text{O}$ (476.70): C 75.6, H 9.5, N 5.9; found: C 75.4, H 9.5, N 6.0. ^1H NMR (300 MHz, C_6D_6): δ – 0.88 (s, 3 H, AlMe), 0.53 (s, 1 H, OH), 1.07 (d, $^3J_{\text{H-H}} = 6.8$ Hz, 6 H, CHMe_2), 1.21 (d, $^3J_{\text{H-H}} = 6.8$ Hz, 6 H, CHMe_2), 1.32 (d, $^3J_{\text{H-H}} = 6.8$ Hz, 12 H, CHMe_2), 1.57 (s, 6 H, CMe), 3.25 (sept, $^3J_{\text{H-H}} = 6.8$ Hz, 2 H, CHMe_2), 3.69 (sept, $^3J_{\text{H-H}} = 6.8$ Hz, 2 H, CHMe_2), 4.93 (s, 1 H, γCH), 7.16–7.07 (m, Ar). EI-MS: m/z (%): 461 (100) [$M^+ - \text{Me}$], 443 (21) [$M^+ - \text{Me} - 2\text{H} - \text{O}$]. IR (Nujol, cm^{-1}) $\tilde{\nu}$: 3728 (AlO-H), 1552, 1530, 1373, 1316, 1256, 1189, 1178, 1106, 1056, 1023, 940, 878, 805, 768, 757, 689, 614.

4.4.8. Synthesis of $\text{LGa}(\text{Me})\text{OH}$ (**8**)

To a solution of 1,3-di-*tert*-butylimidazol-2-ylidene (0.45 g, 2.50 mmol) and $\text{LGa}(\text{Me})\text{Cl}$ (1.34 g, 2.50 mmol) in toluene (50 mL), degassed and distilled water (45 μL , 2.50 mmol) was added slowly with vigorous stirring over a period of 30 min. The mixture was stirred for another 15 min. Volatile components were removed *in vacuo* and the crude product was extracted with *n*hexane (60 mL), where 1,3-di-*tert*-butylimidazolium chloride was filtered through celite. The final solution was concentrated (15 mL) and stored at $-20\text{ }^{\circ}\text{C}$ for two days to afford colorless crystals. Yield (1.00 g, 76 %) Mp: $198\text{--}200\text{ }^{\circ}\text{C}$. Anal. Calcd. for $\text{C}_{30}\text{H}_{45}\text{GaN}_2\text{O}$ (519.41): C 69.37, H 8.73, N 5.39; found C 69.46, H 8.62, N 5.42. ^1H NMR (200 MHz, C_6D_6): δ – 0.57 (s, 3 H, GaMe), 0.08 (s, 1 H, GaOH), 1.08 (d, $^3J_{\text{H-H}} = 6.6\text{ Hz}$, 6 H, CHMe_2), 1.24 (dd, $^3J_{\text{H-H}} = 6.6\text{ Hz}$, 12 H, CHMe_2), 1.34 (d, $^3J_{\text{H-H}} = 6.6\text{ Hz}$, 6 H, CHMe_2), 1.57 (s, 6 H, CMe), 3.20 (sept, $^3J_{\text{H-H}} = 6.5\text{ Hz}$, 2 H, CHMe_2), 3.79 (sept, $^3J_{\text{H-H}} = 6.8\text{ Hz}$, 2 H, CHMe_2), 4.80 (s, 1 H, $\gamma\text{-CH}$), 7.12–7.03 (m, Ar). EI-MS: m/z (%): 518 (6) [M^+], 503 (100) [$M^+ - \text{Me}$], 485 (44) [$M^+ - \text{Me} - 3\text{ H}$]. IR (Nujol, cm^{-1}) $\tilde{\nu}$: 3676 (GaO-H), 1558, 1527, 1442, 1384, 1319, 1262, 1178, 1105, 1056, 1023, 936, 869, 804, 757, 603, 571.

4.4.9. Synthesis of $[\text{LAl}(\text{Me})(\mu\text{-O})\text{AlH}_2]_2$ (**9**)

$\text{LAl}(\text{Me})\text{OH}$ (0.95 g, 2.00 mmol) dissolved in toluene (20 mL) was added dropwise at $0\text{ }^{\circ}\text{C}$ to a stirring (1.0 M) solution of $\text{AlH}_3\cdot\text{NMe}_3$ (2.10 mL, 2.10 mmol) in toluene (15 mL). The solution was allowed to warm to room temperature and further stirred for 15 h. After removal of all the volatiles the residue was extracted with *n*hexane (40 mL). Partial removal of the solvent and storage at room temperature for 2 days afforded colorless crystals of $[\text{LAl}(\text{Me})\text{OAlH}_2]_2$.

Yield (0.75 g, 74 %). Mp: 258-260 °C (decomp.). Anal. Calcd. for $C_{60}H_{92}Al_4N_4O_2$ (1008.65): C 71.40, H 9.19, N 5.55; found C 71.75, H 9.55, N 5.14. 1H NMR (500 MHz, C_7D_8 , -60 °C): δ – 0.81 (s, 3 H, $AlMe$), 0.07 (s, 3 H, $AlMe$), 0.92 (d, $^3J_{H-H} = 6.4$ Hz, 6 H, $CHMe_2$), 1.04 (d, $^3J_{H-H} = 6.4$ Hz, 6 H, $CHMe_2$), 1.14 (d, $^3J_{H-H} = 6.2$ Hz, 6 H, $CHMe_2$), 1.20 (m, 12 H, $CHMe_2$), 1.34 (d, $^3J_{H-H} = 6.3$ Hz, 6 H, $CHMe_2$), 1.39 (s, 6 H, CMe), 1.46 (s, 6 H, CMe), 1.70-1.66 (m, 12 H, $CHMe_2$), 2.97 (sept, $^3J_{H-H} = 6.5$ Hz, 2 H, $CHMe_2$), 3.27 (sept, $^3J_{H-H} = 6.5$ Hz, 2 H, $CHMe_2$), 3.40 (sept, $^3J_{H-H} = 6.5$ Hz, 2 H, $CHMe_2$), 3.54 (sept, $^3J_{H-H} = 6.3$ Hz, 2 H, $CHMe_2$), 3.93 (b, 4 H, AlH_2), 4.79 (s, 1 H, $\gamma-CH$), 4.80 (s, 1 H, $\gamma-CH$), 7.26-6.89 (m, Ar). 1H NMR (500 MHz, C_7D_8 , 100 °C): δ –0.56 (s, 6 H, $AlMe$), 1.10 (m, 24 H, $CHMe_2$), 1.38-1.31 (b, 24 H, $CHMe_2$ and CMe), 1.60 (s, 12 H, CMe), 3.14 (b, 4 H, $CHMe_2$), 3.40 (sept, $^3J_{HH} = 6.7$ Hz, 4 H, $CHMe_2$), 3.65 (b, 4 H, AlH_2), 5.02 (s, 2 H, $\gamma-CH$), 7.16-6.96 (m, Ar). EI-MS: m/z (%): 1007 (92) [$M^+ - H$], 993 (72) [$M^+ - Me$], 979 (60) [$M^+ - Al - 2 H$], 965 (100) [$M^+ - Al - Me - 3 H$], 951 (20) [$M^+ - 2 Al - 3 H$]. IR (Nujol, cm^{-1}) $\tilde{\nu}$: 1850 (asymm. Al–H), 1833 (symm. Al–H), 1552, 1527, 1318, 1260, 1177, 1101, 1055, 1023, 936, 874, 803, 726, 724, 656, 634.

4.4.10. Synthesis of $[LAl(Me)(\mu-O)GaH_2]_2$ (**10**)

$LAl(Me)OH$ (1.43 g, 3.00 mmol) dissolved in toluene (30 mL) was added dropwise at 0 °C to a stirring solution of $GaH_3 \cdot NMe_3$ (0.40 g, 3.00 mmol) in toluene (20 mL). The solution was allowed to warm to room temperature and stirred for 15 h. After removal of all volatiles the residue was extracted with *n*hexane (45 mL). Partial removal of the solvent and storage at room temperature for 5 d afforded colorless crystals of $[LAl(Me)OGaH_2]_2$. Yield (1.30 g, 79 %). Mp: 234 °C (decomp.). Anal. Calcd. for $C_{60}H_{92}Al_2Ga_2N_4O_2$ (1094.81): C 65.82, H 8.47, N 5.12; found C 65.67, H 8.33, N 5.29. 1H NMR (500 MHz, C_7D_8 , -70 °C): δ –0.95 (s, 3 H, $AlMe$), 0.04 (s, 3 H, $AlMe$), 0.92 (d, $^3J_{H-H} = 6.0$ Hz, 6 H, $CHMe_2$), 1.14 (dd, $^3J_{H-H} = 17.3$ Hz, 18 H, $CHMe_2$), 1.40

(s, 12 H, *CMe*), 1.49 (d, $^3J_{\text{H-H}} = 5.8$ Hz, 12 H, *CHMe*₂), 1.68 (d, $^3J_{\text{H-H}} = 17.3$ Hz, 12 H, *CHMe*₂), 2.96 (m, 2 H, *CHMe*₂), 3.32 (m, 2 H, *CHMe*₂), 3.45 (m, 2 H, *CHMe*₂), 3.77 (m, 2 H, *CHMe*₂), 4.63 (s, 1 H, γ -*CH*), 4.70 (s, 1 H, γ -*CH*), 5.05 (s, 2 H, *GaH*₂), 5.20 (s, 2 H, *GaH*₂), 7.22-6.88 (m, *Ar*). ¹H NMR (500 MHz, C₇D₈, 70 °C): δ -0.65 (s, 6 H, *AlMe*), 1.10 (d, $^3J_{\text{H-H}} = 8.7$ Hz, 12 H, *CHMe*₂), 1.17 (d, $^3J_{\text{H-H}} = 6.5$ Hz, 12 H, *CHMe*₂), 1.32 (b, 12 H, *CHMe*₂), 1.43 (b, 12 H, *CHMe*₂), 1.56 (s, 12 H, *CMe*), 3.15 (b, 4 H, *CHMe*₂), 3.48 (b, 4 H, *CHMe*₂), 4.91 {s, 6 H (2 H, γ -*CH* and 4 H, *GaH*₂)}, 7.17-6.96 (m, *Ar*). EI-MS: *m/z* (%): 1094 (24) [*M*⁺], 1079 (100) [*M*⁺ – Me], 1052 (16) [*M*⁺ – Al – Me], 1022 (20) [*M*⁺ – Ga – 2 H], 1007 (20) [*M*⁺ – Me – Ga – 2 H]. IR (Nujol, cm⁻¹) $\tilde{\nu}$: 1929 (asymm. Ga–H), 1901 (symm. Ga–H), 1585, 1551, 1521, 1315, 1293, 1256, 1183, 1176, 1107, 1098, 938, 874, 797, 770, 755, 737, 709, 659, 642, 616, 531, 507.

4.4.11. Synthesis of [LAl(Me)(μ -O)]₂SbNMe₂ (**II**)

To a solution of Sb(NMe₂)₃ (0.25 g, 1.00 mmol) in toluene (15 mL), a solution of LAl(Me)OH (0.95 g, 2.00 mmol) in toluene (25 mL) was added dropwise at 0 °C. The solution was allowed to warm to room temperature and stirred overnight. After removal of all volatiles the product was extracted in *n*hexane (40 mL). Yield (0.67 g, 60 %). Anal. Calcd. for C₆₂H₉₄Al₂N₅O₂Sb (1117.17): C 66.66, H 8.48, N 6.27; found C 66.73, H 8.62, N 6.30. ¹H NMR (200 MHz, C₆D₆): δ -0.57 (s, 3 H, *AlMe*), -0.34 (s, 3 H, *AlMe*), 1.14 (m, 24 H, *CHMe*₂), 1.35, 1.38 (two overlapped d, $^3J_{\text{HH}} = 6.8$ Hz, 18 H, *CHMe*₂), 1.49 (d, $^3J_{\text{HH}} = 6.8$ Hz, 6 H, *CHMe*₂), 1.53 (s, 3 H, *CMe*), 1.56 (s, 9 H, *CMe*), 2.51 (s, 6 H, *SnNMe*₂), 3.30 (two overlapped sept, 4 H, *CHMe*₂), 3.62 (two overlapped sept, $^3J_{\text{H-H}} = 6.8$ Hz, 4 H, *CHMe*₂), 4.86 (s, 1 H, γ -*CH*), 4.95 (s, 1 H, γ -*CH*), 7.14-7.10 (m, *Ar*). IR (Nujol, cm⁻¹) $\tilde{\nu}$: 1533, 1459, 1436, 1382, 1321, 1260, 1195, 1189, 1173, 1109, 1023, 936, 794, 760, 720, 659, 537, 457.

4.4.12. Synthesis of $[LAl(Me)(\mu-O)]Sn\{N(SiMe_3)_2\}$ (12**)**

$LAl(Me)OH$ (0.47 g, 1.00 mmol) dissolved in toluene (20 mL) was added dropwise at 0 °C to a stirring solution of $Sn[N(SiMe_3)_2]_2$ (0.44 g, 1.00 mmol) in toluene (15 mL). The solution was allowed to warm to room temperature and stirred overnight. The color of the solution changes from orange to yellow, after removal of all the volatiles the residue was extracted with *n*hexane (40 mL). Partial removal of the solvent and storage at room temperature for 2 days afforded colorless crystals of **12**. Yield (0.65 g, 86 %). Anal. Calcd. for $C_{36}H_{62}AlN_3OSi_2Sn$ (754.76): C 57.29, H 8.28, N 5.57; found C 57.32, H 8.30, N 5.53. 1H NMR (200 MHz, C_6D_6): δ -0.72 (s, 3 H, $AlMe$), 0.34 (s, 18 H, $SnN(SiMe_3)_2$), 1.12 (d, $^3J_{HH} = 6.8$ Hz, 6 H, $CHMe_2$), 1.25 (d, $^3J_{HH} = 6.8$ Hz, 6 H, $CHMe_2$), 1.31 (d, $^3J_{HH} = 6.8$ Hz, 12 H, $CHMe_2$), 1.58 (s, 6 H, CMe), 3.25 (sept, $^3J_{H-H} = 6.8$ Hz, 2 H, $CHMe_2$), 3.83 (sept, $^3J_{H-H} = 6.8$ Hz, 2 H, $CHMe_2$), 5.02 (s, 1 H, $\gamma-CH$), 7.09-7.12 (m, Ar). IR (Nujol, cm^{-1}) $\tilde{\nu}$: 1531, 1386, 1319, 1257, 1190, 1178, 1108, 1056, 1023, 940, 876, 770, 757, 689, 543, 460.

4.4.13. Synthesis of $[LAl(Me)(\mu-O)]_2Sn$ (13**)**

$LAl(Me)OH$ (0.95 g, 2.00 mmol) dissolved in toluene (30 mL) was added dropwise at 0 °C to a stirring solution of $Sn[N(SiMe_3)_2]_2$ (0.44 g, 1.00 mmol) in toluene (15 mL). The solution was allowed to warm to room temperature and stirred overnight. The color of the solution changes from orange to yellow, after removal of all the volatiles the residue was extracted with *n*hexane (60 mL). Partial removal of the solvent and storage at room temperature for 2 days afforded colorless crystals of **13**. Yield (0.76 g, 71 %). Anal. Calcd. for $C_{60}H_{88}Al_2N_4O_2Sn$ (1070.04): C 67.35, H 8.29, N 5.24; found C 67.33, H 8.31, N 5.28. 1H NMR (200 MHz, C_6D_6): δ -0.80 (s, 3

H, AlMe), 1.13 (d, $^3J_{\text{HH}} = 6.8\text{Hz}$, 12 H, CHMe₂), 1.23 (d, $^3J_{\text{HH}} = 6.8\text{Hz}$, 12 H, CHMe₂), 1.32 (d, $^3J_{\text{HH}} = 6.8\text{Hz}$, 12 H, CHMe₂), 1.40 (d, $^3J_{\text{HH}} = 6.8\text{Hz}$, 12 H, CHMe₂), 1.64 (s, 12 H, CMe), 3.27 (sept, $^3J_{\text{H-H}} = 6.8\text{ Hz}$, 4 H, CHMe₂), 3.95 (sept, $^3J_{\text{H-H}} = 6.8\text{ Hz}$, 4 H, CHMe₂), 5.10 (s, 2 H, γ -CH), 7.07-7.12 (m, Ar). IR (Nujol, cm⁻¹) $\tilde{\nu}$: 1532, 1383, 1320, 1255, 1193, 1172, 1106, 1043, 938, 876, 770, 757, 689, 543, 456.

4.4.14. Synthesis of [LAl(Me)OLi]₃ (14)

Toluene (20 mL) was added to the mixture of LAl(Me)OH (0.48 g, 1.00 mmol) and LiN(SiMe₃)₂ (0.17 g, 1.00 mmol) at room temperature. The resulting solution was stirred for 12 h. After removal of all volatiles *in vacuo* the crude product was extracted with *n*hexane (20 mL). The filtrate was kept at room temperature for 3 d to give colorless crystals. The crystals were collected by filtration and the filtrate was concentrated (ca 10 mL) and kept at 4 °C for 4 d to give another crop. Total yield: (0.21 g, 43%). Mp: 250 °C. Anal. Calcd. for C₉₀H₁₃₂Al₃Li₃N₆O₃ (1447.80): C 74.66, H 9.19, N 5.80; found C 74.42, H 9.34, N 5.38. ¹H NMR (200 MHz, C₇D₈): δ -1.07 (s, 9 H, AlMe), 1.12, 1.26, 1.37, 1.49 (d, $^3J_{\text{H-H}} = 6.8\text{ Hz}$, 12 x 6 H, CHMe₂), 1.64 (s, 3 x 6 H, CH(CMe)₂), 3.69, 3.28 (sept, $^3J_{\text{H-H}} = 6.8\text{ Hz}$, 12 x 1 H, CHMe₂), 4.98 (s, 3 x 1 H, γ -CH), 6.91-7.22 (m, 6 x 3 H, C₆H₃). ⁷Li NMR (116.6 MHz, C₇D₈): δ 1.97. EI-MS: *m/z* (%): 459 (100) [*M*⁺ - Me - Li], 444 (20) [*M*⁺ - 2 Me - Li]. IR (Nujol, cm⁻¹) $\tilde{\nu}$: 1624, 1587, 1552, 1527, 1395, 1320, 1261, 1222, 1100, 1058, 1021, 937, 858, 799, 759, 722, 703, 686, 637, 598, 448.

4.4.15. Synthesis of [LGa(Me)OLi]₃ (15)

Toluene (20 mL) was added to the mixture of LGa(Me)OH (0.77 g, 1.50 mmol) and LiN(SiMe₃)₂ (0.27 g, 1.60 mmol) at -78 °C. The resulting solution was allowed to come to room

temperature and stirred for 12 h. After removal of all volatiles *in vacuo* the precipitate was extracted with *n*hexane (20 mL). The filtrate was kept at room temperature for 3 d to give colorless crystals. The crystals were collected by filtration and the filtrate was concentrated (ca. 10 mL) and kept at 4 °C for 4 d to give another crop. Total yield: (0.46 g, 58 %). Mp: 280 °C (decomp.). Anal. Calcd. for C₉₀H₁₃₂Ga₃Li₃N₆O₃ (1576.04): C 68.59, H 8.44, N 5.33; found C 68.62, H 8.38, N 5.38. ¹H NMR (500 MHz, C₆D₆): δ -0.60 (s, 9 H, GaMe), 1.14, 1.30, 1.34, 1.49 (d, ³J_{H-H} = 6.8 Hz, 12 x 6 H, CHMe₂), 1.64 (s, 3 x 6 H, CH(CMe)₂), 3.36, 3.78 (sept, ³J_{H-H} = 6.8 Hz, 12 x 1 H, CHMe₂), 4.82 (s, 3 x 1 H, γ-CH), 7.11-7.16 (m, 6 x 3 H, C₆H₃). ⁷Li NMR (116.6 MHz, C₆D₆): δ 1.92. EI-MS: *m/z* (%): 503 (100) [*M*⁺ – Me – Li], 487 (40) [*M*⁺ – Me – OLi]. IR (Nujol, cm⁻¹) $\tilde{\nu}$: 1623, 1554, 1523, 1320, 1260, 1196, 1177, 1106, 1057, 1021, 937, 858, 797, 760, 728, 638, 583, 556, 441.

4.4.16. Synthesis of LGa(Me)(μ-O)Zr(Me)Cp₂ (**16**)

Toluene (60 mL) was added at 0 °C to the mixture of LGa(Me)OH (0.52 g, 1.00 mmol) and Cp₂ZrMe₂ (0.25 g, 1.00 mmol). The resulting solution was stirred for 2 h at room temperature, and then continuously for 24 h at 100 °C. The colorless solution was kept at room temperature for 48 h to isolate colorless crystals of LGa(Me)(μ-O)Zr(Me)Cp₂ (0.52 g). After concentration of the filtrate to 15 mL, the solution was kept at 0 °C for three days. An additional crop of **16** (0.18 g) was obtained. Yield (0.70 g, 93 %). Mp: 318 °C (decomp.). Anal. Calcd. for C₄₁H₅₇GaN₂OZr (754.85): C 65.24, H 7.61, N 3.71; found C 65.28, H 7.58, N 3.73. ¹H NMR (200 MHz, CDCl₃): δ -0.32 (s, 3 H, GaMe), -0.12 (s, 3 H, ZrMe), 1.08 (d, ³J_{H-H} = 6.8, 6 H, CHMe₂), 1.25 (d, ³J_{H-H} = 6.8, 6 H, CHMe₂), 1.38, 1.35 (dd, ³J_{H-H} = 6.8 Hz, 12 H, CHMe₂), 1.74 (s, 6 H, CMe), 3.15 (sept, ³J_{H-H} = 6.8 Hz, 4 H, CHMe₂), 4.87 (s, 1 H, γ-CH), 5.29 (s, 10 H, C₅H₅), 7.25–7.24 (m, Ar).

EI-MS: m/z (%): 739 (48) [$M^+ - \text{Me}$], 501 (100) [$M^+ - 2 \text{ Me} - 2 \text{ H} - \text{ZrCp}_2$], 485 (16) [$M^+ - 2 \text{ Me} - 2 \text{ H} - \text{O} - \text{ZrCp}_2$]. IR (Nujol, cm^{-1}) $\tilde{\nu}$: 1554, 1526, 1438, 1316, 1384, 1264, 1253, 1179, 1120, 1100, 1023, 934, 791, 769, 703, 637, 620, 552, 449.

4.4.17. Synthesis of $\text{LGa}(\text{Me})(\mu\text{-OH})\text{SmCp}_3$ (**17**)

Toluene (40 mL) was added to a mixture of $\text{LGa}(\text{Me})\text{OH}$ (0.52 g, 1.00 mmol) and Cp_3Sm (0.35 g, 1.00 mmol) at room temperature. The mixture was stirred overnight where the color of the mixture slowly turned to yellow from orange. After removal of all volatiles *in vacuo* toluene (60 mL) was added and the mixture was heated to 80 °C and filtered while hot. The clear yellow filtrate was kept at room temperature to afford yellow crystals of $\text{LGa}(\text{Me})(\mu\text{-OH})\text{SmCp}_3$ (0.58 g), another crop of yellow crystals was obtained from the mother liquor (0.17 g). Total yield (0.75 g, 86.7 %). Mp: 275 °C. Anal. Calcd. for $\text{C}_{45}\text{H}_{60}\text{Ga}\text{N}_2\text{OSm}$ (865.05): C 62.48, H 6.99, N 3.24; found C 62.17, H 6.80, N 3.22. EI-MS: m/z (%): 504 (72) [$M^+ - \text{Me} - \text{Cp}_3\text{Sm}$]. IR (Nujol, cm^{-1}) $\tilde{\nu}$: 3592 ($\mu\text{-OH}$), 1521, 1442, 1384, 1311, 1255, 1204, 1176, 1105, 1013, 967, 941, 867, 801, 772, 755, 725, 587, 557, 442.

4.4.18. Synthesis of $\text{LGa}(\text{Me})(\mu\text{-OH})\text{NdCp}_3$ (**18**)

Toluene (45 mL) was added to a mixture of $\text{LGa}(\text{Me})\text{OH}$ (0.26 g, 0.50 mmol) and Cp_3Nd (0.17 g, 0.50 mmol) at room temperature. The mixture was stirred overnight where color of the mixture slowly turned light blue-green in color. After removal of all volatiles *in vacuo* toluene (40 mL) was added to the residue. The mixture was heated to 90 °C and filtered while hot. The clear light blue-green filtrate was kept at room temperature to afford greenish crystals of

LGa(Me)(μ -OH)NdCp₃. Yield (0.38 g, 88.4 %). Mp: 254 °C (decomp.). Anal. Calcd. for C₄₅H₆₀GaN₂NdO (858.93): C 62.92, H 7.04, N 3.26; found C 62.69, H 7.13, N 3.22. EI-MS: *m/z* (%): 792 (2) [*M*⁺ – CpH], 503 (24) [*M*⁺ – Me – Cp₃Nd]. IR (Nujol, cm⁻¹) $\tilde{\nu}$: 3591 (μ -OH), 1553, 1521, 1463, 1440, 1378, 1311, 1258, 1204, 1177, 1106, 963, 942, 868, 801, 784, 770, 953, 725, 587, 557, 442.

4.4.19. Synthesis of LGa(Me)(μ -OH)YbCp₃ (**19**)

Toluene (40 mL) was added to a mixture of LGa(Me)OH (0.26 g, 0.50 mmol) and Cp₃Yb (0.18 g, 0.50 mmol) at room temperature. The mixture was stirred overnight where the color of the mixture slowly turned to orange-yellow from green. After removal of all volatiles *in vacuo* toluene (45 mL) was added and the mixture was heated to 90 °C and filtered while hot. The clear orange-yellow filtrate was kept at room temperature to afford yellow crystals of LGa(Me)(μ -OH)YbCp₃. Total yield (0.37 g, 91 %). Mp: 230 °C (decomp.). Anal. Calcd. for C₄₅H₆₀GaN₂Oy (887.73) C 60.88, H 6.81, N 3.16; found C 60.79, H 6.86, N 3.20. EI-MS: *m/z* (%): 726 (50) [*M*⁺ – 2 Cp – 2 Me], 711 (60) [*M*⁺ – 2 Cp – 3 Me]. IR (Nujol, cm⁻¹) $\tilde{\nu}$: 3609 (μ -OH), 1552, 1524, 1440, 1398, 1315, 1261, 1177, 1106, 1015, 940, 832, 817, 797, 760, 643, 555, 444.

4.4.20. Synthesis of C_{tBu}AuCl (**20**)

In a glove box a 100 mL Schlenk flask was charged with Au(CO)Cl (1.90 g, 7.30 mmol) and topped with a dropping funnel containing 1,3-di-*tert*butylimidazol-2-ylidene (1.31 g, 7.25 mmol). Toluene (50 mL) was added to the dropping funnel and the resulting solution was added dropwise to the flask at room temperature. The mixture was stirred until the CO evolution had

ceased. The solution was filtered and the residue was washed with toluene (30 mL). The combined filtrate was concentrated until the compound began to crystallize and then kept at 0 °C for two days to afford colorless crystals of 1,3-di-*tert*butylimidazol-2-ylidene gold(I) chloride $C_{tBu}AuCl$ (1.8 g), the mother liquor afforded another crop (0.6 g). Total yield (2.48 g, 83%). Mp: 170 °C (decomp.). Anal. Calcd. for $C_{11}H_{20}AuClN_2$ (412): C 32.04, H 4.84, N 6.79; found C 32.27, H 5.01, N 6.80. 1H NMR (200 MHz, CD_3CN): δ 1.83 (s, 18 H, *tBu*), 7.26 (s, 2 H, $HC=CH$). ^{13}C NMR (50 MHz, CD_3CN): δ 31.2 (s, CMe_3), 59.0 (s, CMe_3), 117.7 (s, $HC=CH$), 167.6 (s, NCN). EI-MS: m/z (%): 412 (44) [M^+], 376 (14) [$M^+ - H - Cl$], 356 (14) [$M^+ - tBu - H$], 320 (100) [$M^+ - Cl - tBu$], 264 (36) [$M^+ - 2 tBu - Cl - H$]. IR (Nujol, cm^{-1}) $\tilde{\nu}$: 1646, 1543, 1515, 1406, 1387, 1304, 1262, 1236, 1209, 1183, 1097, 1021, 865, 801, 720, 693, 626.

4.4.21. Synthesis of $C_{Mes}AuCl$ (**21**)

The preparation of $C_{Mes}AuCl$ was carried out by using a similar procedure like that for $C_{tBu}AuCl$. The quantities of the reactants used are $Au(CO)Cl$ (1.72 g, 6.60 mmol) and 1,3-dimesityl imidazol-2-ylidene (1.97 g, 6.50 mmol). Yield (2.3 g, 67%). Mp: 210 °C (decomp.). Anal. Calcd. for $C_{21}H_{24}AuClN_2$ (536): C 47.01, H 4.47, N 5.22; found C 46.63, H 4.51, N 4.95. 1H NMR (300 MHz, $THF-D_8$): δ 1.75 (s, 12 H, *o-Me*), 2.13 (s, 6 H, *p-Me*), 6.99 (s, 4 H, *m-H*), 7.46 (s, 2 H, $HC=CH$). ^{13}C NMR (126 MHz, $THF-D_8$): δ 17.4 (s, *o-Me*), 21.3 (s, *p-Me*), 123.6 (s, $HC=CH$), 124.3 (s, mesityl $C_{3,5}$), 130.0 (s, mesityl C_1), 135.6 (s, mesityl $C_{2,6}$), 140.2 (s, mesityl C_4). EI-MS: m/z (%): 536 (28) [M^+], 500 (92) [$M^+ - Cl - H$], 303 (100) [$M^+ - Cl - Au - H$].

4.4.22. Synthesis of $C_{tBu}AuC\equiv CH$ (22)

1,3-Di-*tert*-butylimidazol-2-ylidene gold(I) chloride, $C_{tBu}AuCl$ (1.0 g, 2.43 mmol) was dissolved in THF (30 mL). To this solution was added 5.1 mL (2.55 mmol, 1.05 eq) of 0.5 M, THF solution of ethynyl magnesium chloride. The solution was stirred overnight at room temperature and after the removal of all the volatiles, the crude product was extracted with toluene (45 mL). Crude yield (0.72 g, 72%). Mp: 155 °C (decomp.). Anal. Calcd. for $C_{13}H_{21}AuN_2$ (402): C 38.80, H 5.22, N 6.96; found C 38.79, H 5.10, N 6.85. 1H NMR (500 MHz, THF- D_8) δ 1.22 (s, 1H, $-C\equiv CH$), 1.84 (s, 18 H, *tBu*) 7.29 (d, 2 H, $HC=CH$). ^{13}C NMR (126 MHz, THF- D_8): δ 32.0 (s, CMe_3), 59.2 (s, CMe_3), 89.6 (s, $-C\equiv CH$), 117.3 (s, $HC=CH$), 120.0 (s, $-C\equiv CH$), 187.9 (s, NCN). EI-MS: m/z (%): 402 (100) [M^+], 376 (20) [$M^+ - H - HC=CH$], 320 (60) [$M^+ - tBu - HC=CH$], 290 (80) [$M^+ - tBu - HC=CH - 2 Me$]. IR (Nujol, cm^{-1}) $\tilde{\nu}$: 1979 ($C\equiv C$), 1665, 1667, 1456, 1407, 1375, 1301, 1261, 1234, 1219, 1194, 1094, 1025, 933, 865, 801, 726, 696, 661, 627, 601.

4.4.23. Synthesis of $C_{Mes}AuC\equiv CH$ (23)

The preparation of $C_{Mes}AuC\equiv CH$ was carried out by using a similar procedure like that for $C_{tBu}AuC\equiv CH$. The quantities of the reactants used are 1,3-di-mesitylimidazol-2-ylidene gold(I) chloride, $C_{Mes}AuCl$ (1.0 g, 1.86 mmol) and 4.0 mL (2.0 mmol, 1.07 eq) of 0.5 M, THF solution of ethynyl magnesium chloride. Yield (0.67 g, 72%). Mp: 240 °C (decomp.). Anal. Calcd. for $C_{23}H_{25}AuN_2$ (526.5): C 52.42, H 4.74, N 5.32; found C 51.87, H 4.82, N 5.43. 1H NMR (300 MHz, THF- D_8): δ 0.86 (s, 1 H, $-C\equiv CH$), 2.13 (s, 12 H, *o-Me*), 2.34 (s, 6 H, *p-Me*), 7.04 (s, 4 H, *m-H*), 7.38 (s, 2 H, $HC=CH$). ^{13}C NMR (75 MHz, THF- D_8): δ 18.0 (s, *o-Me*), 21.0 (s, *p-Me*),

88.0 (s, $\text{-C}\equiv\text{CH}$), 123.5 (s, $\text{HC}=\text{CH}$), 124.4 (s, $\text{-C}\equiv\text{CH}$), 130.0 (s, mesityl $\text{C}_{3,5}$), 135.6 (s, mesityl C_1), 136.4 (s, mesityl $\text{C}_{2,6}$), 139.9 (s, mesityl C_4), 190.6 (s, NCN). EI-MS: m/z (%): 526 (64) $[M^+]$, 500 (60) $[M^+ - \text{C}_2\text{H} - \text{H}]$, 303 (100) $[M^+ - \text{C}_2\text{H} - \text{Au} - \text{H}]$. IR (Nujol, cm^{-1}) $\tilde{\nu}$: 1982 ($\text{C}\equiv\text{C}$), 1730, 1606, 1559, 1484, 1409, 1376, 1339, 1290, 1234, 1164, 1028, 926, 852, 755, 705, 629, 574.

5. Handling and Disposal of Solvents and Residual Waste

1. The recovered solvents were distilled or condensed into a liquid nitrogen cold-trap *in vacuo* and collected in halogen-free or halogen-containing solvent containers, and stored for disposal.
2. Used NMR solvents were classified into halogen-free or halogen-containing solvents and disposed accordingly.
3. The acid-bath used for cleaning glassware was neutralized with Na_2CO_3 and the resulting NaCl solution was washed off in the communal water drainage.
4. The residue of the base-bath used for cleaning glassware was poured into a container for waste disposal.
5. Sodium metal used for drying solvents was collected and reacted carefully with *iso*-propanol and poured into base-bath for cleaning glassware.
6. Ethanol and acetone used for low temperature reactions using cold-baths (with solid CO_2 or liquid N_2) were subsequently used for cleaning glassware.

Amounts of various types of disposable wastes generated during the work:

Halogen-containing solvent waste	5 L
Halogen-free solvent waste	30 L
Acid waste	12 L
Basic waste	22 L

6. Crystal Data and Refinement Details

Table 1. Crystal data and structure refinement details for LAl(Me)Cl (1).

Empirical formula	C ₃₀ H ₄₄ AlClN ₂
Formula weight	495.10
Temperature	100(2) K
Wavelength	1.54178 Å
Crystal system	Monoclinic
Space group	<i>P</i> 2 ₁ / <i>c</i>
Unit cell dimensions	<i>a</i> = 12.620(3) Å <i>b</i> = 19.323(4) Å <i>β</i> = 117.29(3)° <i>c</i> = 13.305(3) Å
Volume	2883(1) Å ³
<i>Z</i>	4
Density (calculated)	1.141 Mg/m ³
Absorption coefficient	1.600 (CuKα)/ mm ⁻¹
<i>F</i> (000)	1072
Crystal size	0.20 x 0.20 x 0.01 mm ³
<i>θ</i> range for data collection	4.00 to 58.99°
Index ranges	-14 ≤ <i>h</i> ≤ 13, -21 ≤ <i>k</i> ≤ 21, -14 ≤ <i>l</i> ≤ 14
Reflections collected	23769
Independent reflections	4096 (<i>R</i> _{int} = 0.0386)
Completeness to <i>θ</i> = 58.99°	98.7 %
Refinement method	Full-matrix least-squares on <i>F</i> ²
Data / restraints / parameters	4096 / 3 / 327
Goodness-of-fit on <i>F</i> ²	1.048
Final <i>R</i> indices (<i>I</i> > 2 σ(<i>I</i>))	<i>R</i> 1 = 0.0357, <i>wR</i> 2 = 0.0917
<i>R</i> indices (all data)	<i>R</i> 1 = 0.0445, <i>wR</i> 2 = 0.0977
Largest diff. Peak and hole	0.194 and -0.335 e.Å ⁻³

Table 2. Crystal data and structure refinement details for LGa(Me) Cl (2).

Empirical formula	C ₃₀ H ₄₄ ClGaN ₂
Formula weight	537.84
Temperature	100(2) K
Wavelength	1.54178 Å
Crystal system	Monoclinic
Space group	<i>P</i> 2 ₁ / <i>n</i>
Unit cell dimensions	<i>a</i> = 12.666(3) Å <i>b</i> = 19.287(4) Å <i>β</i> = 117.55(3)° <i>c</i> = 13.299(3) Å
Volume	2880(1) Å ³
Z	4
Density (calculated)	1.240 Mg/m ³
Absorption coefficient	2.292 (CuKα)/ mm ⁻¹
<i>F</i> (000)	1144
Crystal size	0.10 x 0.10 x 0.07 mm ³
<i>θ</i> range for data collection	3.99 to 59.09°
Index ranges	-14 ≤ <i>h</i> ≤ 12, -20 ≤ <i>k</i> ≤ 21, -14 ≤ <i>l</i> ≤ 14
Reflections collected	16011
Independent reflections	4108 (<i>R</i> _{int} = 0.0235)
Completeness to <i>θ</i> = 59.09°	98.8 %
Refinement method	Full-matrix least-squares on <i>F</i> ²
Data / restraints / parameters	4108 / 0 / 322
Goodness-of-fit on <i>F</i> ²	1.047
Final <i>R</i> indices (<i>I</i> > 2 σ(<i>I</i>))	<i>R</i> 1 = 0.0228, <i>wR</i> 2 = 0.0618
<i>R</i> indices (all data)	<i>R</i> 1 = 0.0231, <i>wR</i> 2 = 0.0620
Largest diff. Peak and hole	0.293 and -0.270 e.Å ⁻³

Table 3. Crystal data and structure refinement details for LiIn(Me)Cl (3).

Empirical formula	$\text{C}_{30}\text{H}_{44}\text{ClInN}_2$
Formula weight	582.94
Temperature	100(2) K
Wavelength	1.54178 Å
Crystal system	Monoclinic
Space group	$P2_1/n$
Unit cell dimensions	$a = 12.789(2)$ Å $b = 19.631(3)$ Å $\beta = 117.53(1)^\circ$ $c = 13.294(2)$ Å
Volume	$2960(1)$ Å ³
Z	4
Density (calculated)	1.308 Mg/m ³
Absorption coefficient	7.340 (CuK α)/mm ⁻¹
$F(000)$	1216
Crystal size	0.10 x 0.10 x 0.05 mm ³
θ range for data collection	3.97 to 59.04°
Index ranges	$-14 \leq h \leq 14$, $-19 \leq k \leq 21$, $-13 \leq l \leq 14$
Reflections collected	15305
Independent reflections	4134 ($R_{\text{int}} = 0.0344$)
Completeness to $\theta = 59.04^\circ$	97.1 %
Refinement method	Full-matrix least-squares on F^2
Data / restraints / parameters	4134 / 0 / 322
Goodness-of-fit on F^2	1.070
Final R indices ($I > 2 \sigma(I)$)	$R1 = 0.0215$, $wR2 = 0.0537$
R indices (all data)	$R1 = 0.0218$, $wR2 = 0.0540$
Largest diff. Peak and hole	0.382 and -0.373 e.Å ⁻³

Table 4. Crystal data and structure refinement details for LAl(Me)F (4).

Empirical formula	C ₃₀ H ₄₄ AlFN ₂
Formula weight	478.65
Temperature	100(2) K
Wavelength	1.54178 Å
Crystal system	Monoclinic
Space group	<i>P</i> 2 ₁ / <i>c</i>
Unit cell dimensions	<i>a</i> = 9.002(2) Å <i>b</i> = 9.622(2) Å <i>β</i> = 91.59(3)° <i>c</i> = 32.954(7) Å
Volume	2853(1) Å ³
Z	4
Density (calculated)	1.114 Mg/m ³
Absorption coefficient	0.812 (CuKα)/ mm ⁻¹
<i>F</i> (000)	1040
Crystal size	0.20 x 0.10 x 0.10 mm ³
<i>θ</i> range for data collection	2.68 to 58.95°
Index ranges	-9 ≤ <i>h</i> ≤ 10, -10 ≤ <i>k</i> ≤ 10, -15 ≤ <i>l</i> ≤ 36
Reflections collected	11809
Independent reflections	3966 (<i>R</i> _{int} = 0.0300)
Completeness to <i>θ</i> = 58.95°	96.7 %
Refinement method	Full-matrix least-squares on <i>F</i> ²
Data / restraints / parameters	3966 / 0 / 322
Goodness-of-fit on <i>F</i> ²	1.038
Final <i>R</i> indices (<i>I</i> > 2 σ(<i>I</i>))	<i>R</i> 1 = 0.0336, <i>wR</i> 2 = 0.0861
<i>R</i> indices (all data)	<i>R</i> 1 = 0.0384, <i>wR</i> 2 = 0.0894
Largest diff. Peak and hole	0.245 and -0.210 e.Å ⁻³

Table 5. Crystal data and structure refinement details for LaAlF_2 (5).

Empirical formula	$\text{C}_{29}\text{H}_{41}\text{AlF}_2\text{N}_2$
Formula weight	482.62
Temperature	103(2) K
Wavelength	1.54178 Å
Crystal system	Monoclinic
Space group	$P2_1/n$
Unit cell dimensions	$a = 12.474(3)$ Å $b = 15.853(3)$ Å $\beta = 104.39(3)^\circ$ $c = 14.196(3)$ Å
Volume	$2719(1)$ Å ³
Z	4
Density (calculated)	1.179 Mg/m ³
Absorption coefficient	0.911 (CuK α)/mm ⁻¹
$F(000)$	1040
Crystal size	0.60 x 0.50 x 0.50 mm ³
θ range for data collection	4.23 to 59.09°
Index ranges	$-13 \leq h \leq 13$, $-17 \leq k \leq 16$, $-15 \leq l \leq 15$
Reflections collected	24658
Independent reflections	3916 ($R_{\text{int}} = 0.0462$)
Completeness to $\theta = 59.09^\circ$	99.7 %
Refinement method	Full-matrix least-squares on F^2
Data / restraints / parameters	3912 / 296 / 321
Goodness-of-fit on F^2	1.015
Final R indices ($I > 2 \sigma(I)$)	$R1 = 0.0328$, $wR2 = 0.0809$
R indices (all data)	$R1 = 0.0404$, $wR2 = 0.0859$
Largest diff. Peak and hole	0.194 and -0.219 e.Å ⁻³

Table 6. Crystal data and structure refinement details for LGa(Me)H (6).

Empirical formula	C ₃₀ H ₄₅ GaN ₂
Formula weight	503.40
Temperature	100(2) K
Wavelength	1.54178 Å
Crystal system	Monoclinic
Space group	<i>P</i> 2 ₁ / <i>c</i>
Unit cell dimensions	<i>a</i> = 8.957(2) Å <i>b</i> = 9.664(2) Å <i>β</i> = 91.43(2)° <i>c</i> = 33.123(6) Å
Volume	2866(1) Å ³
Z	4
Density (calculated)	1.167 Mg/m ³
Absorption coefficient	1.432 (CuKα)/ mm ⁻¹
<i>F</i> (000)	1080
Crystal size	0.30 x 0.30 x 0.20 mm ³
<i>θ</i> range for data collection	2.67 to 58.95°
Index ranges	−9 ≤ <i>h</i> ≤ 9, −10 ≤ <i>k</i> ≤ 10, −36 ≤ <i>l</i> ≤ 36
Reflections collected	17143
Independent reflections	4090 (<i>R</i> _{int} = 0.0310)
Completeness to <i>θ</i> = 58.95°	99.2 %
Refinement method	Full-matrix least-squares on <i>F</i> ²
Data / restraints / parameters	4090 / 0 / 316
Goodness-of-fit on <i>F</i> ²	1.062
Final <i>R</i> indices (<i>I</i> > 2 σ(<i>I</i>))	<i>R</i> 1 = 0.0285, <i>wR</i> 2 = 0.0704
<i>R</i> indices (all data)	<i>R</i> 1 = 0.0288, <i>wR</i> 2 = 0.0707
Largest diff. Peak and hole	0.609 and −0.231 e.Å ⁻³

Table 7. Crystal data and structure refinement details for LAl(Me)OH (7).

Empirical formula	C ₃₀ H ₄₅ AlN ₂ O
Formula weight	476.66
Temperature	100(2) K
Wavelength	0.71073 Å
Crystal system	Monoclinic
Space group	<i>P</i> 2 ₁ / <i>c</i>
Unit cell dimensions	<i>a</i> = 9.036(3) Å <i>b</i> = 9.763(4) Å <i>β</i> = 91.40(6)° <i>c</i> = 33.170(6) Å
Volume	2926(6) Å ³
Z	4
Density (calculated)	1.082 Mg/m ³
Absorption coefficient	0.092 (MoKα)/ mm ⁻¹
<i>F</i> (000)	1040
Crystal size	0.80 x 0.70 x 0.70 mm ³
<i>θ</i> range for data collection	7.10 to 50.12°
Index ranges	-10 ≤ <i>h</i> ≤ 10, -9 ≤ <i>k</i> ≤ 11, -35 ≤ <i>l</i> ≤ 39
Reflections collected	6159
Independent reflections	4899 (<i>R</i> _{int} = 0.1157)
Completeness to <i>θ</i> = 50.12°	99.2 %
Refinement method	Full-matrix least-squares on <i>F</i> ²
Data / restraints / parameters	4899 / 0 / 322
Goodness-of-fit on <i>F</i> ²	1.058
Final <i>R</i> indices (<i>I</i> > 2 σ(<i>I</i>))	<i>R</i> 1 = 0.0755, <i>wR</i> 2 = 0.2231
<i>R</i> indices (all data)	<i>R</i> 1 = 0.0846, <i>wR</i> 2 = 0.2303
Largest diff. Peak and hole	0.551 and -0.410 e.Å ⁻³

Table 8. Crystal data and structure refinement details for LGa(Me)OH (8).

Empirical formula	C ₃₀ H ₄₅ GaN ₂ O
Formula weight	519.40
Temperature	100(2) K
Wavelength	1.54178 Å
Crystal system	Monoclinic
Space group	<i>P</i> 2 ₁ / <i>c</i>
Unit cell dimensions	<i>a</i> = 8.943(2) Å <i>b</i> = 9.752(2) Å <i>β</i> = 92.09(2)° <i>c</i> = 33.182(4) Å
Volume	2892(1) Å ³
<i>Z</i>	4
Density (calculated)	1.193 Mg/m ³
Absorption coefficient	1.462 (CuKα)/ mm ⁻¹
<i>F</i> (000)	1112
Crystal size	0.20 x 0.15 x 0.10 mm ³
<i>θ</i> range for data collection	2.66 to 59.08°
Index ranges	−9 ≤ <i>h</i> ≤ 9, −10 ≤ <i>k</i> ≤ 10, −36 ≤ <i>l</i> ≤ 35
Reflections collected	19318
Independent reflections	4120 (<i>R</i> _{int} = 0.0268)
Completeness to <i>θ</i> = 59.08°	98.9 %
Refinement method	Full-matrix least-squares on <i>F</i> ²
Data / restraints / parameters	4120 / 0 / 327
Goodness-of-fit on <i>F</i> ²	1.064
Final <i>R</i> indices (<i>I</i> > 2 σ(<i>I</i>))	<i>R</i> 1 = 0.0268, <i>wR</i> 2 = 0.0666
<i>R</i> indices (all data)	<i>R</i> 1 = 0.0274, <i>wR</i> 2 = 0.0671
Largest diff. Peak and hole	0.252 and −0.302 e.Å ⁻³

Table 9. Crystal data and structure refinement details for [LAl(Me)(μ -O)AlH₂]₂·C₆H₁₄ (9)·C₆H₁₄.

Empirical formula	C ₆₆ H ₁₀₆ Al ₄ N ₄ O ₂ incl. hexane
Formula weight	1095.47
Temperature	103(2) K
Wavelength	1.54178 Å
Crystal system	Monoclinic
Space group	<i>P</i> 2 ₁ / <i>c</i>
Unit cell dimensions	<i>a</i> = 20.420(2) Å <i>b</i> = 17.760(2) Å β = 103.21(2)° <i>c</i> = 18.850(2) Å
Volume	6655.2(8) Å ³
Z	4
Density (calculated)	1.093 Mg/m ³
Absorption coefficient	0.973 (CuK α)/mm ⁻¹
<i>F</i> (000)	2392
Crystal size	0.20 x 0.10 x 0.20 mm ³
θ range for data collection	2.22 to 58.93°
Index ranges	-22 ≤ <i>h</i> ≤ 22, -19 ≤ <i>k</i> ≤ 19, -20 ≤ <i>l</i> ≤ 20
Reflections collected	61271
Independent reflections	9543 (<i>R</i> _{int} = 0.0579)
Completeness to θ = 58.93°	99.8 %
Refinement method	Full-matrix least-squares on <i>F</i> ²
Data / restraints / parameters	9543 / 761 / 786
Goodness-of-fit on <i>F</i> ²	1.029
Final <i>R</i> indices (<i>I</i> > 2 σ (<i>I</i>))	<i>R</i> 1 = 0.0403, <i>wR</i> 2 = 0.1050
<i>R</i> indices (all data)	<i>R</i> 1 = 0.0555, <i>wR</i> 2 = 0.1162
Largest diff. Peak and hole	0.411 and -0.310 e.Å ⁻³

Table 10. Crystal data and structure refinement details for [LAl(Me)(μ -O)GaH₂]₂·C₆H₁₄ (10)·C₆H₁₄.

Empirical formula	C ₆₆ H ₁₀₆ Al ₂ Ga ₂ N ₄ O ₂ incl. hexane
Formula weight	1180.95
Temperature	133(2) K
Wavelength	0.71073 Å
Crystal system	Monoclinic
Space group	<i>P</i> 2 ₁ / <i>m</i>
Unit cell dimensions	<i>a</i> = 9.443(2) Å <i>b</i> = 17.889(2) Å β = 103.12(2)° <i>c</i> = 20.491(5) Å
Volume	3371(2) Å ³
Z	2
Density (calculated)	1.163 Mg/m ³
Absorption coefficient	0.868 (MoK α)/ mm ⁻¹
<i>F</i> (000)	1268
Crystal size	0.30 x 0.20 x 0.20 mm ³
θ range for data collection	3.06 to 49.60°
Index ranges	-9 ≤ <i>h</i> ≤ 11, -21 ≤ <i>k</i> ≤ 21, -24 ≤ <i>l</i> ≤ 24
Reflections collected	20878
Independent reflections	5960 (<i>R</i> _{int} = 0.0515)
Completeness to θ = 49.60°	99.3 %
Refinement method	Full-matrix least-squares on <i>F</i> ²
Data / restraints / parameters	5960 / 621 / 388
Goodness-of-fit on <i>F</i> ²	0.932
Final <i>R</i> indices (<i>I</i> > 2 σ (<i>I</i>))	<i>R</i> 1 = 0.0362, <i>wR</i> 2 = 0.0932
<i>R</i> indices (all data)	<i>R</i> 1 = 0.0503, <i>wR</i> 2 = 0.0999
Largest diff. Peak and hole	0.719 and -0.536 e.Å ⁻³

Table 11. Crystal data and structure refinement details for [LAl(Me)(μ -O)]₂Sb(NMe₂) (11).

Empirical formula	C ₆₂ H ₉₄ Al ₂ N ₅ O ₂ Sb
Formula weight	1117.13
Temperature	100(2) K
Wavelength	1.54178 Å
Crystal system	Triclinic
Space group	<i>P</i> -1
Unit cell dimensions	$a = 13.402(2)$ Å $\alpha = 95.05(2)^\circ$ $b = 16.104(3)$ Å $\beta = 103.26(2)^\circ$ $c = 16.760(3)$ Å $\gamma = 114.43(2)^\circ$
Volume	3137(1) Å ³
Z	2
Density (calculated)	1.183 Mg/m ³
Absorption coefficient	4.084 (CuK α)/ mm ⁻¹
<i>F</i> (000)	1188
Crystal size	0.30 x 0.20 x 0.10 mm ³
θ range for data collection	2.77 to 59.05°
Index ranges	$-14 \leq h \leq 14$, $-17 \leq k \leq 17$, $-18 \leq l \leq 18$
Reflections collected	23935
Independent reflections	8559 (<i>R</i> _{int} = 0.0313)
Completeness to $\theta = 59.05^\circ$	94.7 %
Refinement method	Full-matrix least-squares on <i>F</i> ²
Data / restraints / parameters	8559 / 186 / 714
Goodness-of-fit on <i>F</i> ²	1.048
Final <i>R</i> indices (<i>I</i> > 2 σ (<i>I</i>))	<i>R</i> 1 = 0.0323, <i>wR</i> 2 = 0.0771
<i>R</i> indices (all data)	<i>R</i> 1 = 0.0355, <i>wR</i> 2 = 0.0792
Largest diff. Peak and hole	0.957 and -0.708 e.Å ⁻³

Table 12. Crystal data and structure refinement details for [LiAl(Me)OLi]₃·C₆H₁₄ (14)·C₆H₁₄.

Empirical formula	C ₉₆ H ₁₄₆ Al ₃ Li ₃ N ₆ O ₃ incl. hexane
Formula weight	1533.95
Temperature	100(2) K
Wavelength	1.54178 Å
Crystal system	Hexagonal
Space group	<i>P</i> (6) ₃
Unit cell dimensions	<i>a</i> = 15.848(1) Å <i>b</i> = 15.848(1) Å $\alpha = \beta = 90^\circ, \gamma = 120^\circ$ <i>c</i> = 21.397(1) Å
Volume	4654(1) Å ³
Z	2
Density (calculated)	1.095 Mg/m ³
Absorption coefficient	0.746 (CuKα)/ mm ⁻¹
<i>F</i> (000)	1672
Crystal size	0.25 x 0.20 x 0.10 mm ³
θ range for data collection	3.22. to 58.93°
Index ranges	$-17 \leq h \leq 16, -17 \leq k \leq 17, -23 \leq l \leq 22$
Reflections collected	26427
Independent reflections	4386 (<i>R</i> _{int} = 0.0274)
Completeness to $\theta = 58.93^\circ$	99.7 %
Refinement method	Full-matrix least-squares on <i>F</i> ²
Data / restraints / parameters	4386 / 254 / 414
Goodness-of-fit on <i>F</i> ²	1.082
Final <i>R</i> indices (<i>I</i> > 2 σ(<i>I</i>))	<i>R</i> 1 = 0.0307, <i>wR</i> 2 = 0.0857
<i>R</i> indices (all data)	<i>R</i> 1 = 0.0315, <i>wR</i> 2 = 0.866
Largest diff. Peak and hole	0.305 and -0.393 e.Å ⁻³

Table 13. Crystal data and structure refinement details for [LGa(Me)OLi]₃·C₆H₁₄ (15)·C₆H₁₄.

Empirical formula	C ₉₆ H ₁₄₆ Ga ₃ Li ₃ N ₆ O ₃ incl. hexane
Formula weight	1662.18
Temperature	100(2) K
Wavelength	1.54178 Å
Crystal system	Hexagonal
Space group	<i>P</i> (6) ₃
Unit cell dimensions	<i>a</i> = 15.902(2) Å <i>b</i> = 15.902 (2) Å $\alpha = \beta = 90^\circ, \gamma = 120^\circ$ <i>c</i> = 21.419(3) Å
Volume	4690.7(11) Å ³
<i>Z</i>	6
Density (calculated)	1.177 Mg/m ³
Absorption coefficient	1.376 (CuK α)/ mm ⁻¹
<i>F</i> (000)	1780
Crystal size	0.2 x 0.15 x 0.15 mm ³
θ range for data collection	3.21 to 59.07°
Index ranges	$-17 \leq h \leq 17, -17 \leq k \leq 17, -23 \leq l \leq 23$
Reflections collected	33693
Independent reflections	4490 (<i>R</i> _{int} = 0.0330)
Completeness to $\theta = 59.07^\circ$	99.6 %
Refinement method	Full-matrix least-squares on <i>F</i> ²
Data / restraints / parameters	4490 / 57 / 386
Goodness-of-fit on <i>F</i> ²	1.050
Final <i>R</i> indices (<i>I</i> > 2 σ (<i>I</i>))	<i>R</i> 1 = 0.0218, <i>wR</i> 2 = 0.0601
<i>R</i> indices (all data)	<i>R</i> 1 = 0.0224, <i>wR</i> 2 = 0.0606
Largest diff. Peak and hole	0.263 and -0.197 e.Å ⁻³

Table 14. Crystal data and structure refinement details for LGa(Me)(μ -O)Zr(Me)Cp₂ (16).

Empirical formula	C ₄₁ H ₅₇ GaN ₂ OZr
Formula weight	754.83
Temperature	100(2) K
Wavelength	1.54178 Å
Crystal system	Monoclinic
Space group	<i>P</i> 2 ₁ / <i>n</i>
Unit cell dimensions	<i>a</i> = 10.056(2) Å <i>b</i> = 18.586(3) Å β = 90.20(1)° <i>c</i> = 20.013(3) Å
Volume	3740(1) Å ³
Z	4
Density (calculated)	1.340 Mg/m ³
Absorption coefficient	3.407 (CuK α)/mm ⁻¹
<i>F</i> (000)	1584
Crystal size	0.20 x 0.15 x 0.10 mm ³
θ range for data collection	3.24 to 57.90°
Index ranges	-10 ≤ <i>h</i> ≤ 9, -20 ≤ <i>k</i> ≤ 18, -21 ≤ <i>l</i> ≤ 21
Reflections collected	17776
Independent reflections	4956 (<i>R</i> _{int} = 0.0195)
Completeness to θ = 57.90°	95.5 %
Refinement method	Full-matrix least-squares on <i>F</i> ²
Data / restraints / parameters	4956 / 0 / 432
Goodness-of-fit on <i>F</i> ²	1.061
Final <i>R</i> indices (<i>I</i> > 2 σ (<i>I</i>))	<i>R</i> 1 = 0.0199, <i>wR</i> 2 = 0.0464
<i>R</i> indices (all data)	<i>R</i> 1 = 0.0222, <i>wR</i> 2 = 0.0477
Largest diff. Peak and hole	0.227 and -0.350 e.Å ⁻³

Table 15. Crystal data and structure refinement details for LGa(Me)(μ -OH)SmCp₃ (17).

Empirical formula	C ₄₅ H ₆₀ GaN ₂ OSm
Formula weight	865.01
Temperature	100(2) K
Wavelength	1.54178 Å
Crystal system	Monoclinic
Space group	<i>P</i> 2 ₁ / <i>m</i>
Unit cell dimensions	<i>a</i> = 10.219(2) Å <i>b</i> = 19.616(3) Å β = 109.23(3)° <i>c</i> = 10.586(2) Å
Volume	2003.6(6) Å ³
Z	2
Density (calculated)	1.432 Mg/m ³
Absorption coefficient	11.971 (CuK α)/ mm ⁻¹
<i>F</i> (000)	888
Crystal size	0.10 x 0.10 x 0.20 mm ³
θ range for data collection	4.42 to 59.05°
Index ranges	-11 ≤ <i>h</i> ≤ 10, 0 ≤ <i>k</i> ≤ 21, 0 ≤ <i>l</i> ≤ 11
Reflections collected	18619
Independent reflections	2951 (<i>R</i> _{int} = 0.0536)
Completeness to θ = 59.09°	98.6 %
Refinement method	Full-matrix least-squares on <i>F</i> ²
Data / restraints / parameters	2951 / 0 / 241
Goodness-of-fit on <i>F</i> ²	1.077
Final <i>R</i> indices (<i>I</i> > 2 σ (<i>I</i>))	<i>R</i> 1 = 0.0521, <i>wR</i> 2 = 0.1192
<i>R</i> indices (all data)	<i>R</i> 1 = 0.0528, <i>wR</i> 2 = 0.1197
Largest diff. Peak and hole	1.141 and -1.077 e.Å ⁻³

Table 16. Crystal data and structure refinement details for LGa(Me)(μ -OH)NdCp₃ (18).

Empirical formula	C ₄₅ H ₆₀ GaN ₂ NdO
Formula weight	858.91
Temperature	100(2) K
Wavelength	1.54178 Å
Crystal system	Monoclinic
Space group	<i>P</i> 2 ₁ / <i>m</i>
Unit cell dimensions	<i>a</i> = 10.223(2) Å <i>b</i> = 19.588(3) Å β = 109.26(2)° <i>c</i> = 10.594(2) Å
Volume	2002.7(6) Å ³
Z	2
Density (calculated)	1.424(2) Mg/m ³
Absorption coefficient	10.858 (CuK α)/ mm ⁻¹
<i>F</i> (000)	886
Crystal size	0.10 x 0.10 x 0.15 mm ³
θ range for data collection	4.42 to 58.98°
Index ranges	-11 ≤ <i>h</i> ≤ 10, 0 ≤ <i>k</i> ≤ 21, 0 ≤ <i>l</i> ≤ 11
Reflections collected	18407
Independent reflections	3414 (<i>R</i> _{int} = 0.0408)
Completeness to θ = 58.98°	99.7 %
Refinement method	Full-matrix least-squares on <i>F</i> ²
Data / restraints / parameters	3414 / 2 / 248
Goodness-of-fit on <i>F</i> ²	1.147
Final <i>R</i> indices (<i>I</i> > 2 σ (<i>I</i>))	<i>R</i> 1 = 0.0234, <i>wR</i> 2 = 0.0591
<i>R</i> indices (all data)	<i>R</i> 1 = 0.0236, <i>wR</i> 2 = 0.0592
Largest diff. Peak and hole	0.651 and -0.414 e.Å ⁻³

Table 17. Crystal data and structure refinement details for $C_{18}H_{28}AuClN_2$ (20)· C_7H_8 .

Empirical formula	$C_{18}H_{28}AuClN_2$ incl. toluene
Formula weight	504.84
Temperature	200(2) K
Wavelength	0.71073 Å
Crystal system	Monoclinic
Space group	$P2_1/c$
Unit cell dimensions	$a = 9.355(3)$ Å $b = 10.291(3)$ Å $\beta = 97.84(7)^\circ$ $c = 20.56(3)$ Å
Volume	$1961(3)$ Å ³
Z	4
Density (calculated)	1.710 Mg/m ³
Absorption coefficient	7.637 (MoK α)/ mm ⁻¹
$F(000)$	984
Crystal size	0.80 x 0.30 x 0.30 mm ³
θ range for data collection	3.59 to 24.98°
Index ranges	$-11 \leq h \leq 11$, $-10 \leq k \leq 12$, $-23 \leq l \leq 24$
Reflections collected	5093
Independent reflections	3416 ($R_{int} = 0.0852$)
Completeness to $\theta = 24.98^\circ$	98.7 %
Refinement method	Full-matrix least-squares on F^2
Data / restraints / parameters	3416 / 0 / 206
Goodness-of-fit on F^2	1.092
Final R indices ($I > 2 \sigma(I)$)	$R1 = 0.0489$, $wR2 = 0.1296$
R indices (all data)	$R1 = 0.0532$, $wR2 = 0.1348$
Largest diff. Peak and hole	2.660 and -2.084 e.Å ⁻³

Table 18. Crystal data and structure refinement details for C_{Mes}AuCl (21).

Empirical formula	C ₂₁ H ₂₄ AuClN ₂
Formula weight	536.84
Temperature	100(2) K
Wavelength	1.54178 Å
Crystal system	Orthorhombic
Space group	<i>Fdd2</i>
Unit cell dimensions	$a = 14.715(3) \text{ Å}$ $b = 28.748(6) \text{ Å}$ $\alpha = \beta = \gamma = 90.00^\circ$ $c = 9.678(2) \text{ Å}$
Volume	4094(2) Å ³
Z	8
Density (calculated)	1.742 Mg/m ³
Absorption coefficient	14.732 (CuK α)/ mm ⁻¹
<i>F</i> (000)	2080
Crystal size	0.15 x 0.10 x 0.10 mm ³
θ range for data collection	5.68 to 59.04°
Index ranges	$-16 \leq h \leq 16, -31 \leq k \leq 31, -10 \leq l \leq 10$
Reflections collected	7611
Independent reflections	1454 (<i>R</i> _{int} = 0.0280)
Completeness to $\theta = 59.04^\circ$	99.9 %
Refinement method	Full-matrix least-squares on <i>F</i> ²
Data / restraints / parameters	1454 / 1 / 122
Goodness-of-fit on <i>F</i> ²	1.106
Final <i>R</i> indices (<i>I</i> > 2 $\sigma(I)$)	<i>R</i> 1 = 0.0127, <i>wR</i> 2 = 0.0299
<i>R</i> indices (all data)	<i>R</i> 1 = 0.0128, <i>wR</i> 2 = 0.0300
Largest diff. Peak and hole	0.487 and -0.422 e.Å ⁻³

Table 19. Crystal data and structure refinement details for $\text{C}_{1\text{Bu}}\text{AuC}\equiv\text{CH}\cdot\text{C}_7\text{H}_8$ (22)· C_7H_8 .

Empirical formula	$\text{C}_{20}\text{H}_{29}\text{AuN}_2$ incl. toluene
Formula weight	494.42
Temperature	200(2) K
Wavelength	0.71073 Å
Crystal system	Monoclinic
Space group	$P2_1/c$
Unit cell dimensions	$a = 9.459(4)$ Å $b = 10.350(6)$ Å $\beta = 98.25(6)^\circ$ $c = 20.714(12)$ Å
Volume	$2007(2)$ Å ³
Z	4
Density (calculated)	1.636 Mg/m ³
Absorption coefficient	7.332 (MoK α)/ mm ⁻¹
$F(000)$	968
Crystal size	0.40 x 0.30 x 0.20 mm ³
θ range for data collection	3.57 to 24.92°
Index ranges	$-11 \leq h \leq 11$, $-12 \leq k \leq 12$, $-24 \leq l \leq 24$
Reflections collected	5214
Independent reflections	3471 ($R_{\text{int}} = 0.1460$)
Completeness to $\theta = 24.92^\circ$	98.7 %
Refinement method	Full-matrix least-squares on F^2
Data / restraints / parameters	3471 / 263 / 278
Goodness-of-fit on F^2	1.075
Final R indices ($I > 2 \sigma(I)$)	$R1 = 0.0777$, $wR2 = 0.1839$
R indices (all data)	$R1 = 0.1021$, $wR2 = 0.2084$
Largest diff. Peak and hole	2.814 and -3.564 e.Å ⁻³

7. References

- [1] R. H. Holm, G. W. Everett, A. Chakravorty, *Prog. Inorg. Chem.* **1966**, 7, 83.
- [2] S. G. McGeachin, *Can. J. Chem.* **1968**, 46, 1903.
- [3] L. C. Dorman, *Tetrahedron Lett.* **1966**, 4, 459.
- [4] W. J. Barry, I. Finar, E. F. Mooney, *Spectrochim. Acta* **1965**, 21, 1095.
- [5] R. Bonnett, D. C. Bradley, K. J. Fisher, *J. Chem. Soc., Chem. Commun.* **1968**, 886.
- [6] R. Bonnett, D. C. Bradley, K. J. Fisher, I. F. Rendall, *J. Chem. Soc. (A)* **1971**, 1622.
- [7] J. E. Parks, R. H. Holm, *Inorg. Chem.* **1968**, 7, 1408.
- [8] C. P. Richards, G. A. Webb, *J. Inorg. Nucl. Chem.* **1969**, 31, 3459.
- [9] N. M. Tsybina, V. G. Vinkurov, T. V. Protopopova, A. P. Skoldinov *J. Gen. Chem., USSR* **1966**, 36, 1383; *Zh. Obshh. Khimii* **1966**, 36, 1372.
- [10] F. A. Cotton, B. G. DeBoer, J. R. Pipal, *Inorg. Chem.* **1970**, 9, 783.
- [11] M. Elder, B. R. Penfold, *J. Chem. Soc. (A)* **1969**, 2556.
- [12] C. L. Honeybourne, G. A. Webb, *Mol. Phys.* **1969**, 17, 17.
- [13] C. L. Honeybourne, G. A. Webb, *Chem. Phys. Lett.* **1968**, 2, 426.
- [14] P. B. Hitchcock, M. F. Lappert, D.-S. Liu, *J. Chem. Soc., Chem. Commun.* **1994**, 1699.
- [15] V. C. Gibson, P. J. Maddox, C. Newton, C. Redshaw, G. Solan, A. J. P. White, D. J. Williams, *J. Chem. Soc., Chem. Commun.* **1998**, 1651.
- [16] D. S. Richeson, J. F. Mitchell, K. H. Theopold, *Organometallics* **1989**, 8, 2570.
- [17] A. C. Filippou, C. Völkl, R. D. Rogers, *J. Organomet. Chem.* **1993**, 463, 135.
- [18] V. C. Gibson, C. Newton, C. Redshaw, G. A. Solan, A. J. P. White, D. J. Williams, *Eur. J. Inorg. Chem.* **2001**, 1895.
- [19] B. J. O'Keefe, M. A. Hillmeyer, W. B. Tolman, *J. Chem. Soc., Dalton Trans.* **2001**, 2215.

- [20] J. Feldman, S. J. McLain, A. Parthasarathy, W. J. Marshall, C. J. Calabrese, S. D. Arthur, *Organometallics* **1997**, *16*, 1514.
- [21] P. H. M. Budzelaar, A. B. van Oort, A. G. Orpen, *Eur. J. Inorg. Chem.* **1998**, 1485.
- [22] K. H. Theopold, W.-K. Kim, *Int. Pat. Appl. WO 99/41290* **1999**; *Chem. Abstr.* 131:170748.
- [23] M. Rahim, N. J. Taylor, S. Xin, S. Collins, *Organometallics* **1998**, *17*, 1315.
- [24] P. L. Holland, W. B. Tolman, *J. Am. Chem. Soc.* **1999**, *121*, 7270.
- [25] D. W. Randall, G. S. DeBeer, P. L. Holland, B. Hedman, K. O. Hodgson, W. B. Tolman, E. I. Solomon, *J. Am. Chem. Soc.* **2000**, *122*, 11632.
- [26] C. Cui, H. W. Roesky, H. Hao, H.-G. Schmidt, M. Noltemeyer, *Angew. Chem. Int. Ed.* **2000**, *39*, 1815.
- [27] C. Cui, H. W. Roesky, H.-G. Schmidt, M. Noltemeyer, H. Hao, F. Cimpoesu, *Angew. Chem. Int. Ed.* **2000**, *39*, 4274.
- [28] J. M. Smith, R. L. Lachicotte, P. L. Holland, *J. Chem. Soc., Chem. Commun.* **2001**, 1542.
- [29] J. M. Smith, R. L. Lachicotte, K. A. Pittard, T. R. Cundari, G. Lukat-Rodgers, K. R. Rodgers, P. L. Holland, *J. Am. Chem. Soc.* **2001**, *123*, 9222.
- [30] N. J. Hardman, B. E. Eichler, P. P. Power, *J. Chem. Soc., Chem. Commun.* **2000**, 1991.
- [31] B. Rake, F. Zulch, Y. Ding, J. Prust, H. W. Roesky, M. Noltemeyer, H.-G. Schmidt, Z. *Anorg. Allg. Chem.* **2001**, 627, 836.
- [32] L. W. Pineda, V. Jancik, H. W. Roesky, D. Neculai, A. M. Neculai, *Angew. Chem. Int. Ed.* **2004**, *43*, 1419.
- [33] H. Hao, C. Cui, H. W. Roesky, G. Bai, H.-G. Schmidt, M. Noltemeyer, *J. Chem. Soc., Chem. Commun.* **2001**, 1118.
- [34] S. S. Malhotra, M. C. Whiting, *J. Chem. Soc. Abstr.* **1960**, 3812.
- [35] G. Scheibe, *Ber. Dtsch. Chem. Ges.* **1923**, *56*, 137.

- [36] P. J. Bailey, R. A. Coxall, C. M. E. Dick, S. Fabre, S. Parsons, *Organometallics* **2001**, *20*, 798.
- [37] Y. Ding, H. Hao, H. W. Roesky, M. Noltemeyer, H.–G. Schmidt, *Organometallics* **2001**, *20*, 4806.
- [38] G. Bai, Y. Peng, H. W. Roesky, J. Li, H.–G. Schmidt, M. Noltemeyer, *Angew. Chem. Int. Ed.* **2003**, *42*, 1132.
- [39] Y.–L. Huang, B.–H. Huang, B.–T. Ko, C.–C. Lin, *J. Chem. Soc., Dalton Trans.* **2001**, 2409.
- [40] L. Bourget–Merle, M. F. Lappert, J. R. Severn, *Chem. Rev.* **2002**, *102*, 3031.
- [41] N. N. Greenwood, A. Earnshaw, *Chemistry of the Elements*. 1st ed. Pergamon Press, Oxford, **1984**.
- [42] G. A. Olah (ed.), *Friedel–Crafts and Related Reactions*, Vols. 1–4, Interscience, New York, **1963**: See especially Chap.1 & 2.
- [43] F. Seel, *Atomic Structure and Chemical Bonding*, 4th edn. translated and revised by N. N. Greenwood and H. P. Stadler, Methuen, London, **1963**, pp. 83.
- [44] C. E. Radzewich, G. T. Guzei, R. F. Jordan, *J. Am. Chem. Soc.* **1999**, *121*, 8673.
- [45] B. Qian, D. L. Ward, M. R. Smith, III, *Organometallics* **1998**, *17*, 3070.
- [46] M. Stender, B. E. Eichler, N. J. Hardman, P. P. Power, J. Prust, M. Noltemeyer, H. W. Roesky, *Inorg. Chem.* **2001**, *40*, 2794.
- [47] G. Bai, S. Singh, H. W. Roesky, M. Noltemeyer, H.–G. Schmidt, *J. Am. Chem. Soc.* **2005**, *127*, 3449.
- [48] J. Chai, V. Jancik, S. Singh, H. Zhu, C. He, H. W. Roesky, H.–G. Schmidt, M. Noltemeyer, N. S. Hosmane, *J. Am. Chem. Soc.* **2005**, *127*, 7251.
- [49] H. Zhu, J. Chai, C. He, G. Bai, H. W. Roesky, V. Jancik, H.–G. Schmidt, M. Noltemeyer, *Organometallics* **2005**, *24*, 380.

- [50] H. W. Roesky, G. Bai, V. Jancik, S. Singh. *European Patent*, **2005**, PCT/EP, 2005/002741, Int. Pat. Classification. C07F17/00.
- [51] W. Kaminsky, S. Lenk, V. Scholz, H. W. Roesky, A. Herzog, *Macromolecules* **1997**, *30*, 7647.
- [52] A. Herzog, H. W. Roesky, Z. Zak, M. Noltemeyer, *Angew. Chem. Int. Ed. Engl.* **1994**, *33*, 967.
- [53] A. Herzog, H. W. Roesky, F. Jäger, A. Steiner, M. Noltemeyer, *Organometallics* **1996**, *15*, 909.
- [54] J. Pinkas, H. W. Roesky, *J. Fluorine Chem.* **2003**, *122*, 125, and references therein.
- [55] K. Ziegler, E. Holzkamp, R. Köster, H. Lehmkuhl, *Angew. Chem.* **1955**, *67*, 213.
- [56] E. F. Murphy, R. Murugavel, H. W. Roesky, *Chem. Rev.* **1997**, *97*, 3425.
- [57] H. W. Roesky, *Inorg. Chem.* **1999**, *38*, 5934.
- [58] H. Hohmeister, H. Wessel, P. Lobinger, H. W. Roesky, P. Müller, I. Usón, H.–G. Schmidt, M. Noltemeyer, J. Magull, *J. Fluorine Chem.* **2003**, *120*, 59.
- [59] A. Stasch, H. W. Roesky, D. Vidovic, J. Magull, H.–G. Schmidt, M. Noltemeyer, *Inorg. Chem.* **2004**, *43*, 3625.
- [60] S. Singh, H.–J. Ahn, A. Stasch, V. Jancik, H. W. Roesky, A. Pal, M. Biadene, R. Herbst-Irmer, M. Noltemeyer, H.–G. Schmidt, *Inorg. Chem.* **2006**, *45*, 1853.
- [61] N. Kuhn, A. Kuhn, R. Boese, N. Augart, *J. Chem. Soc., Chem. Commun.* **1989**, 975.
- [62] N. Kuhn, A. Kuhn, M. Speis, D. Bläser, R. Boese, *Chem. Ber.* **1990**, *123*, 1301.
- [63] A. J. Downs, C. R. Pulham, *Chem. Soc. Rev.* **1994**, *23*, 175.
- [64] J. K. Ruff, *Inorg. Synth.* **1967**, *9*, 30.
- [65] B. Twamley, N. J. Hardman, P. P. Power, *Acta Cryst.* **2001**, *E57*, m227.

- [66] C. R. Pulham, A. J. Downs, M. J. Goode, D. W. H. Rankin, H. E. Robertson, *J. Am. Chem. Soc.* **1991**, *113*, 5149.
- [67] A. Storr, V. G. Wiebe, *Can. J. Chem.* **1969**, *47*, 673.
- [68] A. J. Arduengo, III; H. V. R. Dias, J. C. Calabrese, F. Davidson, *J. Am. Chem. Soc.* **1992**, *114*, 9724.
- [69] C. W. Heitsch, C. E. Nordman, R. W. Parry, *Inorg. Chem.* **1963**, *2*, 508.
- [70] N. N. Greenwood, Gallium hydride and its derivatives, Chap. 3 in E. A. V. Ebsworth, A. G. Maddock, A. G. Sharpe (eds.), *New Pathways in Inorganic Chemistry*, pp. 37-64, Cambridge University Press, Cambridge, **1968**.
- [71] K. Masu, H. Machida, *Jpn. Kokai Tokkyo Koho* **2004**, *9*.
- [72] Y. Peng, G. Bai, H. Fan, D. Vidovic, H. W. Roesky, J. Magull, *Inorg. Chem.* **2004**, *43*, 1217.
- [73] A. Stasch, M. Ferbinteanu, J. Prust, W. Zheng, F. Cimpoesu, H. W. Roesky, J. Magull, H.-G. Schmidt, M. Noltemeyer, *J. Am. Chem. Soc.* **2002**, *124*, 5441.
- [74] S. S. Kumar, J. Rong, S. Singh, H. W. Roesky, D. Vidovic, J. Magull, D. Neculai, *Organometallics* **2004**, *23*, 3496.
- [75] N. D. Reddy, S. S. Kumar, H. W. Roesky, D. Vidovic, J. Magull, M. Noltemeyer, H.-G. Schmidt, *Eur. J. Inorg. Chem.* **2003**, 442.
- [76] V. Jancik, Y. peng, H. W. Roesky, J. Li, D. Neculai, A. M. Neculai, R. Herbst-Irmer, *J. Am. Chem. Soc.* **2003**, *125*, 1452.
- [77] S. S. Kumar, S. Singh, H. W. Roesky, J. Magull, *Inorg. Chem.* **2005**, *44*, 1199.
- [78] S. S. Kumar, S. Singh, F. Hongjun, H. W. Roesky, D. Vidovic, J. Magull, *Organometallics* **2004**, *23*, 6328.
- [79] A. Stasch, S. S. Kumar, V. Jancik, H. W. Roesky, J. Magull, M. Noltemeyer, *Eur. J. Inorg. Chem.* **2004**, 4056.

- [80] H. Dorn, H. W. Roesky, *Inorg. Synth.* **2002**, *33*, 230.
- [81] C. Ackerhans, H. W. Roesky, T. Labahn, J. Magull, *Organometallics* **2002**, *21*, 3671.
- [82] J. Janssen, J. Magull, H. W. Roesky, *Angew. Chem. Int. Ed.* **2002**, *41*, 1365.
- [83] H. W. Roesky, M. G. Walawalkar, R. Murugavel, *Acc. Chem. Res.* **2001**, *34*, 201, and references therein.
- [84] H. Sinn, W. Kaminsky, H.-J. Vollmer, R. Woldt, *Angew. Chem. Int. Ed. Engl.* **1980**, *19*, 390.
- [85] E. Y.-X. Chen, T. J. Marks, *Chem. Rev.* **2000**, *100*, 1391.
- [86] M. R. Mason, J. M. Smith, S. G. Bott, A. Barron, *J. Am. Chem. Soc.* **1993**, *115*, 4971.
- [87] C. Schnitter, H. W. Roesky, H.-G. Schmidt, C. Roepken, E. Parisini, G. M. Sheldrick, *Chem. Eur. J.* **1997**, *3*, 1783.
- [88] J. Storre, A. Klemp, H. W. Roesky, H.-G. Schmidt, M. Noltemeyer, R. Fleischer, D. Stalke, *J. Am. Chem. Soc.* **1997**, *119*, 7505.
- [89] M. Veith, M. Jarczyk, V. Huch, *Angew. Chem. Int. Ed. Engl.* **1997**, *36*, 117.
- [90] Y. Koide, A. R. Barron, *Organometallics* **1995**, *14*, 4026.
- [91] G. Bai, H. W. Roesky, J. Li, M. Noltemeyer, H.-G. Schmidt, *Angew. Chem. Int. Ed.* **2003**, *42*, 5502.
- [92] V. Jancik, L. W. Pineda, A. C. Stückl, H. W. Roesky, R. Herbst-Irmer, *Organometallics* **2005**, *24*, 1511.
- [93] A. H. Cowley, F. P. Gabbaï, D. A. Atwood, C. J. Carrano, L. M. Mokry, M. R. Bond, *J. Am. Chem. Soc.* **1994**, *116*, 1559.
- [94] N. M. Boag, K. M. Coward, A. C. Jones, M. E. Pemble, J. R. Thompson, *Acta Crystallogr. Sect. C* **2000**, *56*, 1438.
- [95] W. Uhl, I. Hahn, M. Koch, M. Layh, *Inorg. Chim. Acta* **1996**, *249*, 33.

- [96] D. A. Atwood, A. H. Cowley, P. R. Harris, R. A. Jones, S. U. Koschmieder, C. M. Nunn, J. L. Atwood, S. G. Bott, *Organometallics* **1993**, *12*, 24.
- [97] A. A. Naiini, V. Young, Y. Han, M. Akinc, J. G. Verkade, *Inorg. Chem.* **1993**, *32*, 3781.
- [98] P. J. Nichols, S. Papadopoulos, C. L. Raston, *J. Chem. Soc., Chem. Commun.* **2000**, 1227.
- [99] N. Wiberg, K. Amelunxen, H.-W. Lerner, H. Nöth, W. Ponikwar, H. Schwenk, *J. Organomet. Chem.* **1999**, *574*, 246.
- [100] K. Yamasaki, O. Okada, K. Inami, K. Oka, M. Kotani, H. Yamada, *J. Phy. Chem. B* **1997**, *101*, 13.
- [101] R. J. Wehmschulte, J. M. Steele, M. A. Khan, *Organometallics* **2003**, *22*, 4678.
- [102] A. Sofetis, G. S. Papaefstatthiou, A. Terzis, C. P. Raptopoulou, T. F. Zafiroopoulos, Z. *Naturforsch.* **2004**, *59b*, 291.
- [103] H. W. Roesky, S. Singh, V. Jancik, V. Chandrasekhar, *Acc. Chem. Res.* **2004**, *37*, 969.
- [104] A. Klemp, H. Hatop, H. W. Roesky, H.-G. Schmidt, M. Noltemeyer, *Inorg. Chem.* **1999**, *38*, 5832.
- [105] S. Singh, S. S. Kumar, V. Chandrasekhar, H.-J. Ahn, M. Biadene, H. W. Roesky, N. S. Hosmane, M. Noltemeyer, H.-G. Schmidt, *Angew. Chem., Int. Ed.* **2004**, *43*, 4940.
- [106] F. J. Feher, K. J. Weller, J. W. Ziller, *J. Am. Chem. Soc.* **1992**, *114*, 9686.
- [107] G. Yamamoto, R. Nadano, W. Satoh, Y. Yamamoto, K.-Y. Akiba, *J. Chem. Soc., Chem. Commun.* **1997**, 1325.
- [108] N. B. Sharma, A. Singh, R. C. Mehrotra, *Main Group Metal Chem.* **2004**, *27*, 191.
- [109] Sonika, S. Kumar, A. K. Narula, *J. Ind. Chem. Soc.* **2004**, *81*, 639.
- [110] R. C. Mehrotra, R. R. Goyal, N. C. Jain, *Synth. React. Inorg. Met.-Org. Chem.* **1981**, *11*, 345.
- [111] S. Mathur, A. Singh, R. C. Mehrotra, *Polyhedron* **1993**, *12*, 1073.

- [112] M. Sharma, A. Singh, R. C. Mehrotra, *Ind. J. Chem., Sec. A: Inorg. Bio-Inorg., Phy., Theo. And Anal. Chem.* **1999**, 38A, 1209.
- [113] M. Veith, H. Wolfgang, V. Huch, *Zeitschrift fuer Naturforschung, B: Chem. Sci.* **1995**, 50, 1130.
- [114] A. J. R. Son, M. G. Thorn, P. E. Fanwick, I. P. Rothwell, *Organometallics* **2003**, 22, 2318.
- [115] H. Nöth, A. Schlegel, S. R. Lima, *Zeitschrift fuer Anorg. und Allg. Chem.*, **2001**, 627, 1793.
- [116] J. A. Francis, S. G. Bott, A. R. Barron, *J. Organomet. Chem.* **2000**, 597, 29.
- [117] M. S. Hill, D. A. Atwood, *Main Group Chemistry* **1998**, 2, 285.
- [118] H. Nöth, A. Schlegel, J. Knizek, I. Krossing, W. Ponikwar, T. Seifert, *Chem. Eur. J.* **1998**, 4, 2191.
- [119] H. Nöth, A. Schlegel, J. Knizek, H. Schwenk, *Angew. Chem. Int. Ed. Engl.* **1997**, 36, 2640.
- [120] D. R. Armstrong, R. P. Davies, D. J. Linton, R. Snaith, P. Schooler, A. E. H. Wheatley, *J. Chem. Soc., Dalton Trans.* **2001**, 19, 2838.
- [121] C. N. McMahon, S. J. Obrey, A. Keys, S. G. Bott, A. R. Barron, *J. Chem. Soc., Dalton trans.* **2000**, 2151.
- [122] D. A. Atwood, A. H. Cowley, R. D. Schluter, M. R. Bond, C. J. Carrano, *Inorg. Chem.* **1995**, 34, 2186.
- [123] J. pauls, S. Chitsaz, B. Neumuller, *Zeitschrift fuer Anorg. und Allg. Chem.* **2000**, 626, 2028.
- [124] M. Albrecht, S. Schmid, M. de Groot, P. Weis, R. Froehlich, *J. Chem. Soc., Chem. Commun.* **2003**, 2526.
- [125] W. Uhl, A. Ei-Hamdan, G. Gieseler, K. Harms, *Zeitschrift fuer Anorg. und Allg. Chem.* **2004**, 630, 821.
- [126] F. M. G. de Rege, W. M. Davis, S. L. Buchwald, *Organometallics* **1995**, 14, 4799.
- [127] R. C. Mehrotra, M M. Agarwal, A. Mehrotra, *Synth. Inorg. Met.-Org. Chem.* **1973**, 3, 407.

- [128] K. G. Thomas, P. V. Kamat, *Acc. Chem. Res.* **2003**, *36*, 888.
- [129] M.-C. Daniel, D. Astruc, *Chem. Rev.* **2004**, *104*, 293.
- [130] D. H. Brown, W. E. Smith, *Chem. Soc. Rev.* **1980**, *9*, 217.
- [131] W. A. Herrmann, M. Elison, J. Fischer, C. Kocher, G. R. J. Artus, *Angew. Chem. Int. Ed. Engl.* **1995**, *35*, 2371.
- [132] S. T. Staben, J. J. Kennedy-Smith, F. D. Toste, *Angew. Chem. Int. Ed.* **2004**, *43*, 5350.
- [133] C. Nieto-Oberhuber, M. P. Muñoz, E. Buñuel, C. Nevado, D. J. Cárdenas, A. M. Echavarren, *Angew. Chem. Int. Ed.* **2004**, *43*, 2402.
- [134] G. K. Anderson, *Adv. Organomet. Chem.* **1982**, *20*, 39.
- [135] R. J. Cross, M. F. Davidson, *J. Chem. Soc., Dalton Trans.* **1986**, 411.
- [136] J. Vicente, M.-T. Chicote, M.-D. Abrisqueta, P. G. Jones, *Organometallics* **2000**, *19*, 2629.
- [137] R.-Y. Liao, A. Schier, H. Schmidbaur, *Organometallics* **2003**, *22*, 3199.
- [138] M. J. Irwin, J. J. Vittal, R. J. Puddephatt, *Organometallics* **1997**, *16*, 3541 and references therein.
- [139] W. Lu, N. Zhu, C.-M. Che, *J. Organomet. Chem.* **2003**, *670*, 11.
- [140] B.-C. Tzeng, W.-C. Lo, C.-M. Che, S.-M. Peng, *J. Chem. Soc., Chem. Commun.* **1996**, 181.
- [141] H. Xiao, K.-K. Cheung, C.-M. Che, *J. Chem. Soc., Dalton Trans.* **1996**, 3699.
- [142] V. W.-W. Yam, S. W.-K. Choi, *J. Chem. Soc., Dalton Trans.* **1996**, 4227.
- [143] D. Bourissou, O. Guerret, F. P. Gabbaï, G. Bertrand, *Chem. Rev.* **2000**, *100*, 39.
- [144] H. M. J. Wang, C. Y. L. Chen, I. J. B. Lin, *Organometallics* **1999**, *18*, 1216.
- [145] B. Bovio, A. Burini, B. R. Pietroni, *J. Organomet. Chem.* **1993**, *452*, 287.
- [146] M. V. Baker, P. J. Barnard, S. K. Brayshaw, J. L. Hickey, B. W. Skelton, A. H. White, *J. Chem. Soc., Dalton Trans.* **2005**, 37.

- [147] H. W. Roesky, K. Keller, *J. Fluorine Chem.* **1999**, *100*, 217.
- [148] R.-C. Yu, C.-H. Hung, J.-H. Huang, H.-Y. Lee, J.-T. Chen, *Inorg. Chem.* **2002**, *41*, 6450.
- [149] C. Schnitter, K. Klimek, H. W. Roesky, T. Albers, H.-G. Schmidt, C. Röpken, E. Parisini, *Organometallics* **1998**, *17*, 2249.
- [150] M. Veith, S. Faber, H. Wolfgang, V. Huch, *Chem. Ber.* **1996**, *129*, 381.
- [151] V. Jancik, J. Prust, H. W. Roesky, Unpublished results.
- [152] A. J. Arduengo, III; H. V. R. Dias, R. L. Harlow, M. Kline, *J. Am. Chem. Soc.* **1992**, *114*, 5530.
- [153] J. Storre, A. Klemp, H. W. Roesky, H.-G. Schmidt, M. Noltemeyer, R. Fleischer, D. Stalke, *J. Am. Chem. Soc.* **1996**, *118*, 1380.
- [154] S.-F. Liu, C. Seward, H. Aziz, N.-X. Hu, Z. Popović, S. Wang, *Organometallics* **2000**, *19*, 5709.
- [155] S. J. Rittig, M. Sandercock, A. Storr, J. Trotter, *Can. J. Chem.* **1990**, *68*, 59.
- [156] A. M. Magill, K. J. Cavell, B. F. Yates, *J. Am. Chem. Soc.* **2004**, *126*, 8717.
- [157] R. Shah, J. D. Gale, M. C. Payne, *J. Chem. Soc., Chem. Commun.* **1997**, 131.
- [158] P. Ugliengo, B. Civalleri, C. M. Zicovich-Wilson, R. Dovesi, *Chem. Phys. Lett.* **2000**, *318*, 247.
- [159] S. J. Rittig, A. Storr, J. Trotter, *Can. J. Chem.* **1975**, *53*, 58.
- [160] S.-H. Byeon, S.-S. Lee, J. B. Parise, P. M. Woodward, N. H. Hur, *Chem. Mater.* **2005**, *17*, 3552.
- [161] J. Storre, A. Klemp, H. W. Roesky, R. Fleischer, D. Stalke, *Organometallics* **1997**, *16*, 3074.
- [162] W. E. Hunter, D. C. Hrnčir, R. V. Bynum, R. A. Penttilä, J. L. Atwood, *Organometallics* **1983**, *2*, 750.

- [163] J. F. Clarke, M. G. B. Drew, *Acta Crystallogr.* **1974**, B30, 2267.
- [164] G. Fachinetti, C. Floriani, A. Chiesi-Villa, C. Guastino, *J. Am. Chem. Soc.* **1979**, 101, 1767.
- [165] G. Bai, H. W. Roesky, J. Li, T. Labahn, F. Cimpoesu, J. Magull, *Organometallics* **2003**, 22, 3034.
- [166] L. M. Babcock, V. W. Day, W. G. Klemperer, *J. Chem. Soc., Chem. Commun.* **1988**, 519.
- [167] W. J. Evans, K. A. Miller, J. W. Ziller, *Inorg. Chem.* **2006**, 45, 424.
- [168] M. Kritikos, M. Moustiakimov, M. Wijk, G. Westin, *J. Chem. Soc. Dalton, Trans.* **2001**, 1931.
- [169] H.-W. Wanzlick, H. -J. Schönherr, *Angew. Chem., Int. Ed. Engl.* **1968**, 7, 141.
- [170] K. Öfele, *J. Organomet. Chem.* **1968**, 12, P42.
- [171] A. J. Arduengo, III; R. L. Harlow, M. Kline, *J. Am. Chem. Soc.* **1991**, 113, 361.
- [172] X. Hu, I. Castro-Rodriguez, K. Olsen, K. Meyer, *Organometallics* **2004**, 23, 755.
- [173] R. Fränkel, J. Kniczek, W. Ponikwar, H. Nöth, K. Polborn, W. P. Fehlhammer, *Inorg. Chim. Acta* **2001**, 312, 23.
- [174] H. M. J. Wang, I. J. B. Lin, *Organometallics* **1998**, 17, 972.
- [175] J. F. Britten, C. J. L. Lock, Z. Wang, *Acta Crystallogr., Sect. C: Cryst. Struct. Commun.* **1992**, 48, 1600.
- [176] H. G. Raubenheimer, L. Lindeque, S. Cronje, *J. Organomet. Chem.* **1996**, 511, 177.
- [177] F. Bonati, A. Burini, B. R. Pietrosi, B. Bovio, *J. Organomet. Chem.* **1989**, 375, 147.
- [178] P. J. Barnard, M. V. Baker, S. J. Berners-Price, B. W. Skelton, A. H. White, *J. Chem. Soc., Dalton Trans.* **2004**, 1038.
- [179] M.-T. Lee, C.-H. Hu, *Organometallics* **2004**, 23, 976.
- [180] H. G. Raubenheimer, P. J. Olivier, L. Lindeque, M. Desmet, J. Hrusak, G. J. Kruger, *J. Organomet. Chem.* **1997**, 544, 91.

- [181] F. Bonati, A. Burini, B. R. Pietroni, B. Bovio, *J. Organomet. Chem.* **1991**, 408, 271.
- [182] H. G. Raubenheimer, F. Scott, M. Roos, R. Otte, *J. Chem. Soc., Chem. Commun.* **1990**, 1722.
- [183] H. M. J. Wang, C. S. Vasam, T. Y. R. Tsai, S.-H. Chen, A. H. H. Chang, I. J. B. Lin *Organometallics* **2005**, 24, 486.
- [184] S. Friedrichs, P. G. Jones, *Z. Naturforsch* **2004**, 59b, 793.
- [185] G. Aullón, D. Bellamy, L. Brammer, E. A. Bruton, A. G. Orpen, *J. Chem. Soc., Chem. Commun.* **1998**, 653.
- [186] M. Fujiwara, H. Wessel, H.-S. Park, H. W. Roesky, *Tetrahedron* **2002**, 58, 239.
- [187] H. W. Roesky, G. Anantharaman, V. Chandrasekhar, V. Jancik, S. Singh, *Chem. Eur. J.* **2004**, 10, 4106.
- [188] H. C. L. Abbenhuis, *Chem. Eur. J.* **2000**, 6, 25.
- [189] D. F. Shriver, M. A. Drezdon, *The Manipulation of Air-Sensitive Compounds*, 2nd edn. McGraw-Hill, New York, USA, **1969**.
- [190] "SHELXS-97, Program for Structure Solution": G. M. Sheldrick, *Acta Crystallogr. Sect. A*, **1990**, 46, 467.
- [191] G. M. Sheldrick, SHELXL-97, *Program for Crystal Structure Refinement*, Universität Göttingen, Göttingen, FRG, **1997**.
- [192] O. T. Jr. Beachley, D. B. Rosenblum, D. J. Macrae, *Organometallics* **2001**, 20, 945.
- [193] MeInCl₂ was prepared by the reaction of Me₃In and InCl₃ in 1:2 stoichiometric ratio by using the procedure similar to that reported for MeGaCl₂ (Ref. 192).
- [194] H. W. Roesky, K. Keller, *J. Fluorine Chem.* **1998**, 89, 3.
- [195] S. Saito, Product subclass 2: Aluminum Hydrides. *Science of Synthesis* **2004**, 7, 15.
- [196] D. F. Shriver, A. E. Shirk, *Inorg. Synth.* **1977**, 17, 42.

- [197] A. Kiennemann, G. Levy, F. Schue, C. Tanielian, *J. Organomet. Chem.* **1972**, 35, 143.
- [198] D. H. Harris, M. F. Lappert, *J. Chem. Soc., Chem. Commun.* **1974**, 21, 895.
- [199] C. D. Schaeffer, Jr.; J. J. Zuckerman, *J. Am. Chem. Soc.* **1974**, 96, 7160.
- [200] J. M. Birmingham, G. Wilkinson, *J. Am. Chem. Soc.* **1956**, 78, 42.
- [201] W. Jahn, *Dissertation*, Universität Hamburg, **1983**.
- [202] A. J. Arduengo, III; H. Bock, H. Chen, M. Denk, D. A. Dixon, J. C. Green, W. A. Herrmann, N. L. Jones, M. Wagner, R. West, *J. Am. Chem. Soc.* **1994**, 116, 6641.

List of publications

- [1] *Synthesis, Characterization and X-ray Crystal Structure of a Gallium Monohydroxide and a Hetero-Bimetallic Gallium Zirconium Oxide.* **Sanjay Singh**, Vojtech Jancik, Herbert W. Roesky, and Regine Herbst-Irmer, *Inorg. Chem.* **2006**, 45, 949–951.
- [2] *Syntheses, Characterization and X-ray Crystal Structures of β -diketiminato Group 13 Hydrides, Chlorides and Fluorides.* **Sanjay Singh**, Hans-Jürgen Ahn, Andreas Stasch, Vojtech Jancik, Herbert W. Roesky, Aritra Pal, Mariana Biadene, Regine Herbst-Irmer, Mathias Noltemeyer, and Hans-Georg Schmidt, *Inorg. Chem.* **2006**, 45, 1853–1860.
- [3] *Mononuclear Aluminum Hydroxide for the Design of Well-Defined Homogeneous Catalysts.* Guangcai Bai, **Sanjay Singh**, Herbert W. Roesky, Mathias Noltemeyer, and Hans-Georg Schmidt, *J. Am. Chem. Soc.* **2005**, 127, 3449–3455.
- [4] *Synthesis of a New Class of Compounds Containing a Ln–O–Al Arrangement and Their Reactions and Catalytic Properties.* Jianfang Chai, Vojtech Jancik, **Sanjay Singh**, Hongping Zhu, Cheng He, Herbert W. Roesky, Hans-Georg Schmidt, Mathias Noltemeyer, and Narayan S. Hosmane, *J. Am. Chem. Soc.* **2005**, 127, 7521–7528.
- [5] *A Facile One-step Synthesis of a Lipophilic Gold(I) Carbene Complex. X-ray Crystal Structures of $LAuCl$ and $LAuC\equiv CH$ ($L = 1,3$ -di-*tert*-butylimidazol-2-ylidene).* **Sanjay Singh**, S. Shravan Kumar, Vojtech Jancik, Herbert W. Roesky, Hans-Georg Schmidt and Mathias Noltemeyer, *Eur. J. Inorg. Chem.* **2005**, 3057–3062.
- [6] *Organoaluminum Hydroxide and Bimetallic Derivatives.* **Sanjay Singh**, Herbert W. Roesky. Abstract of papers, 229th National Meeting, American Chemical Society, March 13–17, **2005**. San Diego, California USA.

- [7] *Reaction of LiAlH_2 with tert-Butyl Hydrogenperoxide Under C–H Bond Activation and Substitution Leads to the Formation of a Penta- Coordinated tert-Butylperoxo Aluminum Compound.* S. Shravan Kumar, **Sanjay Singh**, Herbert W. Roesky, and Jörg Magull, *Inorg. Chem.* **2005**, *44*, 1199–1201.
- [8] *Synthesis and Chemical Properties of Tetraalkyl Substituted Thiourea Adducts with Chlorine.* Herbert W. Roesky, Umesh N. Nehete, **Sanjay Singh**, Hans-Georg Schmidt, and Yuiry G. Shermolovich, *Main Group Chemistry*, **2005**, *4*, 11–21.
- [9] *New Synthetic Approach to Yttriumhydroxoacetates, Structural Characterization, and Use as Precursor for Coated Conductors.* Peter Lobinger, Harald Jarzina, Herbert W. Roesky, **Sanjay Singh**, S. Shravan Kumar, Hans-Georg Schmidt, Matthias Noltemeyer, and Herbert C. Freyhardt, *Inorg. Chem.* **2005**, *44*, 9192–9196.
- [10] *Tetranuclear Homo- and Heteroalumoxanes Containing Reactive Functional Groups: Syntheses and X-Ray Crystal Structures of $[\{\text{LAl}(\text{Me})\}(\mu\text{-O})(\text{MH}_2)]_2$; $[\text{M} = \text{Al}, \text{Ga}; \text{L} = \text{HC}\{(\text{CMe})(2,6\text{-iPr}_2\text{C}_6\text{H}_3\text{N})\}_2]$.* **Sanjay Singh**, S. Shravan Kumar, Vadapalli Chandrasekhar, Hans-Jürgen Ahn, Marianna Biadene, Herbert W. Roesky, Narayan S. Hosmane, Mathias Noltemeyer, and Hans-Georg Schmidt, *Angew. Chem.* **2004**, *116*, 5048–5041; *Angew. Chem., Int. Ed.* **2004**, *43*, 4940–4943.
- [11] *A Paradigm Change in Assembling OH Functionalities on Metal Centers.* Herbert W. Roesky, **Sanjay Singh**, Vojtech Jancik and Vadapalli Chandrasekhar, *Acc. Chem. Res.* **2004**, *37*, 969–981.
- [12] *A Planar Dimeric Six-Membered Spirane Aluminum Hydrazide: Synthesis, X-ray Crystal Structure and Theoretical Studies of $[\text{LAlN}(\text{Me})\text{NH}]_2$; $[\text{L} = \text{HC}\{(2,6\text{-i-Pr}_2\text{C}_6\text{H}_3\text{N})(\text{CMe})\}_2]$.* S. Shravan Kumar, **Sanjay Singh**, Fan Hongjun, Herbert W. Roesky, Denis Vidovic, and Jörg Magull, *Organometallics* **2004**, *23*, 6328–6330.

- [13] *Synthesis and Reactivity of Carbaalanes* $(AlH)_6(AlNMe_3)_2(CCH_2C_5H_4FeC_5H_5)_6$ and $(AlH)_6(AlNMe_3)_2(CCH_2Ph)_6$: X-ray Crystal Structure of $(AlH)_6(AlNMe_3)_2(CCH_2C_5H_4FeC_5H_5)_6$. S. Shravan Kumar, Junfeng Rong, **Sanjay Singh**, Herbert W. Roesky, Denis Vidovic, Jörg Magull, Dante Neculai, Vadapalli Chandrasekhar, and Marc Baldus, *Organometallics* **2004**, 23, 3496–3500.
- [14] *Control of Molecular Topology and Metal Nuclearity in Multi-Metallic Assemblies: Designer Metallasiloxanes Derived from Silanetriols*. Herbert W. Roesky, Ganapathi Anantharaman, Vadapalli Chandrasekhar, Vojtech Jancik and **Sanjay Singh**. *Chem. Eur. J.* **2004**, 10, 4106–4114.
- [15] *Adducts of Aluminum and Gallium Trichloride with a N-Heterocyclic Carbene and an Adduct of Aluminum Trichloride with a Thione*. Andreas Stasch, **Sanjay Singh**, Herbert W. Roesky, Mathias Noltemeyer and Hans-Georg Schmidt, *Eur. J. Inorg. Chem.* **2004**, 4052–4055.
- [16] *Synthesis and Structural Characterization of Monomeric Manganese(II) N-Heterocyclic Carbene Complexes* $[MnX_2(C\{N(iPr)C(Me)\}_2)_2]$ ($X = Cl, I, \text{ and } MeCOO$). Jianfang Chai, Hongping Zhu, Ying Peng, Herbert W. Roesky, **Sanjay Singh**, Hans-Georg Schmidt, Mathias Noltemeyer, *Eur. J. Inorg. Chem.* **2004**, 2673–2677.

Patents:

- [17] *Oxygen-bridged Bimetallic Complex, the Production Thereof and its Utilisation for Polymerization Catalyst*. Herbert W. Roesky, Guangcai Bai, Vojtech Jancik and **Sanjay Singh**. European Patent, **2005** PCT/EP, 2005/002741, Int. Pat. Classification. C07F17/00.

Articles In Press/Submitted:

- [18] *Organometallic Hydroxides of Transition Elements*. Herbert W. Roesky, **Sanjay Singh**, K. K. Mohammed Yusuff, John A. Maguire, and Narayan S. Hosmane, *Chem. Rev.* **2006**, In Press.
- [19] *Adducts of Cp_3Ln With $LGa(Me)OH$, Syntheses and X-ray Crystal Structure of $LGa(Me)HO \rightarrow LnCp_3$; ($Ln = Sm, Nd, Yb$ and $L = HC\{C(Me)N(2,6-iPr_2C_6H_3)\}_2$)*. **Sanjay Singh**, Aritra Pal, Herbert W. Roesky, Regine-Herbst Irmer, *Eur. J. Inorg. Chem.* **2006**, Submitted.
- [20] *Fluorine Functionalized Compounds of Group 13 Elements*. **Sanjay Singh**, Herbert W. Roesky, *J. Fluorine Chem.* **2006**, Submitted.

Lebenslauf

Name:		Sanjay Singh
Geboren:		01 October, 1978 in Varanasi
Staatsangehörigkeit:		indisch
Schulbesuch:	1984-1993	Primary School (class I – IX)
	1993-1994	Secondary School Examination (class X)
	1994-1996	Senior School certificate Examination (class XII)
	March 1996	Abitur
Studium:	1997-2000	B. Sc. (Hons.) in Chemie, Banaras Hindu University, Indien
	2000-2002	M. Sc. in Chemie, Indian Institute of Technology Kanpur, Indien
Promotion:	2003-present	Experimentelle Promotionsarbeit im Institut für Anorganische Chemie Göttingen unter der Leitung von Prof. Dr. Dr. h.c. mult. H. W. Roesky